Supersymmetric Gauge Theories from D3-branes on Singularities

by

Pavlos Kazakopoulos

Submitted to the Department of Physics
in partial fulfillment of the requirements for the degree of

Doctor of Philosophy in Physics

at the

MASSACHUSETTS INSTITUTE OF TECHNOLOGY
[September 2005]
June 2005

Author .....
Department of Physics
June 2005

Certified by .....
Amihay Hanany
Associate Professor of Physics
Thesis Supervisor

Accepted by .....
Thomas J. Greytak
Associate Department Head for Education

Supersymmetric Gauge Theories from D3-branes on Singularities

by

Pavlos Kazakopoulos

Submitted to the Department of Physics
on June 2005, in partial fulfillment of the
requirements for the degree of
Doctor of Philosophy in Physics

Abstract

In this thesis we study four-dimensional supersymmetric gauge theories and their string theory realization. After an introduction and a brief review of some basic concepts at the interface of gauge theories and string theory, we begin by examining the duality cascade phenomenon for quiver gauge theories. We give a general formulation for these cascades and use it to identify an example of a duality wall in a theory which can be realized on D3-branes at the apex of the complex cone over the zeroth Hirzebruch surface with the addition of fractional branes. Next, we compute global $U(1)$ charges for the matter fields of the del Pezzo gauge theories and formulate several of their features in the language of exceptional Lie algebras. We suggest the possibility of global symmetry enhancement at infinite coupling for these theories. Finally, we present two contributions to the solution of the geometric engineering problem. We construct the toric phases of the $Y^{p,q}$ theories and then identify and study a new infinite family of quiver gauge theories, $X^{p,q}$, whose dual geometries are known in terms of toric diagrams.

Thesis Supervisor: Amihay Hanany
Title: Associate Professor of Physics

Acknowledgments

First and foremost I want to express my gratitude to my advisor Ami Hanany for sharing his knowledge and insight with me during the years we have been working together, and for guiding me through the crucial phases of my graduate studies. Ami has always been available when his advice or help was needed. I always felt that he was on my side, a person whose guidance I could trust, and for this I truly thank him.

I also want to thank my other collaborators in the works presented in this thesis, Sergio Benvenuti, Sebastian Franco, Yang He and Brian Wecht for our collaborations and interesting discussions. Brian Fore, Umut Gursoy, Chris Kouvaris, Leonidas Pantelidis, Kyriakos Papadodimas, Nikolaos Prezas, Jan Troost and the other colleagues with whom I had many enlightening discussions during my years at MIT. Barton Zwiebach for his academic advice. My thesis committee members, Bill Bertozzi and Wati Taylor, for their time.

My thanks also go to my parents and my wonderful friends, in Greece and in the US, who stood by me and helped me stay happy and optimistic during the stressful times. May I always have the strength to support them as they supported me.

Last but most certainly not least I thank Deepa Isac for her extraordinary love.

Contents

List of Figures

List of Tables

Chapter 1

Introduction

This thesis consists of four works completed during the last two years on the subject of supersymmetric gauge theories in four dimensions, using concepts and methods deriving from string theory. Although Supersymmetry has not yet been discovered in high energy experiments, many people are confident that it will indeed be discovered in the next generation of these experiments. These will be conducted at the Large Hadron Collider of CERN, with energies in the range of a few TeV/nucleon. Most phenomenological models predict traces of Supersymmetry to appear at 1-1.5 TeV, so if Supersymmetry is real, there is a good chance it will be found there[1]. The phenomenological implications would then be far-reaching, beacause any model for unification will necessarily be a model with spontaneously broken Supersymmetry. This is one reason why supersymmetric gauge theories are worth studying, because in the next few years there is a chance we will be learning that nature is supersymmetric.

Apart from that though, we already know that all except gravitational interactions, at least at the highest energies that we can currently probe, are very accurately described by gauge theories like Quantum Chromodynamics. Supersymmetric gauge theories are in many ways similar to non-supersymmetric ones, exhibiting phenomena like chiral symmetry breaking, asymptotic freedom and confinement. However, the larger amount of symmetry relates bosons to fermions and constrains their interac-

[1]There is also the opinion that we already have enough evidence that the Higgs particle has a mass around 114 GeV, and this by itself is a good indication for Supersymmetry, because only it can provide the cancellation of radiative corrections needed for such a low mass.

tions, making it possible to extract more information with less effort. They are in this sense a theoretical laboratory in which we can test ideas and acquire understanding that will enlighten us as to the structure of more realistic theories. String theory, which gained momentum as a candidate for a unified theory of all interactions, gravitational and gauge, can also be seen as a way to approach gauge theories regardless of its relevance for unifying the forces at a fundamental level (although I do believe that in the end some version of it will be relevant to the actual unification). It is in this spirit mainly that my research has been conducted.

Many supersymmetric Yang-Mills theories admit a very natural realization in string theory, where the endpoints of open strings behave at low energies (low meaning far below the string mass scale, which could be as high as the Planck mass) like charged particles with gauge interactions determining their dynamics. It is natural in the sense that one does not need to add these interactions by hand, instead they emerge from the quantization of the string. This makes it possible to use properties of the string background (e.g. geometric or topological data of the spacetime in which the strings are moving) in order to compute data of the gauge theory. In many cases it is much easier to use this method instead of doing calculations in the field theory. It can also reveal patterns that would be hard to spot by looking at the field theory by itself. We will see an example of this in Chapter 4. However, given an open string background, it is often a hard question to read off the resulting gauge theory. Chapters 5 and 6 contain a contribution to answering this question.

The main concepts and methods we use derive from three important theoretical developements of the 1990's. In chronological order these are: Seiberg's duality for $\mathcal{N} = 1$ supersymmetric gauge theories, the discovery of D-branes, and AdS/CFT. We will discuss the relevant aspects of each of these in more detail in the next chapter[2], but a very brief description is in order here. Seiberg's duality was proposed in the early nineties for the theory known as supersymmetric QCD (SQCD). It asserts that when this theory flows to a conformal fixed point there is a dual description in terms of a different set of degrees of freedom that is physically indistinguishable

[2]The appropriate references will also be given there.

from the original theory at the fixed point. In some cases, one of the two theories is strongly coupled while its dual is weakly coupled, making this a strong-weak duality. The duality was extensively studied and generalized to other theories, including theories with product gauge group and matter fields in bifundamental representations (**quiver** gauge theories), which are the focus of the works presented here. D-branes were discovered in 1995, marking the beginning what is sometimes called the second superstring revolution. They are extended objects in string theory, on which the endpoints of open strings are confined. One very interesting property is that in the low energy limit the theory on their world-volume is a field theory, usually of Yang-Mills type. It is possible to "engineer" a wide variety of gauge theories using D-branes, and as mentioned before many problems which are hard from the field theory point of view are more tractable when translated to problems in string theory. Not long after the discovery of D-branes, the AdS/CFT correspondence was conjectured. It states that the low energy conformal field theory on the worldvolume of a large number of D3-branes is holographically dual to Type IIB string theory in the near horizon geometry of the D3-branes (it makes similar statements for other kinds of branes, but we will not discuss these cases). One very interesting aspect of this duality is that the strong coupling limit of the field theory corresponds to the supergravity limit of the Type IIB theory, allowing one to get results for a strongly coupled quantum field theory by doing computations in classical supergravity.

The plan of the thesis is as follows. In Chapter 2 we review the basic concepts that we use throughout the next chapters. Then in Chapter 3 we study the duality cascade phenomenon. A duality cascade is a RG flow for an $\mathcal{N} = 1$ supersymmetric gauge theory, in which when a gauge coupling becomes strong one uses Seiberg duality to get a dual theory in which this coupling becomes weaker as the flow proceeds. Then further down the energy scale another coupling becomes strong which requires a new dualization and so on, resulting in a process which deserves the name "duality cascade". In this way we can continue a RG flow beyond the point of strong coupling. The use of Seiberg duality in this manner is motivated from the holographically dual geometry. This is how the first example of a cascade was discovered, deforming the

AdS/CFT pair for the conifold by the addition of fractional branes and matching the supergravity solution with a RG flow for the gauge theory. Subsequently more examples were discovered that lent support to the duality cascade method. In our work we approach the phenomenon from the field theory side. We provide a general formalism for performing a duality cascade on a quiver gauge theory. Then we apply this to examples of gauge theories that can be embedded in string theory. The surprising result is the appearance of a duality wall, i.e. a duality cascade in which the distance on the energy scale between successive dualizations decreases fast enough that the cascade cannot proceed towards the UV beyond a finite energy. Although examples of duality walls had been found before, this was the first example that admitted a string theory realization.

In Chapter 4, we turn our attention to global symmetries in the del Pezzo gauge theories. These are quiver gauge theories that arise on D3-branes placed at the tip of a complex cone over the del Pezzo surfaces. Using topological data of the del Pezzo surfaces and results from AdS/CFT, namely the correspondence between D3-branes wrapped on three-cycles in the base of the cone and dibaryon operators in the gauge theory, we identify the global $U(1)$ charges of all bifundamental fields in these theories using a natural basis provided by the geometry. In this basis the charges turn out to be the Dynkin coefficients of representations of exceptional Lie algebras. This makes it possible to express supepotentials, Higgsing, Seiberg dualities in the Lie algebra language, giving a much more symmetric description of these theories than one would have without use of the geometry. Moreover, it raises the possibility of an enhanced exceptional global symmetry at infinite gauge coupling. Examples of supersymmetric gauge theories featuring enhanced symmetry at infinite coupling have been proposed in three and five dimensions, using string theory setups. The del Pezzo theories provide a plausible case for the existence of such a limit in four dimensions.

Chapters 5 and 6 deal with answering the question: given a background geometry in which D3-branes can be placed, what will be the low energy theory on these branes? Chapter 5 is a follow-up on the discovery of the theories for a certain (infinite) class of geometries, called $Y^{p,q}$. The theories living on the branes for these geometries

are also called $Y^{p,q}$ and are quiver gauge theories. However, Seiberg duality tells us that in fact there is an infinite class of theories (the Seiberg duals) that flow to the same conformal fixed point in the infrared. We use Seiberg duality to construct a subclass of these theories, called the **toric phases** in which all gauge group factors have the same rank. We provide a simple description for these phases in terms of "impurities" on the quiver diagram[3]. We also give a prescription of how to break conformal invariance in the $Y^{p,q}$ theories while preserving supersymmetry.

Finally, in Chapter 6 we find a new infinite family of quiver gauge theories, dubbed $X^{p,q}$, for which the algebraic description of the background geometry is known. This algebraic description is given in terms of toric diagrams, a notion that will be reviewed in Section 2.2.1. The theories are constructed based on the way we expect them to behave after Higgsing. We explain why the geometry predicts that each $X^{p,q}$ theory can be Higgsed to $Y^{p,q}$ or $Y^{p,q-1}$, depending on the field that gets the vacuum expectation value and we use this information to "reverse engineer" the theories. We study aspects of these theories, including toric phases and global symmetries and comment on some of their properties.

[3]The quiver diagram is a graphical representation of a quiver gauge theory. It will be defined in Section 2.1

Chapter 2

A Brief Review of Relevant Concepts

In this chapter review some of the relevant aspects of concepts used frequently in the next chapters. These include Seiberg duality, D-branes and the AdS/CFT correspondence.

2.1 Seiberg duality

Supersymmetric QCD (SQCD) is a $\mathcal{N} = 1$ supersymmetric gauge theory with gauge group $SU(N_c)$, N_f quarks Q in the fundamental ($\mathbf{N_c}$) representation and N_f anti-quarks $\tilde{Q}$ in the antifundamental representation ($\overline{\mathbf{N}}_\mathbf{c}$) of the gauge group. The theory has zero superpotential. For $\frac{3}{2}N_c < N_f < 3N_c$ the theory is aymptotically free and flows to an interacting conformal fixed point in the infrared. This range of values of the number of flavors is called the conformal window. Seiberg [1] conjectured that at that point there is a dual theory with gauge group $SU(N_f - N_c)$, N_f flavors $q, \tilde{q}$, a scalar field M and superpotential

$$W = Mq\tilde{q} \tag{2.1}$$

This theory also flows to an interacting conformal field point in the infrared at which it is physically indistinguishable from the original theory, although the two theories are perturbatively different. Evidence for the validity of the duality include the matching of global symmetries, quantum moduli spaces and chiral rings of the two theories. There is also a map between deformations of the two theories, according to which the operator $\tilde{Q}Q$ is mapped to M in the dual theory. This will be important for us since we will be considering theories with superpotential, which we want to translate in the alphabet of fields of the dual theory.

The theories we study are $\mathcal{N} = 1$ quiver gauge theories. These have a gauge group of the form $SU(N_1) \times SU(N_2) \times \ldots \times SU(N_p)$ with matter fields transforming in bifundamental representations. We use the usual graphical representation for these theories, in which every gauge group factor is represented by a node. A field X_{ij} transforming in the fundanental representation of the ith factor and the antifundamental representation of the jth factor is represented by an arrow starting from node i and ending on node j. The superpotential for such a theory consists of terms of the form $\mathrm{tr}(X_{i_1 i_2} X_{i_2 i_3} \ldots X_{i_r i_1})$, where the trace is taken over the color indices. These theories are believed to flow to superconformal fixed points in the IR when all the beta functions for gauge and superpotential couplings vanish. We will describe this method for finding fixed points in detail in Chapter 3. When such a fixed point exists, it has been shown [2, 3] that one can apply Seiberg duality to any one of the gauge group factors (nodes). What we mean by this is: imagine deforming the theory by turning off all superpotential couplings and all gauge couplings except the one for the node under consideration. One is left with a SQCD theory, on which the duality can be applied. Then one turns on the rest of the couplings, written in terms of the new variables. This is the dual theory.

2.2 D-Branes and gauge theories

D-Branes came to the center of the stage in string theory when it was realized [4] that they are the sources for the antisymmetric form fields appearing in the massless

spectrum of superstring theories. A Dp-brane is an object extending in p dimensions of space and time, so its worldvolume is $p+1$ dimensional. The defining property is that the ends of open strings must end on a D-brane. One is forced to consider D-branes when trying to extend the T-duality of closed strings to the open string sector [5]. Then one encounters Neumann boundary conditions for the endpoints of the open strings, and the hypersurface on which these points are constrained is precisely the D-brane. Far from being only a ficticious hypersurface though, a Dp-brane is a physical object with tension

$$T_p \sim \frac{1}{g_s l_s^{p+1}} \tag{2.2}$$

where g_s is the string coupling and l_s is the length of the string. A D-brane has its own dynamics, which for a single (bosonic) Dp-brane are given by the Born-Infeld action:

$$S = -T_p \int d^{p+1}\sigma e^{-\phi} \sqrt{-\det\left(G_{ij} + B_{ij} + 2\pi\alpha' F_{ij}\right)}. \tag{2.3}$$

Here ϕ is the dilaton, G_{ij} and B_{ij} are the induced metric on the brane and the pullback of the Kalb-Ramond field respectively, and F_{ij} is the field strength of the $U(1)$ gauge field living on the D-brane worldvolume.

D-branes have many very interesting applications in string theory, but the one we will be interested in is the property that at low energies the theory on their worldvolume is a gauge field theory. The simplest possible configuration that gives a non-abelian gauge symmetry is having a stack of N parallel and coincident Dp-branes in flat space. This setup breaks the spacetime Lorentz symmetry $SO(9,1) \to SO(p,1) \times SO(9-p)$ where $SO(p,1)$ is the Lorentz symmetry on the Dp-brane worldvolume and $SO(9-p)$ is the rotational symmetry in the transverse space, where the D-brane is pointlike. The low energy theory is then the dimensional reduction of the ten-dimentional supersymmetric $U(N)$ Yang-Mills theory to $(p+1)$ dimensions [7]. The bosonic part of the action for this theory is

$$S = \frac{1}{4g_{YM}^2} \int d^{p+1}\sigma \mathrm{Tr}\left(-F_{ij}F^{ij} - 2(D_i X^m)^2 + [X^m, X^n]^2\right) \tag{2.4}$$

where i, j index the directions along the D-brane worldvolume and m, n index the transverse coordinates. Here F_{ij} is the $U(N)$ field strength and X^m are fields in the adjoint representation of $U(N)$. The Yang-Mills coupling is related to the D-brane tension:

$$\frac{1}{g_{YM}^2} = T_p l_s^4 \tag{2.5}$$

For the case of D3-branes this is the four-dimensional $\mathcal{N} = 4$ supersymmetric Yang-Mills theory, with a dimensionless coupling $g_{YM}^2 = g_s$.

This theory is very interesting, but we want to engineer theories with less supersymmetry, since these are closer to the real-world particle theories. There are two ways in which this can be done, either by using setups of branes or by placing the branes in curved space, possibly with fluxes. We will be dealing with the second method, in which the space transverse to the branes is curved. In particular, we will be interested in $\mathcal{N} = 1$ supersymmetric gauge theories in four dimensions. These can be constructed by placing parralel D3-branes in ten-dimensional spacetime of the form $\mathbb{R}^{1,3} \times CY_3$ where $\mathbb{R}^{1,3}$ is the four-dimensional Minkowski spacetime spanned by the D3-branes and CY_3 is a Calabi-Yau threefold. A Calabi-Yau manifold CY_n is a n-complex-dimemensional manifold of $SU(n)$ holonomy. This means that a vector transported around a closed loop will be rotated by an element of $SU(n)$. This contrasts with the case of a generic oriented $2n$-real-dimensional Riemannian manifold which has $SO(2n)$ holonomy. Anticipating the discussion of the AdS/CFT correspondence, let us say that that we will be interested in configurations where the Calabi-Yau threefold is a real cone over a compact five dimensional Sasaki-Einstein space X^5. The near horizon limit of this geometry is a space of the form $AdS_5 \times X^5$. The D3-branes are placed at the tip of the cone. The resulting gauge theories on the D-branes are quiver gauge theories, with all matter fields transforming in two-index representations (adjoint or bifundamental) of the gauge group factors. In general, the gauge theory will have $\mathcal{N} = 1$ supersymmetry. A particular subclass of these Calabi-Yau cones includes the ones that also happen to be toric varieties. These admit an algebraic description that makes it easier to identify the gauge theory living on the

D-brane worldvolume and study its properties. We briefly discuss toric geometry in the next subsection, along the lines of [8].

2.2.1 Toric geometry

Toric varieties are a generalization of the complex projective space:

$$\mathbb{CP}^n = \frac{\mathbb{C}^{n+1} - \{\vec{0}\}}{\mathbb{C}^*} \tag{2.6}$$

where the $\mathbb{C}^*$ acts by

$$z_i \to \lambda z_i \ , \ i = 1, \ldots, n+1. \tag{2.7}$$

We can generalize this to a toric variety V as follows:

$$V = \frac{\mathbb{C}^{n+m} - F}{\mathbb{C}^{*m}}. \tag{2.8}$$

F here denotes the set of points that we have to remove for the quotient to be well defined. The action of the m copies of $\mathbb{C}^*$ is now given by

$$(z_1, \ldots, z_{n+m}) \to (\lambda_a^{Q_1^a} z_1, \ldots, \lambda_a^{Q_{n+m}^a} z_{n+m}) \ , \ a = 1, \ldots, m. \tag{2.9}$$

The Q_i^a are integers and can be arranged in a $m \times (m+n)$ matrix. One way to look at this quotient is to use the decomposition $\mathbb{C}^* = \mathbb{R}^+ \times U(1)$. This is called the *symplectic quotient*. One first imposes the m constrains

$$\sum_{i=1}^{n+m} Q_i^a |z_i|^2 = t_a \tag{2.10}$$

where t_a are arbitrary real parameters and then takes the quotient by the $U(1)^m$ action, which is given by (2.9) with $|\lambda_a| = 1$. Putting all $t_a = 0$ yields a cone, with the conical singularity located at $z_i = 0$, $i = 1, \ldots, m+n$.

It is possible to encode a toric variety in a *toric diagram*, which consists of $n+m$

integer vectors v_i in $\mathbb{Z}^{n-1}$ that satisfy the set of relations

$$\sum_{i=1}^{n+m} Q_i^a v_i = 0. \tag{2.11}$$

These relations define the charges Q_i^a which in turn define the quotient giving the toric variety. For a three complex dimensional Calabi-Yau manifold, which is what we will be dealing with, the vectors v_i lie on a plane. We will make use of these toric diagrams in Chapter 6. We will discuss there how we can extract information from these about the gauge theoruy living on the D3-branes at the tip of the Calabi-Yau cone.

2.3 AdS/CFT

The AdS/CFT correspondence [9, 10, 11] is an example of a holographic duality, i.e. the duality between a theory with gravity and one without gravity. The correspondence relates two seemingly different limits of the same physical system: a stack of parallel and coincident D3-branes in Type IIB string theory. The supergravity solution for this system is

$$\begin{aligned} ds^2 &= f^{-1/2}(-dt^2 + dx_1^2 + dx_2^2 + dx_3^2) + f^{1/2}(dr^2 + r^2 d\Omega_5^2) \\ F_5 &= (1+*)dt dx_1 dx_2 dx_3 df^{-1} \ , \ f = 1 + \frac{R^4}{r^4} \ , \ R^4 = 4\pi g_s \alpha'^2 N \end{aligned} \tag{2.12}$$

where the coordinates x_1, x_2, x_3 are along the brane and the second term in the metric is the transverse space written in spherical coordinates. In the near horizon limit, $r << R$, we can drop the 1 in f and the metric becomes that of $AdS_5 \times S^5$, with N units of fiveform flux through the S^5. The radius of curvature of both spaces is R. On the other hand one has at low energies the gauge theory on the branes, which as mentioned before will be the $\mathcal{N} = 4$ super Yang-Mills theory in four dimensions, with gauge group $U(N)$. This theory is exactly conformal, because the large amount of supersymmetry makes the beta functions vanish identically.

In its strongest form, Maldacena's conjecture states that Type IIB string theory on $AdS_5 \times S^5$ with N units of fiveform flux is the same (holographically dual) to $\mathcal{N} = 4$ super Yang-Mills with gauge group $U(N)$. Actually, the $U(1)$ factor of $U(N)$ is just a free vector multiplet corresponding to the center of mass motion of the D-branes, so the AdS theory actually describes the $SU(N)$ part of the gauge theory. The coupling of the gauge theory is related to the radius of curvature through

$$N g_{YM}^2 = \frac{R^4}{\alpha'^2}. \tag{2.13}$$

From (2.13) we see that for small g_s, α' and large R, N such that the t'Hooft coupling $\lambda = N g_{YM}^2$ is large, one gets a duality between a strongly coupled gauge theory and classical supergravity!

The natural objects to consider in a conformal field theory are operators $O(x)$. The correspondence is based on a dictionary that relates operators $O(x)$ in the CFT to fields $\phi(x, r)$ in AdS, or equivalently states of the string theory on AdS. Here r denotes a radial coordinate in AdS space and x denotes the coordinates in four dimensional Minkowski space. The correlation functions of $O(x)$ can be computed from the relation

$$\langle e^{\int \mathrm{d}^4 x \phi_0(x) O(x)} \rangle_{\mathrm{CFT}} = \mathcal{Z}_{\mathrm{string}} \left[\phi(x, r)|_{\partial \mathrm{AdS}} = \phi_0(x) \right] \tag{2.14}$$

where $\phi_0(x)$ is an arbitrary field on the boundary of AdS_5, which is four dimensional Minkowski space and $\mathcal{Z}_{\mathrm{string}}$ is the string partition function with the given boundary condition. One can take derivatives of the left hand side with respect to $\phi_0(x)$ to obtain the correlation functions of $O(x)$, so the correspondence is in principle complete. This relation also determines the conformal dimensions Δ of the operators in terms of the masses m of the dual AdS fields as:

$$\Delta = \frac{d}{2} + \sqrt{\frac{d^2}{4} + m^2 R^2} \tag{2.15}$$

for AdS_{d+1}.

The correspondence can also be generalized to other kinds of branes and backgrounds. The generalization that is of interest to us is placing the D3-branes at the apex of a Calabi-Yau cone CY_3, whose base is a five-dimensional Sasaki-Einstein manifold X_5. The metric on this cone is

$$ds^2_{CY} = dr^2 + r^2 ds^2_{X_5} \tag{2.16}$$

and the near horizon limit of the background gives $AdS_5 \times X_5$ with N units of fiveform flux. The Maldacena conjecture naturally extends to this case [12, 13] and says that Type IIB string theory in this near horizon limit is holographically dual to the IR conformal fixed point of the gauge theory on the D3-branes. A basic difference with D3-branes in flat space is that the gauge theory now is not exactly conformal, but it is conformal at the IR end of its RG flow. It is to this fixed point that the duality applies. In all the examples that have been studied this gauge theory has matter fields in two-index representations only. We will see many examples of such theories in this thesis, since they are our main object of study. One very interesting consequence of this generalization is that it allows us to test and use the operator-state correspondence for states that are not seem in supergravity but are string theory states. These are states describing D3-branes wrapped on non-trivial supersymmetric three-cycles in X_5. The dual operators are the so called dibaryon operators, which are constructed from fully antisymmetrizing the gauge indices of bifundamental fields. The simplest example is

$$\epsilon_{i_1 i_2 \cdots i_N} \epsilon^{j_1 j_2 \cdots j_N} X^{i_1}_{j_1} X^{i_2}_{j_2} \cdots X^{i_N}_{j_N} \tag{2.17}$$

for a bifundamental field charged under two $SU(N)$ factors. The conformal dimension of this operator is N times the conformal dimension of the simple X^i_j field. The dual state is a D3-brane wrapped N times on a supersymmetric three-cycle. For large N, the mass of the state and the conformal dimension of the operator are both large and (2.15) can be approximated by $\Delta \approx mR$. The mass m is in turn proportional to the volume of the cycle that the brane is wrapping, so that one can compute conformal dimensions of fields at a strongly coupled fixed point by calculating the volume of

a three-cycle. This has proven very useful and we will discuss it further and make liberal use of it throughout the following chapters.

Chapter 3

Duality Cascades and Duality Walls

3.1 Introduction

The "Duality Cascade" phenomenon, discovered by Klebanov and Strassler [17], has been one of the most interesting applications of the AdS/CFT correspondence. It is part of the ongoing programme to extend the correspondence to more general, in this case non-conformal, classes of field theories.

The introduction of M fractional D3 branes in addition to N regular ones on the conifold singularity breaks conformal invariance. The authors of [17] studied the resulting field theory which is a four-dimensional $\mathcal{N} = 1$ $SU(N + M) \times SU(N)$ non-conformal gauge theory. They showed that the radial variation of the fiveform flux in the dual near-horizon geometry can be identified with the running of the gauge couplings in the gauge theory. When one of the couplings becomes strong, one can, à la Seiberg, dualize the theory and flow to the IR, to one with gauge group $SU(N - M) \times SU(N)$. To the UV one may follow this RG flow in the field theory *ad infinitum*. This RG flow by means of successive Seiberg dualizations was referred to as a duality cascade [17].

Nice examples of duality cascades from the field theory side have been studied. Notably, in [18] the cascade has been described in terms of properties of the adjacency

matrix of the quiver, which for the examples studied in this work happens to be a Cartan matrix. Then Seiberg duality is a Weyl reflection in the associated root space. The UV behaviour then depends markedly on whether the Cartan matrix is hyperbolic (with a single negative eigenvalue and the rest positive) or not. Indeed for some simple quiver examples (without a known stringy realization), it was shown that the RG flow slows down in the UV and in fact (quite surprisingly) there is a finite accumulation point at which the scale of the dualizations pile up. This raises the interesting possibility of non-trivial UV completions for these field theories. This kind of UV behavior of a duality cascade was originally dubbed "Duality Wall" in [19].

The issue seems to persist as one studies field theories that can be realized on D-branes . As a first example that is chiral and arising from standard string theory constructions, [20] discussed the case of our familiar $\mathbb{C}^3/\mathbb{Z}_3$ singularity. Using naive beta-functions without consideration for the anomalous dimensions, [20] analysed in detail how one encounters duality walls for this string theoretic gauge theory. This is however only a toy example, since the anomalous dimensions of the fields are ignored.

Despite our lack for explicit metrics and supergravity solutions for wider classes of examples, we are in fact well armed from the gauge theory perspective. There are several instances of D3-branes probing conical singularities where the gauge theory on the branes is known. This theory is generally a $\mathcal{N} = 1$ supersymmetric quiver gauge theory, with product gauge group and matter in bifundamental representations. These theories generically flow to an IR conformal fixed point. One can then use Seiberg duality on individual gauge group factors (nodes) to get a dual quiver gauge theory equivalent to the original one. Seiberg duality can be applied succesively on different nodes. An interesting structure emerges from this duality: the *tree structure* of the space of dual theories. As we dualize a node in the quiver at each stage, a new branch is added to the tree. The topology of the tree is of interest. For example, whether there are any closed cycles which would signify that certain dualities may be trapped within a group of theories. To get a duality cascade however, one needs to break conformal invariance. Seiberg duality is then used in a different way. Following the

flow to the UV, the gauge coupling of some nodes becomes large at a finite energy scale. One can formally use Seiberg duality on this node at this point, reversing the sign of the beta function so the the flow can be continued beyond this point. We say "formally" because the theory is not conformal. However, the dual supergravity solution, when available, seems to agree with the gauge theory flow, lending support to using Seiberg duality in this unconventional way.

Dualizations in the tree is precisely the desired cascading procedure. As the theory flows to the UV and successive dualizations are performed, a particular path is traced out on the tree. Of course the computation of the RG flow requires knowledge of the beta-function, including the corrections coming from the anomalous dimensions. The form of the exact beta function has been computed by [21] for $\mathcal{N} = 1$ gauge theories and by [22] for quiver theories in particular. The beta function can be expressed in terms of the anomalous dimensions of the matter fields of the quiver theory, which are in turn proportional to the $U(1)_R$ charges of the fields. The excellent work by [23] provides us with a way to systematically determine the R-symmetry and hence all anomalous dimensions. One only has to maximize a cubic function of the $U(1)$ charges. This computation works only for conformal theories but as we shall see, in the example studied here the symmetries of the quiver constrain the corrections to the anomalous dimensions in such a way that they can be ignored in a first approximation.

The structure of this chapter is as follows. We will first require three ingredients the combination of which will form the crux of our calculation. The first piece we need is four dimensional $\mathcal{N} = 1$ super conformal field theory (SCFT), especially quiver theories. In particular we remind the reader of the computations of anomalous dimensions in the beta function. This will be the subject of Section 3.2. The second piece we need is the so-called "duality tree" which arises from iterative Seiberg-like dualisations of quiver theories. This, with concrete examples from the zeroth del Pezzo, will constitute Section 3.3. The final piece we need is to recall the rudiments of the Klebanov-Strassler cascade for the quiver theory associated to the conifold. We do this in Section 3.4.

Thus equipped, we examine a simple but illustrative gauge theory in Section

3.5. This is a fairly well-studied quiver theory arising from D3-branes probing the singular complex cone over the zeroth Hirzebruch surface. The duality tree for the conformal phases of the theory form a flower. With the appropriate addition of fractional branes to take us away from conformality, we compute the beta function running in Section 3.5.2, by determining, using the abovementioned maximization principle, all anomalous dimensions. We will find in Section 3.5.3 that there is indeed a duality wall, i.e. an energy scale beyond which dualities cannot proceed.

3.2 Computing anomalous dimensions in a SCFT

We devote this section to a summary of beta-functions in 4D $\mathcal{N} = 1$ SCFT and of how to compute in particular the anomalous dimensions. The remainder of the chapter will make extensive use of the values of these anomalous dimensions.

The necessary and sufficient conditions for a $\mathcal{N} = 1$ supersymmetric gauge theory with superpotential to be conformally invariant, are (1) the vanishing of the beta function for each gauge coupling and (2) the requirement that the couplings in the superpotential be dimensionless. Both these conditions impose constraints on the anomalous dimensions of the matter fields, that is, chiral operators of the theory. This is because supersymmetry relates the gauge coupling beta functions to the anomalous dimensions of the matter fields due to the form of the NSVZ beta functions [21, 22].

The examples which we study in this chapter are a class of SUSY gauge theories known as quiver theories. These have product gauge groups of the form $\prod_i SU(N_{c_i})$ together with N_{f_i} bifundamental matter fields for the i-th gauge factor. There is also a polynomial superpotential. Such theories can be conveniently encoded by quiver diagrams where nodes are gauge factors and arrows are bifundamentals. The SCFT conditions for these quiver theories can be written as:

$$\begin{aligned} \beta_i \sim 3N_{c_i} - N_{f_i} + \frac{1}{2}\sum_j \gamma_j = 0 \\ -d(h) + \frac{1}{2}\sum_k \gamma_k = 0 \end{aligned} \tag{3.1}$$

where β_i is the beta-function for the i-th gauge factor, and γ_j, the anomalous dimensions. The index j labels the fields charged under the j-th gauge group factor while k indexes the fields appearing in the k-th term of the superpotential with coupling h, whose naive mass dimension is $d(h)$.

These conditions (3.1) constitute a linear system of equations. However they do not always uniquely determine the anomalous dimensions because there will be more variables than constraints. One or more of the γ's are left as free parameters. Intriligator and Wecht [23] provided a general method for fixing this freedom in aribitrary 4D SCFT, whereby completely specifying the anomalous dimensions. They showed that the R-charges of the matter fields, which in an SCFT are related to the γ's, are those that (locally) maximize the central charge a of the theory. The central charge a is given in terms of the R-charges by

$$a = \frac{3}{32}(3\,\mathrm{Tr}\,R^3 - \mathrm{Tr}\,R)\ , \tag{3.2}$$

where the trace is taken over the fermionic components of the vector and chiral multiplets.

In a quiver theory with gauge group $\prod_i SU(N_i)$ and chiral bifundamental multiplets with multiplicities f_{ij} between the i-th and j-th gauge factors (the matrix f_{ij} is the adjacency matrix of the quiver), we can give an explicit expression for (3.2) in terms of the R-charges R_{ij} of the lowest components of the bifundamentals

$$a = \frac{3}{32}\left[2\sum_i N_i^2 + \sum_{i<j} f_{ij}N_iN_j\left[3(R_{ij}-1)^3 - (R_{ij}-1)\right]\right]\ . \tag{3.3}$$

Parenthetically, we remark that in some cases, such as the ones to be discussed in Section 3.4 and Section 3.5, anomalous dimensions can be fixed by using some discrete symmetries of the quiver and the superpotential, without the need to appeal to the systematic maximization of a.

Now in (3.3) we need to know the R-charges. However, in a SCFT the conformal dimension D of a chiral operator is related to its R-charge by $D = \frac{3}{2}|R|$. Moreover,

for bifundamental matter the relation between D and γ is $D = 1 + \frac{\gamma}{2}$. Therefore we can write the R-charges and hence (3.3) in terms of the anomalous dimensions by

$$\frac{3}{2}|R| = 1 + \frac{\gamma}{2} \, . \tag{3.4}$$

Therefore, after solving the conformality constraints (3.1) we can write a in terms of the still unspecified γ's by (3.3) and then maximize it in order to completely determine all the anomalous dimensions.

The freedom in the anomalous dimensions after using the SCFT conditions reflects the presence of non-anomalous $U(1)$ flavor symmetries in the IR theory. Initially, there is one $U(1)$ flavor symmetry for each arrow of the quiver. All the matter fields lying on an arrow have the same charge under this $U(1)$. Now we must impose the anomaly free condition for each node, this is the condition that for the adjacency matrix f_{ij} at the i-th node we have

$$\sum_j f_{ij} N_j = \sum_j f_{ji} N_j \, . \tag{3.5}$$

In other words, the ranks of the gauge groups, as a vector, must lie in the integer nullspace of the antisymmetrized adjacency matrix:

$$(f - f^T)_{ij} \cdot \vec{N} = 0 \, . \tag{3.6}$$

After imposing this condition (3.6), we are left with (# of arrows - # of nodes) non-anomalous $U(1)$'s. The invariance of the superpotential reduces their number even more, giving one linear relation between their charges for each of its terms. But the number of independent such relations is not always sufficient to eliminate all the abelian flavor symmetries. The charges of those that still remain in the IR can indeed be read off from the expressions for the anomalous dimensions of the fields in terms of those that remain free after imposing the conditions (3.1).

The way in which the charge matrix of the remaining $U(1)$ flavor symmetries appears in this framework is as the matrix of coefficients that express the anomalous

dimensions of the bifundamental fields as linear combinations of numerical constants and some set of independent anomalous dimensions. Specifically, suppose we start with n anomalous dimensions and that the solution to (3.1) specifies k of them in terms of the other $n-k$:

$$\gamma_i = \gamma_{0_i} + q_{ij}\gamma_j \quad , \quad i = 1, \ldots, k \quad , \quad j = k+1, \ldots, n. \tag{3.7}$$

The corresponding R-charges are related to the γ's by $R = \frac{\gamma+2}{3}$. The charges of the matter fields under these residual $U(1)$'s from are given by the q_{ij} matrix in (3.7). The constants γ_{0_i} are mapped to the test values of R charges. It is important to keep in mind that it is possible to change the basis of $U(1)$'s (correspondingly the set of independent anomalous dimensions), in which case the charge matrix would be modified.

3.3 Duality structure of SUSY gauge theories: Duality trees

Having reviewed the methodology of computing anomalous dimensions, we turn to the next ingredient, the duality trees which arise from Seiberg-like dualities performed on the quivers. An interesting way to encode dual gauge theories and their relations is by using *duality trees*. This construction was introduced in [24], for the specific case of D3-branes probing a complex cone over dP_0, the zeroth del Pezzo surface.

In general, for a quiver theory with adjacency matrix f_{ij} and n gauge group factors, there are n different choices of nodes on which to perform Seiberg duality. In other words, we can dualize any of the n nodes of the quiver to obtain a new one, for which we again have n choices for dualisation. We recall that dualisation on node i_0 proceeds as follows. Define I_{in} := nodes having arrows going into i_0, I_{out} := those having arrow coming from i_0 and I_{no} := those unconnected with i_0.

1. Change the rank of the node i_0 from N_c to $N_f - N_c$ with $N_f = \sum_{i \in I_{in}} f_{i,i_0} N_i =$

$\sum_{i \in I_{out}} f_{i_0,i} N_i$;

2. $f_{ij}^{dual} = f_{ji}$ if either $i, j = i_0$;

3. Only arrows linking I_{in} to I_{out} will be changed and all others remain unaffected;

4. $f_{AB}^{dual} = f_{AB} - f_{i_0 A} f_{B i_0}$ for $A \in I_{out}, \quad B \in I_{in}$;
   If this quantity is negative, we simply take it to mean an arrow going from B to A. This step is simply the addition of the Seiberg dual mesons (as a mass deformation if necessary).

We remark that the fourth of these dualisation rules accounts for the antisymmetric part of the intersection matrix, which does not encode bi-directional arrows. Such subtle cases arise when there are no cubic superpotentials needed to give masses to the fields associated with the bi-directional arrows. This will not be an issue for the theories studied in this paper.

The subsequent data structure is that of a tree, where each site represents a gauge theory, with n branches emanating from it, connecting it to its dual theories. This is called a "duality tree". We will see along the chapter that duality trees exhibit an extremely rich structure, with completely distinct topologies for the branches for gauge theories coming from different geometries.

As an introduction, let us recall the simple example considered in [24]. The probed geometry in this case was a complex cone over dP_0. This cone is simply the non-compact $\mathbb{C}^3/\mathbb{Z}_3$ orbifold singularity. The generic quiver for any one in the tree of Seiberg dual theories for this geometry will have the form as given in Figure 3-1. The superpotential is cubic because there are only cubic gauge invariant operators in this theory, given by closed loops in the quiver diagram.

Since there are three gauge group factors, there will be three branches coming out from each site in the duality tree. The tree is presented in Figure 3-2. For clarity we color-coded the tree so that sites of the same colour correspond to equivalent theories, i.e., theories related to one another by some permutation of the gauge groups and/or charge conjugation of all fields in the quiver (in other words theories whose quivers

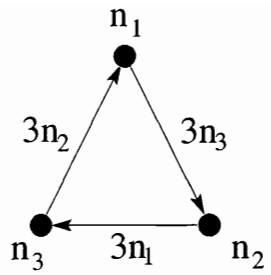

Figure 3-1: Generic quiver for any of the Seiberg dual theories in the duality tree corresponding to a D3-brane probing $\mathbb{C}^3/\mathbb{Z}_3$, the complex cone over dP_0.

are permutations and/or transpositions of each other). We have also included, the quivers to which the various coloured sites correspond in Figure 3-3.

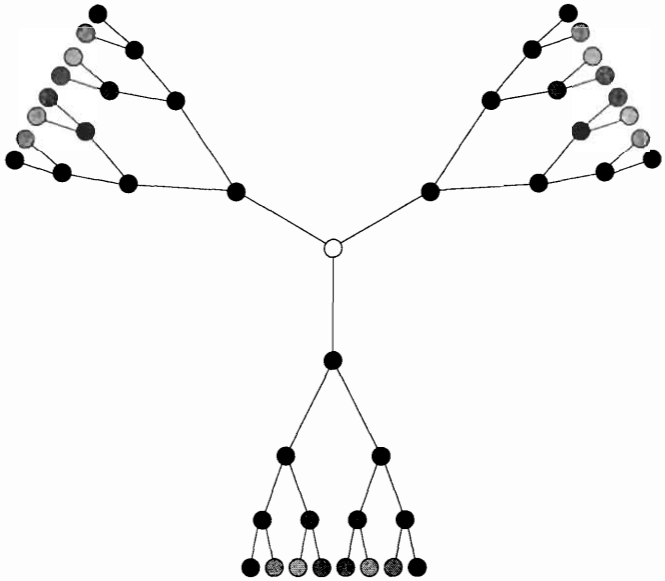

Figure 3-2: Tree of Seiberg dual theories for dP_0. Each site of the tree represents a gauge theory, and the branches between sites indicate how different theories are related by Seiberg duality transformations.

One important invariant associated to an algebraic singularity is the trace of the total monodromy matrix around the singular point. This can typically be recast into an associated Diophantine equation in the intersection numbers, i.e. the f_{ij}'s [25, 26, 27]. This equation captures all the theories that can be obtained by Seiberg duality and hence classifies the sites in the tree.

From Figure 3-1, we see that there exists a simple relation between the intersection numbers and the ranks of the gauge groups for dP_0, namely for rank (n_1, n_2, n_3), the

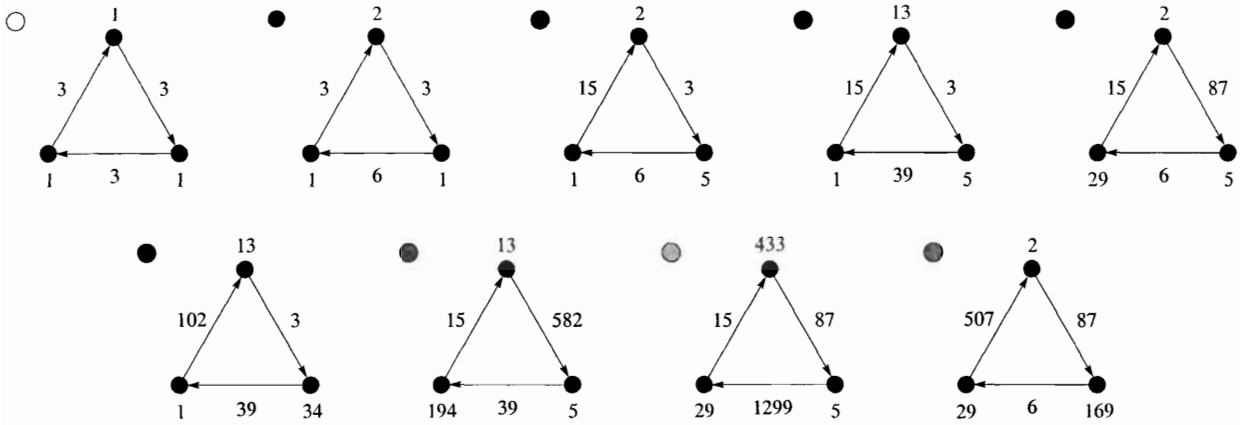

Figure 3-3: Some first cases of the Seiberg dual phases in the duality duality tree for the theory corresponding to a D3-brane probing $\mathbb{C}^3/\mathbb{Z}_3$, the complex cone over dP_0.

intersection matrix is given by $3\begin{pmatrix} 0 & n_1 & -n_3 \\ -n_1 & 0 & n_2 \\ n_3 & -n_2 & 0 \end{pmatrix}$. The Diophantine equation in terms of the ranks reads

$$n_1^2 + n_2^2 + n_3^2 - 3n_1n_2n_3 = 0 \ . \tag{3.8}$$

This turns out to be the well-studied Markov equation.

It is important to stress that, up to this point, duality trees do not provide any information regarding RG flows. In fact, if the theories under study are conformal the trees just represent the set of dual gauge theories and how they are interconnected by Seiberg duality transformations within the conformal window. We will extend our discussion about this point in Section 3.4 and Section 3.5, where we will obtain non-conformal theories by the inclusion of fractional branes.

3.4 The conifold cascade

A famous example of successive Seiberg dualisations is the Klebanov-Strassler cascade in gauge theory [17] associated to the warped deformed conifold. In light of the duality tree structure in the previous section, we now present the third and last piece of preparatory work and summarize some key features of this example, in order to illustrate the concept of duality cascade, as well as to introduce the methods and approximations that will be used later.

Let us begin by considering the gauge theory that appears on a stack of N D3-branes probing the conifold. This theory has an $SU(N) \times SU(N)$ gauge symmetry. The matter content consists of four bifundamental chiral multiplets $A_{1,2}$ and $B_{1,2}$ and the quiver diagram is shown in Figure 3-4. This model has also interactions given by

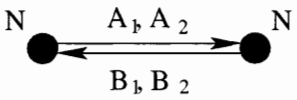

Figure 3-4: Quiver diagram for the gauge theory on N D3-branes probing the conifold.

the following quartic superpotential

$$W = \frac{\lambda}{2}\epsilon^{ij}\epsilon^{kl}\,\mathrm{Tr}\,A_i B_k A_j B_l \tag{3.9}$$

for some coupling λ, and where we trace over color indices.

This gauge theory is self dual under Seiberg duality transformations, by applying the duality rules in Section 3.3. Accordingly, its "duality tree" is the simplest one, consisting of a single point representing the $SU(N) \times SU(N)$ theory, which transforms into itself when dualizing either of its two gauge groups. This is shown in Figure 3-5.

Figure 3-5: The "duality tree" of the conifold. Its single site represents the standard $SU(N) \times SU(N)$ theory. The closed link coming out the site and returning to it represents the fact that the theory, being self-dual, transforms into itself under Seiberg duality.

We will see below that when we apply the procedure for finding anomalous dimensions outlined in Section 3.3 to this specific case, taking into account its symmetries, we conclude that all the anomalous dimensions are in fact equal to $-1/2$ and that the theory is conformal, i.e. both the gauge and superpotential couplings have vanishing beta functions and (3.1) are satisfied. In order to induce a non-trivial RG

flow the theory has to be deformed. One way of doing this is by the inclusion of fractional branes [17]. It is straightforward to see what kind of fractional branes can be introduced.

In general, introducing fractional branes is done by determining, for a given quiver, the most general gauge groups consistent with anomaly cancellation. Now recall from (3.6), possible ranks of the gauge factors must reside in the integer nullspace of the intersection matrix. Therefore a basis for probe and fractional branes is simply given by a basis for this nullspace. For the conifold, we find that the most general gauge group is $SU(N+M) \times SU(N)$. We will refer to N as the number of probe branes and to M as the number of fractional branes.

We see that indeed, for any non-vanishing M, there is no possible choice of anomalous dimensions satisfying (3.1) and thus we are indeed moving away from the conformal point. This case has been widely studied (see [17, 28, 29] and references therein) and leads to a *duality cascade*. What this means is that at every step in the dualisation procedure of this now non-conformal quiver theory, one of the gauge couplings is UV free while the other one is IR free. As we follow the RG flow to the IR, we reach a scale at which the inverse coupling of the UV free gauge factor vanishes. At this point, one has to switch to a more suitable description of the physics, in terms of different microscopic degrees of freedom, by performing a Seiberg duality transformation on the strongly coupled gauge group. This procedure generates the duality cascade when iterated. Indeed, the tree of Figure 3-5 can be interpreted as representing a duality cascade resulting from the addition of fractional branes.

3.4.1 Moving away from the conformal point

Let us now study this cascade in detail, setting the framework we will later use to analyze cascades for general quiver theories. Recall, from (3.1), that a key ingredient required for the computation of the beta functions are the values of the anomalous dimensions. We have already provided a method to compute anomalous dimensions in the absence of fractional branes, that is, in a conformal theory, in Section 3.2. There is no analogue for such a procedure when the theory is taken away from con-

formality. However it is possible to work in a limit such that their values are under control and the beta functions that govern the RG flow can be computed to some approximation. Since M/N measures the departure from conformal invariance, any anomalous dimension will be of the generic form

$$\gamma = \gamma_c + O(M/N) \ , \tag{3.10}$$

where γ_c is its value for the conformal case of $M = 0$. Now, this theory is symmetric under the transformation

$$\begin{aligned} M &\to -M \\ N &\to N + M \ , \end{aligned} \tag{3.11}$$

which, in the limit $N/M \ll 1$ (i.e., we are taking a standard large N limit), simplifies to

$$\begin{aligned} M &\to -M \\ N &\to N \ . \end{aligned} \tag{3.12}$$

This indicates that, in fact, at large N, γ must be an even function in M/N and so the expansion (3.10) has to start from the second order [17]:

$$\gamma = \gamma_c + O(M/N)^2 \ . \tag{3.13}$$

The expression (3.13) is of great aid to us as it gives us the control over the anomalous dimensions we were pursuing. Inspecting (3.1), we see that because the departure of the γ's from their conformal values is of order $(M/N)^2$ at large N, the order (M/N) contributions to the beta functions can be computed simply by substituting the anomalous dimensions calculated at the conformal point into (3.1), and using the gauge groups with the M corrections.

Let us be concrete and proceed to compute the cascade for this example. First let

us consider the anomalous dimensions at the conformal point where $M = 0$. They are the result of requiring the beta functions for both $SU(N)$ gauge groups and for the single independent coupling in the superpotential to vanish in accordance with (3.1). In this case, these three conditions coincide and are reduced to

$$\gamma_{c,A} + \gamma_{c,B} = -1 \ , \tag{3.14}$$

where $\gamma_{c,A}$ (resp. $\gamma_{c,B}$) is the critical value for the anomalous dimension for field A (resp. B). Once we take into account the symmetry condition $\gamma_{c,A} = \gamma_{c,B}$, we finally obtain

$$\gamma_c = -1/2 \ . \tag{3.15}$$

Now let us consider the beta functions for the gauge couplings in the non-conformal case of $M \neq 0$. They are

$$\begin{aligned} SU(N+M): &\qquad \beta_{g_1} = N(1+\gamma_A+\gamma_B) + 3M \\ SU(N): &\qquad \beta_{g_2} = N(1+\gamma_A+\gamma_B) + (-2+\gamma_A+\gamma_B)M. \end{aligned} \tag{3.16}$$

Note that there is no solution to the vanishing of these beta functions for $M \neq 0$. Replacing the anomalous dimensions at the conformal point $\gamma_c = -1/2$ into (3.16) we obtain the leading contribution to the beta functions

$$\begin{aligned} SU(N+M): &\qquad \beta_{g_1} = +3M \\ SU(N): &\qquad \beta_{g_2} = -3M \ . \end{aligned} \tag{3.17}$$

Since the theory at any point in the cascade is given by the quiver in Figure 3-4 with gauge group replaced by $SU(N+(n+1)M) \times SU(N+nM)$ for some $n \in \mathbb{Z}$ (where the role of the two gauge groups is permuted at every step), we see that the gauge couplings run as shown in Figure 3-6, where the beta function for each gauge group changes from $\pm 3M$ to $\mp 3M$ with each dualization. In Figure 3-6 we use he standard notation to which we adhere throughout the chapter: the squared inverse couplings are denoted as $x_i = 1/g_i^2$ and the logarithm of the scale is $t = \log \mu$.

An important feature of this RG flow is that the separation between successive dualizations in the t axis remains *constant* along the entire cascade. We will see in Section 3.5.3 how the gauge theory for a D3-brane probing more general geometries, such as a complex cone over the Zeroth Hirzebruch surface, can exhibit a dramatically different behavior.

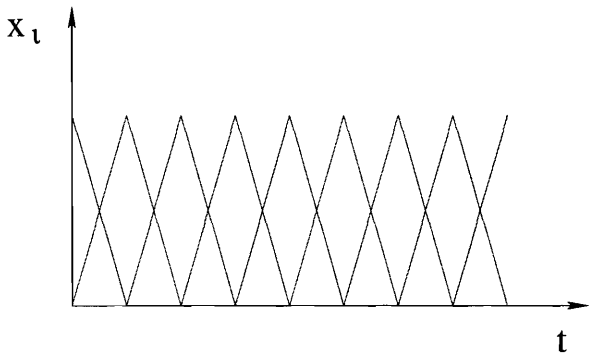

Figure 3-6: Running of the inverse square gauge couplings $x_i = \frac{1}{g_i^2}$, i=1,2. against the log of energy scale $t = \log \mu$, for the conifold. The distance between consecutive dualizations is constant and the ranks of the gauge groups grow linearly with the step in the cascade.

3.5 Phases of F_0

We are now well-equipped with techniques of computing anomalous dimensions, of duality trees and duality cascades. Let us now initiate the study of some more complicated gauge theories. Our first example will be the D-brane probe theory on a complex cone over the zeroth Hirzebruch surface F_0, which is itself simply $\mathbb{P}^1 \times \mathbb{P}^1$.

There are some reasons motivating the choice of this theory. The first is its relative simplicity. The second is that its Seiberg dual phases generically have multiplicities of bifundamental fields greater than 2, whereby providing some interesting properties. Indeed, from the general analysis of [18, 20], a qualitative change in a RG flow towards the UV behavior is expected when such a multiplicity is exceeded. Finally, as we will discuss later, this theory admits the addition of fractional branes. The presence of fractional branes makes the theory non-conformal, driving a non-trivial RG flow. All together, this theory is a promising candidate for a rich RG cascade structure.

The duality tree in this case is shown in Figure 3-7. We have drawn sites that correspond to different theories with different colours; the colour-coded theories are summarized in Figure 3-8. Since the quiver has four gauge groups, there are four possible ways of performing Seiberg duality and thus there are four branches coming out from each node of the tree. The numbers on each branch corresponds to the node which was dualised. A novel point that was not present in the tree for dP_0 is the existence of closed loops.

The possible existence of RG flows corresponding to these closed loops is constrained by the requirement that the number of degrees of freedom increases towards the UV, in accordance to the c-conjecture/theorem. As it was stressed for the dP_0 and the conifold examples, the duality tree for F_0 merely represents the infinite set of conformal theories which are Seiberg duals. Non-vanishing beta functions and the subsequent RG flow are generated when fractional branes are included in the system.

3.5.1 F_0 RG flows

In this section we will follow the RG flow towards the UV of the theory living on D3-branes probing F_0, with the addition of fractional branes to obtain a non-conformal theory. As in the conifold example, the possible anomaly free probe and fractional branes are determined by finding the integer null space of the intersection matrix that defines the quiver (3.6). This can be done for any of the dual quivers that appear in the duality tree, but the natural choice is the simplest of the F_0 quivers as was done in [27] which is shown in Figure 3-8 as the first one (blue dot). The intersection matrix for this quiver is given by

$$A_{ij} = \begin{pmatrix} 0 & 2 & 0 & 0 \\ 0 & 0 & 2 & 0 \\ 0 & 0 & 0 & 2 \\ 2 & 0 & 0 & 0 \end{pmatrix} \Rightarrow f_{ij} = \begin{pmatrix} 0 & 2 & 0 & -2 \\ -2 & 0 & 2 & 0 \\ 0 & -2 & 0 & 2 \\ 2 & 0 & -2 & 0 \end{pmatrix} . \tag{3.18}$$

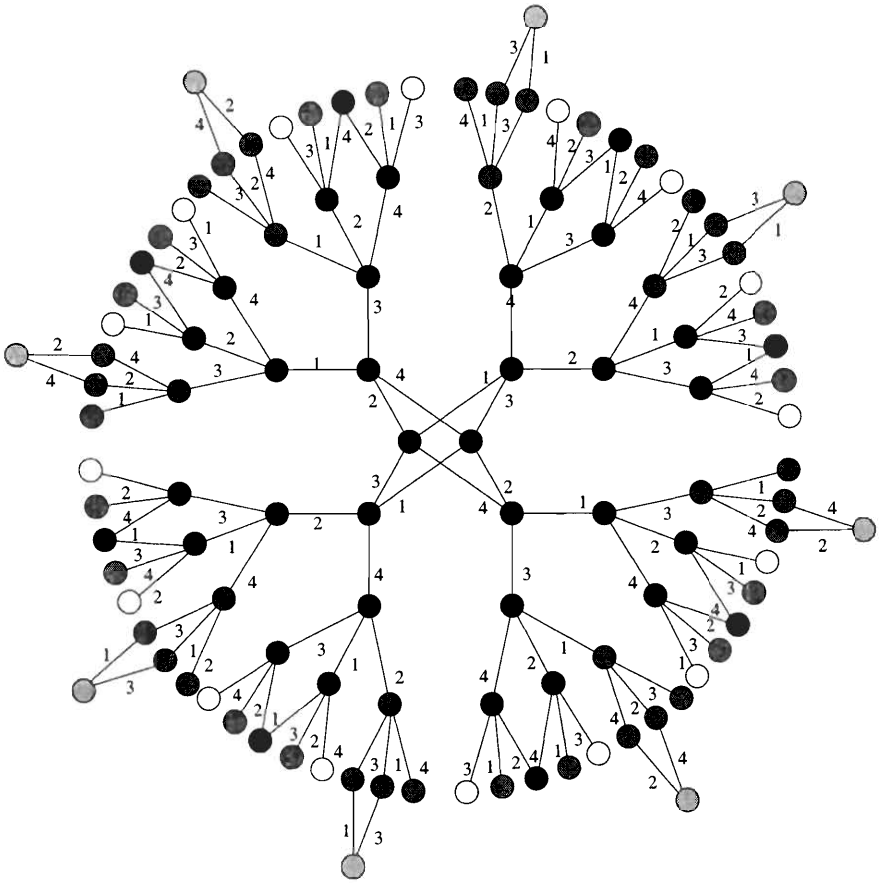

Figure 3-7: The "duality tree" of Seiberg dual theories for F_0.

A suitable basis for the nullspace of (3.18) is $v_1 = (1,1,1,1)$ and $v_2 = (0,1,0,1)$. Therefore, the most generic ranks for the nodes in the quiver, consistent with anomaly cancellation, are

$$(n_1, n_2, n_3, n_4) = N(1,1,1,1) + M(0,1,0,1) \ . \tag{3.19}$$

Following the discussion in Section 3.4, we will refer to N as the number of probe branes and M as the number of fractional branes. The theory is then conformal for $M = 0$ and non-conformal otherwise. For $M \neq 0$, there will exist an RG cascade. The specific path to the UV is determined by the initial conditions of the flow, namely the gauge couplings at a given scale Λ_0. As we will see, very different qualitative behaviours can be obtained, depending on these initial conditions.

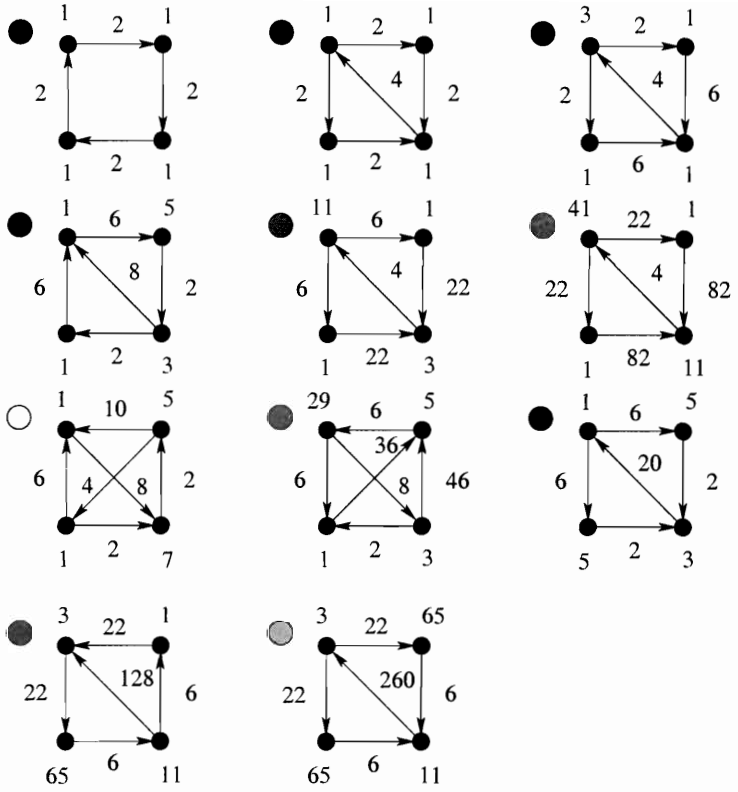

Figure 3-8: Some Seiberg dual phases for F_0.

A crucial step in solving the conifold cascade was the identification of a symmetry that provided us with control over the anomalous dimensions in the $M/N \ll 1$ limit. It is possible to find an analogous symmetry for F_0. Examining (3.19) we see that this theory is invariant under

$$\begin{aligned} M &\to -M \\ N &\to N + M \ . \end{aligned} \tag{3.20}$$

In the limit $M/N \ll 1$, this symmetry transformation becomes

$$\begin{aligned} M &\to -M \\ N &\to N \ . \end{aligned} \tag{3.21}$$

Up to now, we have only considered a single theory (the first quiver in Figure 3-8)

and showed that for $M/N \ll 1$ it is symmetric under (3.22). But the whole tree of Seiberg dual theories can be constructed using this model as the starting point. Since the transformations in (3.22) map the initial theory onto itself, the models derived from it by Seiberg duality are also invariant. Therefore, (3.22) constitute a symmetry of the entire tree.

In analogy to the conifold case this symmetry implies that, for all the dual theories, the odd order terms in the M/N expansion of the anomalous dimensions of all their bifundamental fields vanish and thus

$$\gamma = \gamma_c + O(M/N)^2 \ . \tag{3.22}$$

This means that the leading, $O(M/N)$, non-zero contribution to the beta functions can be computed using the anomalous dimensions calculated at the conformal point. Schematically,

$$\beta(\gamma) = \beta(\gamma_c) + O(M/N)^2 \tag{3.23}$$

for all the beta functions.

The procedure outlined in Section 3.2 can thus be applied to determine the conformal anomalous dimensions, which then can be used to work out the beta functions in the limit $M/N \ll 1$ and study the running of the gauge couplings as we flow to the UV. Let us do so in detail. The beta-functions in (3.1), for a quiver theory with k gauge group factors, ranks $\{n\}_i$, adjacency matrix A_{ij} and loops indexed by h corresponding to gauge invariant operators that appear in the superpotential, now becomes

$$\begin{aligned} \beta_{i\in\text{nodes}} &= 3n_i - \frac{1}{2}\sum_{j=1}^{k}(A_{ij}+A_{ji})n_j + \frac{1}{2}\sum_{j=1}^{k}(A_{ij}\gamma_{ij}+A_{ji}\gamma_{ji})n_j \\ \beta_{h\in\text{loops}} &= -d(h) + \frac{1}{2}\sum_{h}\gamma_{h_i h_j} \ , \end{aligned} \tag{3.24}$$

where in the second expression $\beta_{h\in\text{loops}}$ associated with the terms in the superpotential the index in the sum over $\gamma_{h_i h_j}$ means consecutive arrows in a loop and $d(h)$

is determined by 3 minus the number of fields in the loop.

We will make liberal use of (3.24) throughout. For our example for the first phase of F_0, the ranks $(n_1, n_2, n_3, n_4) = (1, 1, 1, 1)$, together with intersection matrix from (3.18), (3.24) reads

$$\begin{aligned} 1 \ + \ & \gamma_{1,2} + \gamma_{4,1} = 0, \ \ 1 + \gamma_{1,2} + \gamma_{2,3} = 0, \ \ 1 + \gamma_{2,3} + \gamma_{3,4} = 0, \\ 1 \ + \ & \gamma_{3,4} + \gamma_{4,1} = 0, \ \ 1 + \frac{1}{2}(\gamma_{1,2} + \gamma_{2,3} + \gamma_{3,4} + \gamma_{4,1}) = 0 \ , \end{aligned} \tag{3.25}$$

which admits the solution

$$\{\gamma_{1,2} \to -1 - \gamma_{4,1}, \quad \gamma_{2,3} \to \gamma_{4,1}, \quad \gamma_{3,4} \to -1 - \gamma_{4,1}\} \ . \tag{3.26}$$

We see that there is one undetermined γ. To fix this we appeal to the maximization method presented in Section 3.2. The central charge (3.3) now takes the form (where $\gamma_{4,5}$ is understood to mean $\gamma_{4,1}$.

$$a = \frac{3}{4} + \frac{1}{16}\sum_{i=1}^{4}\left(1 + \frac{(-1+\gamma_{i,i+1})^3}{3} - \gamma_{i,i+1}\right) \ . \tag{3.27}$$

Upon substituting (3.26) into (3.27), we obtain

$$a(\gamma_{4,1}) = -\frac{3}{8}(-2 + \gamma_{4,1} + \gamma_{4,1}^2) \ , \tag{3.28}$$

the maximum of which occurs at $\gamma_{4,1} = -\frac{1}{2}$. And so we have in all, upon using (3.26),

$$\gamma_{1,2} = \gamma_{2,3} = \gamma_{3,4} = \gamma_{4,1} = -1/2 \ . \tag{3.29}$$

Let us remark, before closing this section, that there is an alternative, though perhaps less systematic, procedure to determine anomalous dimensions that does not rely on the maximization of a. For every theory in the F_0 cascade the space of solutions to (3.25) is one dimensional. Fixing this freedom at any given point determines the anomalous dimensions in the entire duality tree. Maximization of the

central charge a is a possible way of determining this free parameter. For F_0, a simple alternative is to make use of the symmetries of the theory (quiver and superpotential). Our theory (3.18) for example, instantly has all γ's equal by the $\mathbb{Z}_4$ symmetry of the quiver. Therefore, in conjunction with the solutions (3.26) to conformality, gives (3.29) as desired. Once the anomalous dimensions of theory (3.18) are determined, the freedom that existed in the conformal solutions of all the dual theories is fixed. This is done by matching the scaling dimensions of composite Seiberg mesons every time a Seiberg duality is performed and by noting that the anomalous dimensions of fields that are neutral under the dualized gauge group are unchanged.

3.5.2 Closed cycles in the tree and cascades

Now we wish to find the analogue of the conifold cascade in Section 3.4 here. For this we wish to look for "closed cycles" in the duality tree (Figure 3-7). In the conifold case the theory was self dual and we cascaded by adding appropriate fractional branes. Here we do indeed see a simple cycle involving two sites. We will call these two theories models A and B respectively and draw them in Figure 3-9. Model A is the example we addressed above.

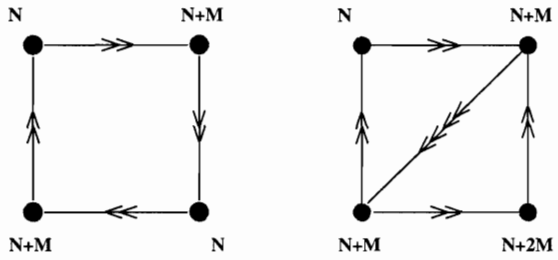

Figure 3-9: Quivers for Models A and B. Model A corresponds to the choice of ranks $(n_1, n_2, n_3, n_4)_A = N(1,1,1,1) + M(0,1,0,1)$, from which model B is obtained by dualizing node 3. It has ranks $(n_1, n_2, n_3, n_4)_B = N(1,1,1,1) + M(0,1,2,1)$.

The starting point will be model A, its superpotential and the set of gauge couplings at a scale Λ_0. We recall from (3.29) that the anomalous dimensions at the conformal point are $\gamma_{1,2} = \gamma_{2,3} = \gamma_{3,4} = \gamma_{4,1} = -1/2$. This leads to the following

values for the beta functions for the 4 gauge group factors:

$$\begin{aligned} \beta_1 &= -3M & \beta_2 &= 3M \\ \beta_3 &= -3M & \beta_4 &= 3M \ . \end{aligned} \tag{3.30}$$

These beta-functions are constants, which means that the running of x_i, the inverse squared couplings as a function of the log scale is linear, with slopes given by (3.30). Let us thus run x_i to the UV accordingly. We see that β_1 and β_3 are negative so at some point the inverse couplings for the first or the third node will reach 0. Which of them does so first depends on the value of the initial inverse couplings we choose for n_1 and n_3. We dualise the node for which the inverse coupling first reaches 0, say node 3. This will give us Model B. If instead node 1 has the inverse coupling going to 0 first, we would dualise on 1 and obtain a theory that is equivalent to Model B after a reflection of the quiver (we can see this from Figure 3-7).

Next we compute the anomalous dimensions for Model B at the conformal point. In analogy to (3.25) and (3.27) we now obtain $\gamma_{1,2} = \gamma_{3,2} = \gamma_{4,3} = \gamma_{4,1} = -1/2$ and $\gamma_{2,4} = 1$, which gives the beta functions for the next step:

$$\begin{aligned} \beta_1 &= -3M & \beta_2 &= 0 \\ \beta_3 &= 3M & \beta_4 &= 0 \ . \end{aligned} \tag{3.31}$$

From these we run the couplings at this stage again, find the node for which the inverse coupling first goes to 0. And dualise that node. We see a remarkable feature in (3.31). To the level of approximation that we are using, only the first gauge group factor has a negative beta function. This implies that the next node to be dualized is precisely node 1. Performing Seiberg duality thereupon takes us to a quiver that is exactly of the form of Model A, only with the ranks differing in contributions proportional to M, i.e., different fractional brane charges

By iterating this procedure it is possible to see that the entire cascade corresponds to a chain that alternates between type A and type B models. Furthermore, the length of the even steps of the cascade, measured on the $t = \log \mu$ axis is constant.

The same statement applies to the length of the odd steps. This cascade is presented in Figure 3-10 for the initial conditions $(x_1, x_2, x_3, x_4) = (2, 1, 1, 0)$.

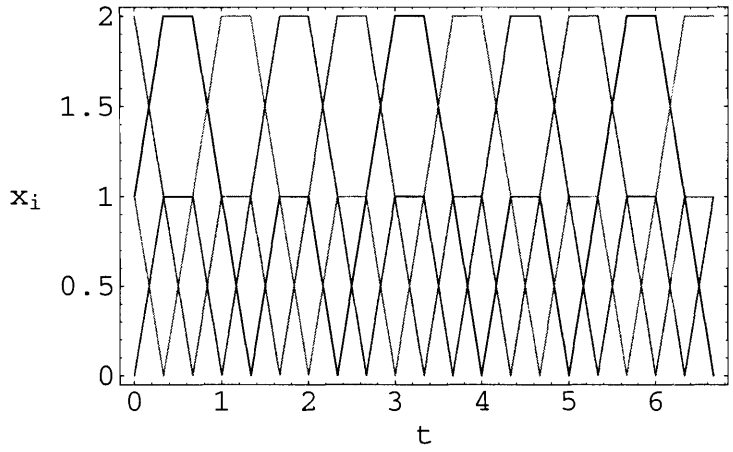

Figure 3-10: Duality cascade alternating between the A and B toric models.

3.5.3 Duality wall

We have seen in Section 3.5.2 that models A and B form a closed cascade and are not connected to the other theories in the F_0 duality tree by the RG flow, regardless of initial conditions. This motivates the study of duality cascades having other Seiberg dual theories as their starting points. The simplest choice corresponds to the model in Figure 3-11. This theory is obtained from Model A by Seiberg dualizing node 2 followed by 1. We will call this Model C.

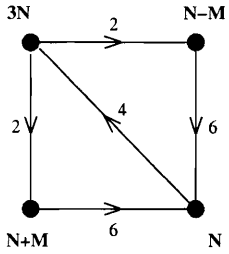

Figure 3-11: Model C for the F_0 theory. It is obtained from dualising node 2 and then 1 from the simplest Model A.

Decreases in the Step

Applying the formalism developed in previous sections we can proceed to compute, for any initial condition, the RG cascade as the theory evolves to the UV. The starting point is the computation of the anomalous dimensions for Model C at the conformal point. These, by the techniques above, turn out to be $\gamma_{1,2} = \gamma_{1,4} = -3/2$, $\gamma_{2,3} = \gamma_{4,3} = 5/2$ and $\gamma_{3,1} = -1$. Using them to calculate the beta functions, we obtain

$$\begin{aligned} \beta_1 &= 0 & \beta_2 &= -3M \\ \beta_3 &= 0 & \beta_4 &= 3M \ . \end{aligned} \tag{3.32}$$

With these let us evolve to the UV. Let us first consider the case in which the initial condition for the inverse gauge couplings are $(x_1, x_2, x_3, x_4) = (1, 1, 1, 0)$. Figure 3-12 shows the evolution of the four inverse gauge couplings both as a function of the step in the cascade and as a function of the logarithm of the scale. An interesting feature

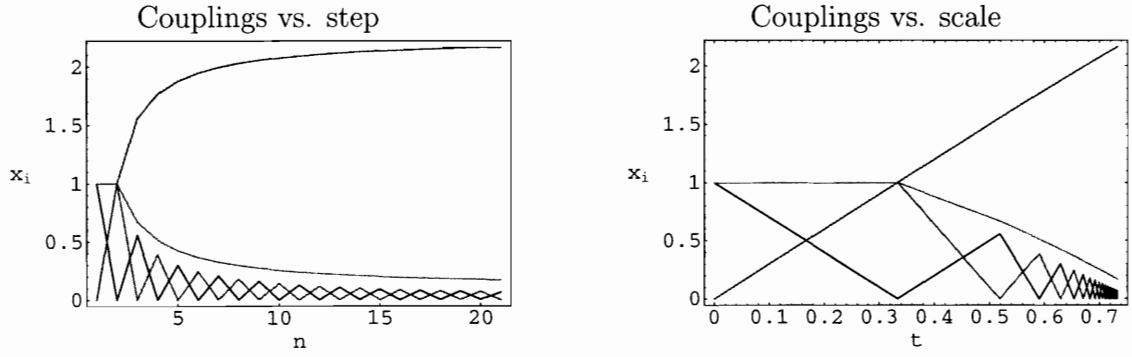

Figure 3-12: Evolution of gauge couplings with **(a)** the step in the duality cascade and **(b)** the energy scale for initial conditions $(x_1, x_2, x_3, x_4) = (1, 1, 1, 0)$. The colouring scheme is such that orange, black, green, and red respectively represent nodes 1, 2, 3 and 4.

is that the distance, Δ_i, between successive dualizations is monotonically decreasing. This marks a departure from the behaviors observed in the conifold cascade and from the example presented in Section 3.5.2, where Δ_i remained constant (cf. Figure 3-6). However, this fact does not necessarily mean the convergence of the dualization scales. Indeed, we plot the intervals Δ_i in Figure 3-13.a while Figure 3-13.b shows

the resulting dualization scales. The slope of this curve is decreasing, reflecting the

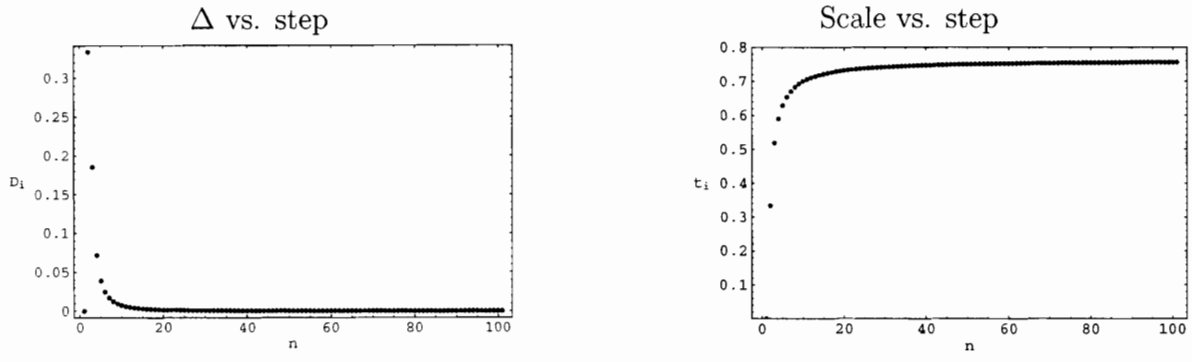

Figure 3-13: The evolution of Δ, the size of the increment during each dualisation and the energy scale increase as we dualise, for the initial conditions $(x_1, x_2, x_3, x_4) = (1, 1, 1, 0)$.

decreasing behavior of Δ_i. Nevertheless, *ad infinitum*, the scale may diverge.

A Duality Wall

Let us now consider a different set of initial conditions, given by $(x_1, x_2, x_3, x_4) = (1, 1, 4/5, 0)$. The flow of the inverse couplings is now shown in Figure 3-14.

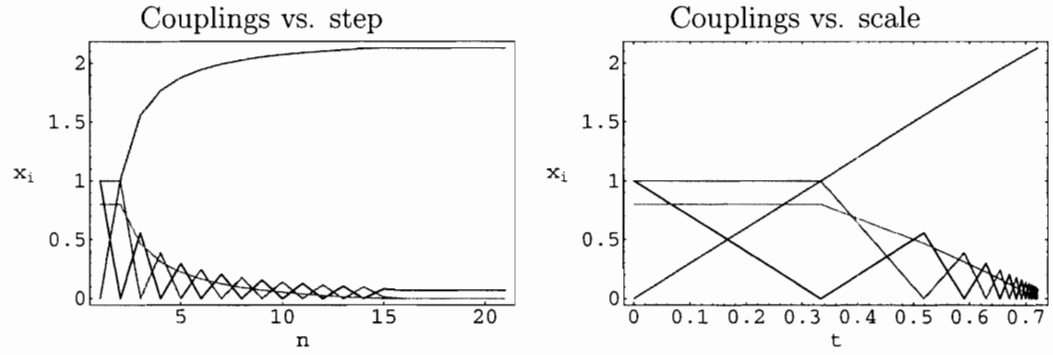

Figure 3-14: Evolution of gauge couplings with **(a)** the step in the duality cascade and **(b)** the energy scale for initial conditions $(x_1, x_2, x_3, x_4) = (1, 1, 4/5, 0)$. The colouring scheme is such that orange, black, green, and red respectively represent nodes 1, 2, 3 and 4.

A completely new phenomenon appears in this case. Something very drastic

happens after the fourteenth step in the cascade. As a consequence of lowering the initial value of x_3, the third node gets dualized at this step, producing an explosive growth of the number of chiral and vector multiplets in the quiver. This statement can be made precise: *at the 14-th step node 3 is dualized and the subsequent quivers have all their intersection numbers greater than 2.* In this situation the results of [18, 20] suggest that a duality wall is expected. This phenomenon is characterized by a flow of the dualization scales towards an UV *accumulation point* with an exponential divergence in the number of degrees of freedom.

Figure 3-14 shows a very small running of the gauge couplings beyond this point. This is not due to a vanishing of the beta functions, but to the extreme reduction of the length of the Δ_i intervals.

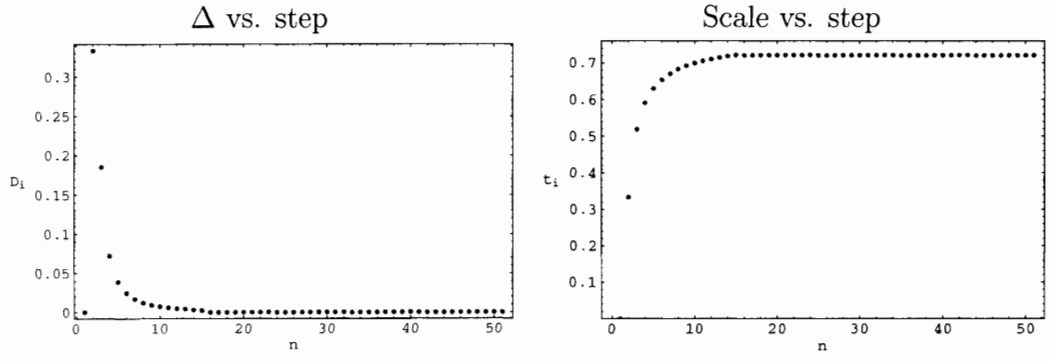

Figure 3-15: The evolution of Δ, the size of the increment during each dualisation and the energy scale increase as we dualise, for the initial conditions $(x_1, x_2, x_3, x_4) = (1, 1, 4/5, 0)$.

In contrast to Figure 3-13, for the initial conditions $(1, 1, 4/5, 0)$, we have drawn the plots in Figure 3-15.a and Figure 3-15.b. Both of them indicate that a limiting scale which cannot be surpassed is reached as the theory flows towards the UV. This is precisely what we call a *duality wall.*

3.5.4 Location of the wall

We have just seen that starting from the quiver in Figure 3-11 for F_0 with initial conditions $(x_1, x_2, x_3, x_4) = (1, 1, 4/5, 0)$ a duality wall is reached. Let us briefly examine

the sensitivity of the location of the duality wall to the initial inverse couplings.

Let our initial inverse gauge couplings be $(1, x_2, x_3, 0)$, with $0 < x_2, x_3 < 1$, and we repeat the analysis of the previous two subsections. We study the running of the beta functions, and determine the position of the duality wall, t_{wall}, for various initial values. We plot in Figure 3-16, the position of the duality wall against the initial values x_2 and x_3, both as a three-dimensional plot in I and as a contour plot in II. We see that the position is a stepwise function. A similar behavior has been already observed in [20] for dP_0 in the case of vanishing anomalous dimensions.

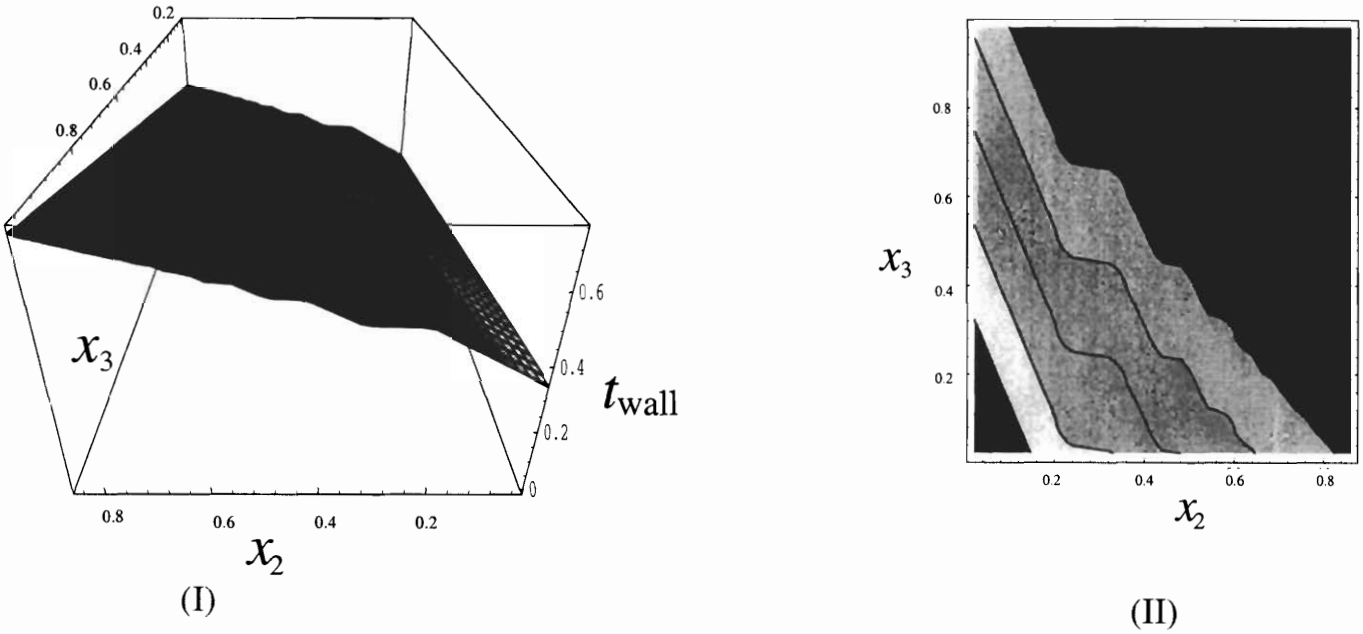

Figure 3-16: A plot of the position t_{wall} against the initial gauge coupling values $(1, x_2, x_3, 0)$. (I) is the 3-dimensional plot and (II) is the contour plot versus x_2 and x_3.

3.6 Conclusions

We have presented a general framework for studying duality cascades in quiver gauge theories and used this technology to find an example of a duality wall for a gauge theory that can be realized in string theory. Subsequently to this work, the authors of [30] studied duality cascades in the del Pezzo theories, and found partial super-

gravity solutions dual to these cascades. Similar results were also obtained for duality cascades in the $Y^{p,q}$ theories, which we will discuss in Chapters 5 and 6, in [31].

Chapter 4

Exceptional Symmeties in 4-d SUSY Gauge Theories

4.1 Introduction

In this chapter we turn our attention to global symmetries in the del Pezzo gauge theories, identifying the $U(1)$ global symmetries for all the bifundamental fields and reformulating many features of these interesting theories in a Lie algebra language. We do this using topological data of the string theory background in which these theories are realized in conjunction with the AdS/CFT correspondence.

One of the possible ways in which gauge theories can be engineered in String Theory is by considering the low energy limit of D-branes probes on singularities. When D3-branes are used to probe local Calabi-Yau threefolds, the resulting theory on their worldvolume is a $\mathcal{N} = 1$, $d = 4$ quiver gauge theory. A large class of interesting geometries is given by toric singularities. The gauge group, matter content and interaction superpotential of the gauge theory are dictated by the underlying geometry. A particular class of interesting singularities is the one of complex cones over del Pezzo surfaces dP_n. In [32] a map between bifundamental fields in certain del Pezzo quivers and 2-cycles in the geometry was established. Furthermore, a set of n global $U(1)$ symmetries, together with the corresponding charges of the bifundamental fields were identified. The main objective of this chapter is to exploit this map between

geometry and field theory in order to reformulate properties of the del Pezzo theories in a more symmetric manner. Interestingly, we find that the matter fields of these theories have $U(1)$ charges that coincide with the Cartan elements of exeptional Lie algebras E_n and we are able to rewrite many features of the theories in terms of representations of these algebras.

This structure, i.e. the grouping of matter fields into E_n representations and the resulting successful reformulation of several properties of the gauge theories in the language of group theory of these exceptional Lie algebras seems to point towards the existence of a fixed point with enhanced exceptional global symmetry for each of the del Pezzo theories. The enhanced E_n symmetry is hidden in the sense that it does not appear in the perturbative Lagrangian definition of the theories, and one can only argue for the existence of a superconformal fixed point where the symmetry is realized. For $n = 6, 7, 8$ this is of course to be expected, since there are no known Lagrangians that manifest this type of global symmetry. Examples of hidden global symmetry enhancement have been discovered in three and five dimensional gauge theories. In three dimensions, a $N = 4$ $U(1)$ gauge theory with 2 charged hypermultiplets flows to a fixed point with enhanced $SU(2)$ global symmetry and infinite gauge coupling [33]. More generally, the theories on D2 branes probing ADE singularities of an ALE space are argued to possess a fixed point (at infinite gauge coupling) with hidden global symmetry of the corresponding ADE type [34]. In the T-dual picture one has three-branes suspended between NS fivebranes and the global symmetry can be seen as the gauge symmetry living on the NS fivebranes [35]. In five dimensions, the $\mathcal{N} = 1$ gauge theory on a D4 brane probing a certain type I′ background is shown to have a fixed point with enhanced E_n global symmetry, depending on the number of D8 branes in the background [36]. Here also the fixed point resides at infinite gauge coupling. More examples can be found in [37] (see also [38]). The study of hidden symmetry enhancement in five dimensions can also be approached through (p, q) web techniques as in [39, 41] and the symmetry is made manifest in the string theory construction with the introduction of 7-branes [42]. The theories we have at hand bear striking similarities to these examples, namely the appearance of the E_n Lie groups as hidden

global symmetries and the realization of the enhanced symmetry only at zero inverse gauge coupling. On the other hand, all the aforementioned examples are theories with eight supercharges in contrast to the four supercharges of the theories on D3-branes probing cones over del Pezzo surfaces. To the best of our knowledge, this is the first example of gauge theories with $\mathcal{N} = 1$ supersymmetry in four dimensions that may exhibit a hidden exceptional global symmetry.

There are several problems that can be addressed once quivers are classified using global symmetries. An especially challenging task when deriving gauge theories that live on D-branes on singularities is the determination of the corresponding superpotentials. After organizing the matter content into representations, while ignoring their quiver gauge quantum numbers, the building blocks for superpotentials are given by invariant combinations of such irreducible representations. This is a key observation since, with this amount of supersymmetry, superpotentials are only affected by closed string complex moduli and will not be affected by changing Kähler moduli. As a result it is possible to compute the superpotentials at the enhanced point were the full E_n symmetry is enhanced and restrict only to E_n invariants. Once the symmetry is broken by turning on gauge interactions some of the terms in the superpotential become non-gauge invariant and are projected out. We are left then with the gauge invariant projection of the original E_n symmetric terms. In particular, the computation of superpotentials for non-toric del Pezzos is an interesting problem. We will see in this chapter how these superpotentials can also be derived by considering symmetric combinations and, in some cases, using simple inputs regarding the behavior of the theory under (un)higgsings.

As we proceed with the study of del Pezzo quivers, we will encounter a complication. The matter content of some quivers does not even seem to fit into irreducible representations of the corresponding E_n group. We will see that it is still possible to treat all the examples within a unified framework, through the use of *partial representations*. This idea simply states that the missing fields can be postulated to exist as massive fields, thus completing the representation to its actual size. Our tools allow us to identify all the quantum numbers of such missing states. A crucial ingredient

in such a construction is the possibility to add a global symmetry invariant mass term for these fields such that at energies smaller than this mass such fields will be integrated out and we will be left with what appears to be a "partial representation".

The outline of this chapter is as follows. In Section 4.2, we review how E_n symmetries arise in del Pezzo surfaces, and we establish the general framework that will be used along the paper to make these symmetries explicit in the corresponding quiver theories. In Section 3, we follow this methodology and, starting from dP_3, construct the divisors associated to bifundamental fields for all del Pezzo quivers up to dP_6 by performing successive blow-ups. We classify the bifundamental matter into irreducible representations of the global symmetry group and show how invariance under the global symmetry group determines superpotentials. Section 4.4 describes the concept of partial representations and shows in explicit examples how to determine which are the fields that are missing from them. In Section 4.5 we identify the blow-downs that take from dP_n to dP_{n-1} with higgsing of the global symmetry group E_n down to E_{n-1} by a non-zero VEV in the fundamental representation. This offers a systematic approach to the connection among theories for different del Pezzos. Section 4.6 presents a simple set of rules for transforming the E_n representation content of a quiver under Seiberg duality.

4.2 E_n symmetries and del Pezzo surfaces

Let us have a look at how exceptional symmetries appear in del Pezzo theories. Del Pezzo surfaces dP_n are manifolds of complex dimension 2 constructed by blowing up $\mathbb{P}^2$ at n generic points, $n = 0, \ldots, 8$. The lattice $H_2(dP_n, \mathbb{Z})$ is generated by the set $\{D, E_1, E_2, \ldots, E_n\}$. Here D is the pullback of the generator of $H_2(\mathbb{P}^2, \mathbb{Z})$ under the projection that collapses the blown-up exceptional curves $E_1, E_2, \ldots, E_n$. The intersection numbers for this basis are

$$D \cdot D = 1 \qquad D \cdot E_i = 0 \qquad E_i \cdot E_j = -\delta_{ij} \qquad i, j = 1, \ldots, n \tag{4.1}$$

One can use a vector notation for the elements of $H_2(dP_n, \mathbb{Z})$ which will be useful later for counting dibaryons. In this notation the basis elements read

$$\begin{aligned} D &: (1,0,0,...,0) \\ E_1 &: (0,1,0,...,0) \\ E_2 &: (0,0,1,...,0), \text{ etc} \end{aligned} \tag{4.2}$$

and the intersection numbers are computed by taking the scalar product between vectors using the Lorentzian metric diag $(1,-1,\ldots,-1)$.

The first Chern class for dP_n is $c_1 = 3D - \sum_{i=1}^{n} E_i$. The canonical class is $K_n = -c_1$. The orthogonal complement of K_n according to the above intersection product is a natural sublattice of $H_2(dP_n, \mathbb{Z})$, called the *normal sublattice*. There is an isomorphism between the normal sublattice and the root lattice of the E_n Lie algebra for $n \geq 3$. If we take as basis for this sublattice the set of vectors

$$\begin{aligned} &\alpha_i = E_i - E_{i+1} \qquad\qquad i = 1,...,n-1 \\ &\alpha_n = D - E_1 - E_2 - E_3 \end{aligned} \tag{4.3}$$

then the intersection numbers for the α_i are

$$\alpha_i \cdot \alpha_j = -A_{ij} \ , \ i,j = 1,\ldots,n, \tag{4.4}$$

where A_{ij} is the Cartan matrix of the Lie Algebra E_n. Thus, the α_i correspond to the simple roots of E_n. It is useful to keep in mind that $E_1 = U(1)$, $E_2 = SU(2) \times U(1)$, $E_3 = SU(2) \times SU(3)$, $E_4 = SU(5)$ and $E_5 = SO(10)$. Given an element $\mathcal{C}$ of $H_2(dP_n, \mathbb{Z})$, we can assign a weight vector of E_n to it, with Dynkin coefficients given by its projection on the normal sublattice

$$\lambda_i = -\mathcal{C} \cdot \alpha_i \ . \tag{4.5}$$

Let us now consider the quiver gauge theories that appear on a stack of N D3-branes probing complex cones over del Pezzo surfaces. For dP_n, the gauge group is $\prod_{i=1}^{k} U(d_i N)$, where the d_i are appropriate integers and $k = n + 3$, the Euler

characteristic of the del Pezzo. The near horizon geometry of this configuration will be $AdS_5 \times X_5$ where X_5 is a $U(1)$ fibration over the the del Pezzo surface dP_n. The AdS/CFT correspondence [9, 10, 11] conjectures a mapping between operators in the conformal gauge theory and states of the bulk string theory. Although this mapping is not known in its generality, it has been sufficiently explored for the special case of BPS operators. One such class of operators are dibaryons [43, 15]. These are generalizations of the usual baryons to theories with bifundamental matter. In the gravity dual dibaryons correspond to D3-branes wrapping certain 3-cycles in X_5. These 3-cycles are holomorphic 2-cycles of dP_n together with the $U(1)$ fiber of X_5. Therefore, it is possible to assign a curve in $H_2(dP_n, \mathbb{Z})$ to every dibaryon [32, 44] (more details of this correspondence later). In the special case where the quiver theory is in the so-called toric phase[1], i.e. when all the gauge group factors are $SU(N)$, there are some dibaryons which are formed by the anti-symmetrization of N copies of a single bifundamental field

$$\epsilon_{i_1 i_2 \cdots i_N} \epsilon^{j_1 j_2 \cdots j_N} X^{i_1}_{j_1} X^{i_2}_{j_2} \cdots X^{i_N}_{j_N}. \tag{4.6}$$

This can be repeated for every bifundamental field, allowing us to extend the correspondence between holomorphic 2-cycles (also called divisors) and dibaryons and assign an element of $H_2(dP_n, \mathbb{Z})$ to each bifundamental matter field in the quiver [32]. Thus, if $X_{\alpha\beta}$ is a bifundamental field extending from node α to node β in the quiver representation then we can associate to it an element $L_{\alpha\beta}$ of $H_2(dP_n, \mathbb{Z})$. In fact, the $L_{\alpha\beta}$ of toric quivers can be written as differences of divisors L_α associated to the nodes. The precise nature of the node divisors was clarified in [44], where they were identified with the first Chern class of the sheaves in the dual exceptional collection associated to the quiver. This result has been generalized in [44] to the case in which the ranks of the gauge groups are not necessarily equal, yielding the following expressions

[1]We want to bring to the reader's attention the particular use we are making here of the concept of a toric phase. It simply refers to a quiver in which all $d_i = 1$, i.e. all the gauge groups are equal to $SU(N)$. In particular, there can be toric quivers for non-toric del Pezzos, as we will see along the paper.

$$L_{\alpha\beta} = \frac{L_\beta}{d_\beta} - \frac{L_\alpha}{d_\alpha} \qquad \text{if} \quad \frac{L_\beta}{d_\beta} - \frac{L_\alpha}{d_\alpha} \geq 0$$
$$L_{\alpha\beta} = \frac{L_\beta}{d_\beta} - \frac{L_\alpha}{d_\alpha} + c_1 \quad \text{if} \quad \frac{L_\beta}{d_\beta} - \frac{L_\alpha}{d_\alpha} < 0. \tag{4.7}$$

where the sign refers to the sign of $(L_\beta/d_\beta - L_\alpha/d_\alpha) \cdot c_1$. The supersymmetric gauge theories living on the stack of D3-branes probing these geometries are invariant under a set of global $U(1)$ symmetries. One of these is the $U(1)_R$ symmetry which is part of the superconformal algebra. There are also n flavor $U(1)$ symmetries under which the bifundamentals are charged. Dibaryons are correspondingly charged under these symmetries, thus we refer to them as baryonic $U(1)$'s. The aforementioned correspondence allows us to readily calculate the charges of bifundamentals under the *baryonic* $U(1)$'s and $U(1)_R$ contained in the global symmetry group of the quivers. In particular, the R charge, being proportional to the volume of the 3-cycle wrapped by the D3-brane in the dual geometry, is given by

$$R(X_{\alpha\beta}) = -2\frac{K_n \cdot L_{\alpha\beta}}{K_n \cdot K_n}. \tag{4.8}$$

The global baryonic $U(1)$ symmetries are gauge symmetries in the AdS_5 bulk, with the $U(1)$ gauge fields coming from the reduction of the RR gauge field C_4 on n independent 3-cycles of X_5. The flavor currents J_i of these $U(1)$'s must be neutral under the R-symmetry, which translates in the dual geometry as $J_i \cdot K_n = 0$. Therefore, the divisors J_i corresponding to these are elements of the normal sublattice and can be chosen to be the basis vectors α_i defined in (4.3). The vector of $U(1)$ charges for each bifundamental $X_{\alpha\beta}$ is then

$$q_i = L_{\alpha\beta} \cdot J_i. \tag{4.9}$$

According to (4.5), these are (modulo an unimportant overall minus sign) the Dynkin coefficients of the weight vector $L_{\alpha\beta}$. We can indeed compute the weight vectors for all the toric phases of the del Pezzos (and will in fact do so in Section 3). What one finds using these weight vectors is that the bifundamental matter fields

can be accommodated into irreducible representations of the E_n Lie algebra for each of these theories. The matter fields within a representation have the same R charge, which is characteristic of the representation.

These theories also have nonzero superpotentials. Each term in the superpotential must be invariant under the $U(1)$ flavor symmetries and have R-charge equal to two. The superpotential for all these models can actually be written as the gauge invariant part of singlets of E_n formed by products of these irreducible representations. As we will see, this description makes it possible to recast most of what is known about the del Pezzo theories, including superpotentials, Seiberg duality relations and higgsing relations, in an elegant group theoretic language. Although the global symmetry of these models at a generic point in the moduli space is just the $U(1)^n \times U(1)_R$ symmetry, in the limit where all the gauge couplings $g_i \to \infty$ the full E_n symmetry is restored. This enhancement of the symmetry leaves its mark on the theory even for finite g_i, if appropriately combined with the principle of gauge invariance. In fact, the $U(1)^n \times U(1)_R$ global symmetry algebra forms the Cartan sub-algebra of the affine algebra, $\hat{E}_n$, with $U(1)_R$ being the Cartan element associated with the imaginary root of the affine algebra. It is important to note that the sub-algebras which can be enhanced by tuning the inverse gauge coupling are always finite dimensional and, as usual, the affine algebra is never completely enhanced. It will be interesting to study the signature of the affine algebras on these quiver theories.

4.2.1 The Weyl group and dibaryons

Let $\mathcal{C}$ be an element of $H_2(dP_n, \mathbb{Z})$ corresponding to a dibaryon state in dP_n. The degree of this curve is defined as:

$$k = -(K_n \cdot \mathcal{C}). \tag{4.10}$$

There is a natural action of the Weyl group of E_n on these curves that preserves their degree. If $\alpha_i \in H_2(dP_n, \mathbb{Z})$, $i = 1, \ldots, n$ is any of the simple roots in (4.3) then the corresponding Weyl group element acts on $\mathcal{C}$ as

$$w_{\alpha_i} \ : \ \mathcal{C} \to \mathcal{C} + (\mathcal{C} \cdot \alpha_i)\ \alpha_i \tag{4.11}$$

and the curve produced by this action has the same degree k, because $K_n \cdot \alpha_i = 0$. Thus, the curves of a given degree form a representation of the Weyl group of E_n. So there is some E_n related structure for dibaryon states at a generic point in the moduli space, even though they do not form complete E_n representations because of the requirement of gauge invariance in their construction. On the other hand, every representation of E_n is the union of irreducible representations of the Weyl group (Weyl orbits). For basic representations, i.e. representations whose highest weight vector has only one nonzero element, equal to one, it can be shown that they consist of a single nontrivial Weyl orbit (plus n Weyl singlets in the case of the adjoint). This means that for low levels k the dimensions of Weyl orbits and irreducible E_n representations coincide (modulo a difference of n for the adjoint).

4.3 Global symmetry classification of quivers

The discussion in Section 4.2 provides us with a systematic procedure to classify del Pezzo quivers according to the transformation properties of bifundamental fields under the corresponding E_n groups, which can be summarized as follows. The divisors associated to bifundamental fields are computed from the divisors assigned to the quiver nodes using (4.7). The baryonic $U(1)$ and R charges are calculated from the intersection numbers of these divisors with the normal sublattice and the canonical class according to (4.9) and (4.8). The vector of $U(1)$ charges for each of the matter fields in dP_n is actually a weight vector of the E_n Lie algebra and, as we will see by computing them, these weight vectors form irreducible representations of E_n.

In this section we will summarize the transformation properties under global symmetries of bifundamental fields in different phases of gauge theories on D3-branes probing complex cones over del Pezzo surfaces. This information will be used in the subsequent sections of the paper. We will closely examine the toric phases of the del Pezzo theories, dP_n for $3 \leq n \leq 6$.

The corresponding superpotentials of these theories are singlets under the global symmetry transformations. Thus, they can be written as a sum of products of irreducible representations, with the understanding that from each of these products we consider the E_n singlet included in it and that only the gauge invariant terms in this singlet actually contribute to the superpotential. We will only write down those superpotential terms from which some contributions survive the projection onto gauge invariants, although sometimes more terms that are invariant under global transformations can be written down.

The only subtlety we encounter in using this description is the appearance of *partial representations.* This is just a name for groups of fields whose $U(1)$ charges do not completely fill representations of E_n. A detailed discussion of partial representations is deferred to Section 4.4. For now it will suffice to say that the missing components in these representations are actually massive matter fields that do not appear in the low energy limit of the theory.

In writing down these theories, we have decided to number the gauge groups following the order of the corresponding external legs of the associated (p, q) webs (see [45, 46] for a description of the connection between (p, q) webs and 4d gauge theories on D3-branes probing toric singularities). This ordering is closely related to the one of the associated dual exceptional collection. In fact, both ordering prescriptions are almost identical, differing at most by a possible reordering of nodes within each block (set of parallel external legs in the (p, q) web description).

There are different ways to go about calculating the divisors associated to nodes and bifundamental fields in these quiver theories. According to [44], the divisors corresponding to the nodes are the elements of a dual exceptional collection, obtained through a certain braiding operation from the exceptional collection used to construct the quiver theory. We will follow here another procedure, also used in [32], which makes use of the fact that these phases are related to one another by Seiberg dualities and/or higgsing. We can compute the divisor configurations starting from any of these models and using Seiberg duality and blowing down or blowing up cycles in the geometry, which means higgsing or unhiggsing the quiver theory respectively. We will

primarily focus on toric phases. By the use of Seiberg dualities on selfdual nodes (i.e. nodes whose rank does not change upon dualisation) we can 'move' among different toric phases of the theory, while the operation of blowing cycles up or down takes us from the dP_n theory to dP_{n+1} or dP_{n-1} respectively. The ways these operations act on the divisors are described in [32]. Here is a quick review of the rules for quivers in which all the gauge groups are equal to $SU(N)$:

- **Seiberg duality:** when a self-dual node α (i.e., for the class of quivers under consideration, a node with $2N$ flavors) is dualised, the divisor L_α changes to $L'_\alpha = L_\beta + L_\gamma - L_\alpha$ where β and γ are the nodes where arrows starting from α end or, equivalently, where arrows that end at α begin. In the case of a double arrow, β and γ can be the same.

- **Blow-down:** to blow down from dP_n to dP_{n-1} we eliminate E_n from the divisors and identify the nodes that have the same divisor after the elimination.

- **Blow-up:** to go from dP_{n-1} to dP_n we add a new node and attribute to it a divisor such that the field that is unhiggsed in the quiver corresponds to the divisor E_n that we blow up. Moreover, all other divisors can differ from their blown-down counterparts only by E_n.

We now present the results of this classification for the toric phases of the del Pezzo theories, dP_n for $3 \leq n \leq 6$.

4.3.1 del Pezzo 3

There are four toric phases for dP_3, related to one another by Seiberg dualities [54]. For each of them we list the divisors corresponding to the nodes and fields, the assignment of fields to representations and the superpotential written as an E_3 singlet.

Model I

This model has 12 fields.

Node	L_α		$L_{\alpha\beta}$	J_1	J_2	J_3	R
		X_{45}	E_1	-1	0	1	$1/3$
		X_{23}	E_2	1	-1	1	$1/3$
		X_{61}	E_3	0	1	1	$1/3$
1	$D+E_3$	X_{34}	$D-E_1-E_2$	0	1	-1	$1/3$
2	$2D-E_2$	X_{56}	$D-E_1-E_3$	1	-1	-1	$1/3$
3	$2D$	X_{12}	$D-E_2-E_3$	-1	0	-1	$1/3$
4	E_3	X_{51}	$D-E_1$	1	0	0	$2/3$
5	E_1+E_3	X_{35}	$D-E_2$	-1	1	0	$2/3$
6	D	X_{13}	$D-E_3$	0	-1	0	$2/3$
		X_{24}	$D-E_1$	1	0	0	$2/3$
		X_{62}	$D-E_2$	-1	1	0	$2/3$
		X_{46}	$D-E_3$	0	-1	0	$2/3$

(4.12)

The quiver diagram for this model is displayed in Figure 4-1. The fields are arranged in irreducible representations of $E_3 = SU(2)\times SU(3)$ as shown in (4.13). The assignment is done by comparing the $U(1)$ charges above with the Dynkin labels of the weight vectors of an E_3 irreducible representation. We remind the reader that because of the difference in their definitions there is an overall minus sign difference that must be taken into account in this comparison. From now on, repeated representations will be identified with lowercase subscript (a, b, c, etc).

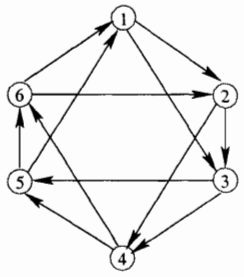

Fields	$SU(2)\times SU(3)$
$(X_{12}, X_{23}, X_{34}, X_{45}, X_{56}, X_{61})$	$(2,3)$
(X_{13}, X_{35}, X_{51})	$(1,\bar{3})_a$
(X_{24}, X_{46}, X_{62})	$(1,\bar{3})_b$

(4.13)

Figure 4-1: Quiver diagram for Model I of dP_3.

The superpotential can then be written as

$$W_I = (2,3)^6 + (2,3)^2 \otimes (1,\bar{3})_a \otimes (1,\bar{3})_b + (1,\bar{3})_a^3 + (1,\bar{3})_b^3 \tag{4.14}$$

Model II

There are 14 fields in this phase. We can get it by dualising node 1 of the previous model. Again, we calculate the divisors and charges and compare them with E_3 weight vectors in order to assign the fields to representations. The results are shown in the tables below.

$Node$	L_α		$L_{\alpha\beta}$	J_1	J_2	J_3	R
		X_{32}	E_1	-1	0	1	$1/3$
		X_{65}	E_2	1	-1	1	$1/3$
		X_{42}	E_3	0	1	1	$1/3$
		X_{53}	$D-E_1-E_2$	0	1	-1	$1/3$
1	D	X_{21}	$D-E_1-E_3$	1	-1	-1	$1/3$
2	E_1+E_3	X_{54}	$D-E_2-E_3$	-1	0	-1	$1/3$
3	E_3	X_{41}	$D-E_1$	1	0	0	$2/3$
4	E_1	X_{16}	$D-E_2$	-1	1	0	$2/3$
5	$2D$	X_{64}	$D-E_3$	0	-1	0	$2/3$
6	$2D-E_2$	X_{63}	$D-E_1$	1	0	0	$2/3$
		Y_{16}	$D-E_2$	-1	1	0	$2/3$
		X_{31}	$D-E_3$	0	-1	0	$2/3$
		X_{15}	D	0	0	1	1
		X_{26}	$2D-E_1-E_2-E_3$	0	0	-1	1

(4.15)

The quiver for this model is shown in Figure 4-2. The representation structure is shown in (4.16).

Using this, we can write the superpotential as

$$\begin{aligned} W_{II} \;=\; & (2,3)^4 \otimes (1,\bar{3})_a + (2,3)^4 \otimes (1,\bar{3})_b \\ & +(2,3) \otimes (2,1) \otimes (1,\bar{3})_a + (2,3) \otimes (2,1) \otimes (1,\bar{3})_b \\ & +(1,\bar{3})_a^2 \otimes (1,\bar{3})_b + (1,\bar{3})_a \otimes (1,\bar{3})_b^2 \end{aligned} \tag{4.17}$$

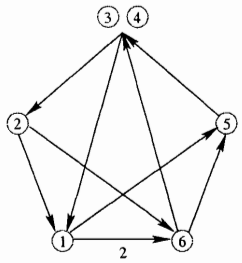

Fields	$SU(2) \times SU(3)$
$(X_{54}, X_{65}, X_{53}, X_{32}, X_{21}, X_{42})$	$(2,3)$
(X_{63}, X_{31}, X_{16})	$(1,\bar{3})_a$
(X_{64}, X_{41}, Y_{16})	$(1,\bar{3})_b$
(X_{26}, X_{15})	$(2,1)$

(4.16)

Figure 4-2: Quiver diagram for Model II of dP_3.

Model III

Dualising node 2 of Model II we obtain Model III. This phase has 14 fields.

$Node$	L_α
1	D
2	E_1
3	E_3
4	0
5	$2D$
6	$2D - E_2$

	$L_{\alpha\beta}$	J_1	J_2	J_3	R
X_{42}	E_1	-1	0	1	$1/3$
X_{65}	E_2	1	-1	1	$1/3$
X_{43}	E_3	0	1	1	$1/3$
X_{53}	$D - E_1 - E_2$	0	1	-1	$1/3$
X_{64}	$D - E_1 - E_3$	1	-1	-1	$1/3$
X_{52}	$D - E_2 - E_3$	-1	0	-1	$1/3$
X_{21}	$D - E_1$	1	0	0	$2/3$
X_{16}	$D - E_2$	-1	1	0	$2/3$
X_{31}	$D - E_3$	0	-1	0	$2/3$
X_{15}	D	0	0	1	1
X_{14}	$2D - E_1 - E_2 - E_3$	0	0	-1	1

(4.18)

Figure 4-3 shows the quiver diagram and Table (4.19) summarizes how the fields fall into representations.

The superpotential for this theory can be written in an invariant form as

$$\begin{aligned} W_{III} &= (2,3)^2 \otimes (1,\bar{3})_a^2 + (2,3)^2 \otimes (1,\bar{3})_a \otimes (1,\bar{3})_b + (2,3)^2 \otimes (1,\bar{3})_b^2 \\ &\quad + (2,3) \otimes (2,1) \otimes (1,\bar{3})_a + (2,3) \otimes (2,1) \otimes (1,\bar{3})_b \end{aligned} \tag{4.20}$$

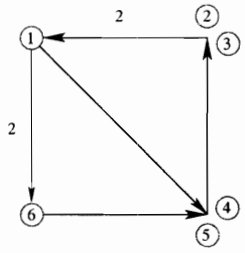

Fields	$SU(2) \times SU(3)$
$(X_{21}, X_{64}, X_{23}, X_{43}, X_{62}, X_{41})$	$(2,3)$
(X_{15}, X_{56}, X_{35})	$(1,\bar{3})_a$
(Y_{15}, Y_{56}, Y_{35})	$(1,\bar{3})_b$
(X_{54}, X_{52})	$(2,1)$

(4.19)

Figure 4-3: Quiver diagram for Model III of dP_3.

Model IV

There are 18 fields in this phase, which is produced by dualising node 6 of Model III.

$Node$	L_α
1	E_1
2	E_2
3	E_3
4	$2D$
5	0
6	D

	$L_{\alpha\beta}$	J_1	J_2	J_3	R
X_{51}	E_1	-1	0	1	$1/3$
X_{52}	E_2	1	-1	1	$1/3$
X_{53}	E_3	0	1	1	$1/3$
X_{43}	$D - E_1 - E_2$	0	1	-1	$1/3$
X_{42}	$D - E_1 - E_3$	1	-1	-1	$1/3$
X_{41}	$D - E_2 - E_3$	-1	0	-1	$1/3$
X_{16}	$D - E_1$	1	0	0	$2/3$
X_{26}	$D - E_2$	-1	1	0	$2/3$
X_{36}	$D - E_3$	0	-1	0	$2/3$
X_{64}	D	0	0	1	1
X_{65}	$2D - E_1 - E_2 - E_3$	0	0	-1	1

(4.21)

The table below shows how the fields are organized in representations.

The superpotential is

$$W_{IV} = (2,3) \otimes [(1,\bar{3})_a + (1,\bar{3})_b] \otimes [(2,1)_a + (2,1)_b + (2,1)_c] \tag{4.23}$$

4.3.2 del Pezzo 4

There are two toric phases for dP_4. The organization of matter fields into E_4 representations is in this case more subtle than in the preceding examples. The classification of

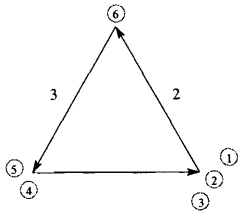

Fields	$SU(2) \times SU(3)$
$(X_{51}, X_{52}, X_{53}, X_{41}, X_{42}, X_{43})$	$(2,3)$
(X_{16}, X_{26}, X_{36})	$(1,\bar{3})_a$
(Y_{16}, Y_{26}, Y_{36})	$(1,\bar{3})_b$
(X_{64}, X_{65})	$(2,1)_a$
(Y_{64}, Y_{65})	$(2,1)_b$
(Z_{64}, Z_{65})	$(2,1)_c$

(4.22)

Figure 4-4: Quiver diagram for Model IV of dP_3.

these theories can be achieved with the same reasoning as before, by introducing the idea of partial representations. Partial representations are ordinary representations in which some of the fields are massive, being integrated out in the low energy limit. We will summarize the results in this section, and postpone a detailed explanation of partial representations to Sections 4.4 and 4.6.

Model I

This theory has 15 fields.

			$L_{\alpha\beta}$	J_1	J_2	J_3	J_4	R
		X_{45}	E_1	-1	0	0	1	$2/5$
		X_{23}	E_2	1	-1	0	1	$2/5$
$Node$	L_α	X_{46}	E_3	0	1	-1	1	$2/5$
		X_{71}	E_4	0	0	1	0	$2/5$
1	D	X_{36}	$D - E_1 - E_2$	0	1	0	-1	$2/5$
2	E_1	X_{24}	$D - E_1 - E_3$	1	-1	1	-1	$2/5$
3	E_3	X_{57}	$D - E_1 - E_4$	1	0	-1	0	$2/5$
4	$2D - E_4$	X_{35}	$D - E_2 - E_3$	-1	0	1	-1	$2/5$
5	0	X_{12}	$D - E_2 - E_4$	-1	1	-1	0	$2/5$
6	$D - E_4$	X_{67}	$D - E_3 - E_4$	0	-1	0	0	$2/5$
7	$2D - E_2 - E_4$	X_{51}	$D - E_1$	1	0	0	0	$4/5$
		X_{72}	$D - E_2$	-1	1	0	0	$4/5$
		X_{61}	$D - E_3$	0	-1	1	0	$4/5$
		X_{13}	$D - E_4$	0	0	-1	1	$4/5$
		X_{14}	$2D - E_1 - E_2 - E_3 - E_4$	0	0	0	-1	$4/5$

(4.24)

Comparing the charges with weight vectors of $SU(5)$ representations we find the

assignment tabulated in (4.25).

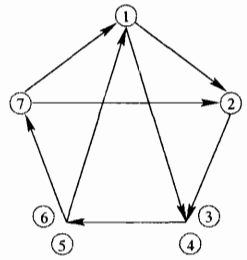

Fields	$SU(5)$
$(X_{45}, X_{23}, X_{46}, X_{71}, X_{36}, X_{24}, X_{57}, X_{35}, X_{12}, X_{67})$	10
$(X_{51}, X_{72}, X_{67}, X_{13}, X_{14})$	$\bar{5}$

(4.25)

Figure 4-5: Quiver diagram for Model I of dP_4.

The superpotential is written in terms of singlets as

$$W_I = 10 \otimes \bar{5}^2 + 10^3 \otimes \bar{5} \tag{4.26}$$

One might wonder whether a $\mathbf{10}^5$ term should be present in $W_{dP_{4,I}}$. At first sight it appears as a valid contribution, since this product of representations contains an E_4 singlet and we see from Figure 4-5 that it would survive the projection onto gauge invariant states. As we shall discuss in Section 4.5, this model can be obtained from Model I of dP_5 by higgsing. All the gauge invariants in that theory are quartic. In particular, since there are no cubic terms, masses are not generated when turning on a non-zero vev for a bifundamental field. Then, we conclude that any fifth order term in $W_{dP_{4,I}}$ should have its origin either in a fifth or sixth order term in $W_{dP_{5,I}}$. Since $W_{dP_{5,I}}$ is purely quartic, we conclude that the $\mathbf{10}^5$ is not present in $W_{dP_{4,I}}$.

Model II

Upon dualisation of node 7 of Model I we get Model II. There are 19 fields in this model.

Node	L_α		$L_{\alpha\beta}$	J_1	J_2	J_3	J_4	R
		X_{52}	E_1	-1	0	0	1	$2/5$
		X_{74}	E_2	1	-1	0	1	$2/5$
		X_{53}	E_3	0	1	-1	1	$2/5$
		X_{76}	E_4	0	0	1	0	$2/5$
		X_{43}	$D-E_1-E_2$	0	1	0	-1	$2/5$
1	D	X_{75}	$D-E_1-E_3$	1	-1	1	-1	$2/5$
2	E_1	X_{63}	$D-E_1-E_4$	1	0	-1	0	$2/5$
3	E_3	X_{42}	$D-E_2-E_3$	-1	0	1	-1	$2/5$
4	$2D-E_4$	X_{17}	$D-E_2-E_4$	-1	1	-1	0	$2/5$
5	0	X_{62}	$D-E_3-E_4$	0	-1	0	0	$2/5$
6	$2D-E_2$	X_{21}	$D-E_1$	1	0	0	0	$4/5$
7	$2D-E_2-E_4$	X_{16}	$D-E_2$	-1	1	0	0	$4/5$
		X_{31}	$D-E_3$	0	-1	1	0	$4/5$
		X_{14}	$D-E_4$	0	0	-1	1	$4/5$
		X_{15}	$2D-E_1-E_2-E_3-E_4$	0	0	0	-1	$4/5$
		X_{27}	$2D-E_1-E_2-E_4$	0	1	-1	0	$6/5$
		X_{37}	$2D-E_2-E_3-E_4$	-1	0	0	0	$6/5$

(4.27)

This is the first example where partial representations appear. We will study this further in Section 4.4, and for the moment it will suffice to say that the missing fields (indicated by asterisks in Table (4.28)) are massive and the terms containing those fields in the singlets forming the superpotential should be thrown out, as they are not a part of the low energy theory.

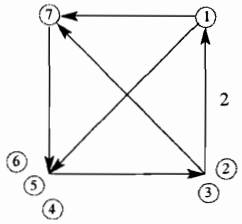

Figure 4-6: Quiver diagram for Model II of dP_4.

Fields	$SU(5)$
$(X_{52}, X_{74}, X_{53}, X_{76}, X_{43}, X_{75}, X_{63}, X_{42}, X_{17}, X_{62})$	10
$(X_{21}, X_{16}, X_{31}, X_{14}, X_{15})$	$\bar{5}_a$
$(Y_{21}, Y_{31}, *, *, *)$	partial $\bar{5}_b$
$(X_{27}, X_{37}, *, *, *)$	partial 5

(4.28)

The superpotential for this theory is

$$\begin{aligned} W_{II} &= 10 \otimes \bar{5}_a^2 + 10 \otimes \bar{5}_a \otimes \bar{5}_b \\ &\quad + 10^3 \otimes \bar{5}_a + 10^3 \otimes \bar{5}_b + 10^2 \otimes 5 \end{aligned} \tag{4.29}$$

where the superpotential corresponds only to those E_4 invariant contributions that survive the projection onto gauge invariant terms. The terms including the partial $\bar{\mathbf{5}}_\mathbf{b}$ representation are naturally understood to be truncated to fields actually appearing in the quiver.

4.3.3 del Pezzo 5

Let us study the three toric phases of dP_5. Models II and III exhibit again the phenomenon of partial representations.

Model I

This model has 16 fields.

$Node$	L_α
1	E_1
2	E_3
3	$D - E_4$
4	$D - E_5$
5	$2D - E_2 - E_4 - E_5$
6	D
7	$2D - E_4 - E_5$
8	0

	$L_{\alpha\beta}$	J_1	J_2	J_3	J_4	J_5	R
X_{81}	E_1	−1	0	0	0	1	1/2
X_{57}	E_2	1	−1	0	0	1	1/2
X_{82}	E_3	0	1	−1	0	1	1/2
X_{36}	E_4	0	0	1	−1	0	1/2
X_{46}	E_5	0	0	0	1	0	1/2
X_{72}	$D - E_1 - E_2$	0	1	0	0	−1	1/2
X_{58}	$D - E_1 - E_3$	1	−1	1	0	−1	1/2
X_{13}	$D - E_1 - E_4$	1	0	−1	1	0	1/2
X_{14}	$D - E_1 - E_5$	1	0	0	−1	0	1/2
X_{71}	$D - E_2 - E_3$	−1	0	1	0	−1	1/2
X_{45}	$D - E_2 - E_4$	−1	1	−1	1	0	1/2
X_{35}	$D - E_2 - E_5$	−1	1	0	−1	0	1/2
X_{23}	$D - E_3 - E_4$	0	−1	0	1	0	1/2
X_{24}	$D - E_3 - E_5$	0	−1	1	−1	0	1/2
X_{67}	$D - E_4 - E_5$	0	0	−1	0	1	1/2
X_{68}	$2D - E_1 - E_2 - E_3 - E_4 - E_5$	0	0	0	0	−1	1/2

(4.30)

All sixteen fields here are accommodated in a single **16** representation of $E_5 = SO(10)$.

The superpotential consists simply of all quartic gauge invariants and can be written as

$$W_I = 16^4 \tag{4.32}$$

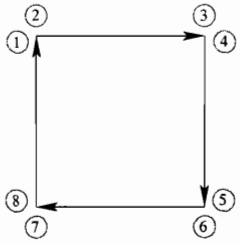

Fields	$S0(10)$
$(X_{81}, X_{57}, X_{82}, X_{36}, X_{46}, X_{72}, X_{58}, X_{13}, X_{14}, X_{71}, X_{45}, X_{35}, X_{23}, X_{24}, X_{67}, X_{68})$	16

(4.31)

Figure 4-7: Quiver diagram for Model I of dP_5.

Model II

Model II is can be obtained by dualising node 5 of model I. The divisors and charges are as shown in the tables.

$Node$	L_α
1	D
2	$2D - E_4 - E_5$
3	0
4	E_1
5	E_2
6	E_3
7	$D - E_4$
8	$D - E_5$

	$L_{\alpha\beta}$	J_1	J_2	J_3	J_4	J_5	R
X_{34}	E_1	−1	0	0	0	1	1/2
X_{35}	E_2	1	−1	0	0	1	1/2
X_{36}	E_3	0	1	−1	0	1	1/2
X_{71}	E_4	0	0	1	−1	0	1/2
X_{81}	E_5	0	0	0	1	0	1/2
X_{26}	$D - E_1 - E_2$	0	1	0	0	−1	1/2
X_{25}	$D - E_1 - E_3$	1	−1	1	0	−1	1/2
X_{47}	$D - E_1 - E_4$	1	0	−1	1	0	1/2
X_{48}	$D - E_1 - E_5$	1	0	0	−1	0	1/2
X_{24}	$D - E_2 - E_3$	−1	0	1	0	−1	1/2
X_{57}	$D - E_2 - E_4$	−1	1	−1	1	0	1/2
X_{58}	$D - E_2 - E_5$	−1	1	0	−1	0	1/2
X_{67}	$D - E_3 - E_4$	0	−1	0	1	0	1/2
X_{68}	$D - E_3 - E_5$	0	−1	1	−1	0	1/2
X_{12}	$D - E_4 - E_5$	0	0	−1	0	1	1/2
X_{13}	$2D - E_1 - E_2 - E_3 - E_4 - E_5$	0	0	0	0	1	1/2
X_{82}	$D - E_4$	0	0	−1	1	1	1
X_{72}	$D - E_5$	0	0	0	−1	1	1
X_{83}	$2D - E_1 - E_2 - E_3 - E_4$	0	0	0	1	−1	1
X_{73}	$2D - E_1 - E_2 - E_3 - E_5$	0	0	1	−1	−1	1

(4.33)

The meson fields created by the dualization form a partial **10** representation of $SO(10)$.

The superpotential is

$$W_{II} = 16^4 + 16^2 \otimes 10 \tag{4.35}$$

Model III

The last toric phase of dP_5 is produced by dualising on node 6 of model II and has 24 fields, arranged as follows.

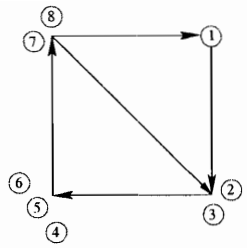

Fields	$S0(10)$
$(X_{34}, X_{35}, X_{36}, X_{71}, X_{81}, X_{26}, X_{25}, X_{47}, X_{48}, X_{24}, X_{57}, X_{58}, X_{67}, X_{68}, X_{12}, X_{13})$	16
$(X_{82}, X_{72}, X_{83}, X_{73}, *, *, *, *, *, *)$	partial 10

(4.34)

Figure 4-8: Quiver diagram for Model II of dP_5.

$Node$	L_α
1	E_1
2	E_3
3	E_2
4	$D - E_4 - E_5$
5	$2D - E_4 - E_5$
6	0
7	$D - E_4$
8	$D - E_5$

	$L_{\alpha\beta}$	J_1	J_2	J_3	J_4	J_5	R
X_{61}	E_1	−1	0	0	0	1	1/2
X_{63}	E_2	1	−1	0	0	1	1/2
X_{62}	E_3	0	1	−1	0	1	1/2
X_{48}	E_4	0	0	1	−1	0	1/2
X_{47}	E_5	0	0	0	1	0	1/2
X_{52}	$D - E_1 - E_2$	0	1	0	0	−1	1/2
X_{53}	$D - E_1 - E_3$	1	−1	1	0	−1	1/2
X_{17}	$D - E_1 - E_4$	1	0	−1	1	0	1/2
X_{18}	$D - E_1 - E_5$	1	0	0	−1	0	1/2
X_{51}	$D - E_2 - E_3$	−1	0	1	0	−1	1/2
X_{37}	$D - E_2 - E_4$	−1	1	−1	1	0	1/2
X_{38}	$D - E_2 - E_5$	−1	1	0	−1	0	1/2
X_{27}	$D - E_3 - E_4$	0	−1	0	1	0	1/2
X_{28}	$D - E_3 - E_5$	0	−1	1	−1	0	1/2
X_{64}	$D - E_4 - E_5$	0	0	−1	0	1	1/2
X_{54}	$2D - E_1 - E_2 - E_3 - E_4 - E_5$	0	0	0	0	1	1/2
X_{85}	$D - E_4$	0	0	−1	1	1	1
X_{75}	$D - E_5$	0	0	0	−1	1	1
X_{86}	$2D - E_1 - E_2 - E_3 - E_4$	0	0	0	1	−1	1
X_{76}	$2D - E_1 - E_2 - E_3 - E_5$	0	0	1	−1	−1	1

(4.36)

A second copy of the partial **10** representation appears here.

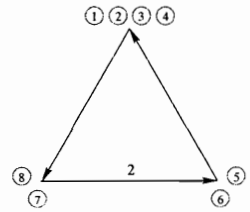

Fields	$S0(10)$
$(X_{61}, X_{63}, X_{62}, X_{48}, X_{47}, X_{52}, X_{53}, X_{17}, X_{18}, X_{51}, X_{37}, X_{38}, X_{27}, X_{28}, X_{64}, X_{54})$	16
$(X_{85}, X_{75}, X_{86}, X_{76}, *, *, *, *, *, *)$	partial 10_a
$(Y_{85}, Y_{75}, Y_{86}, Y_{76}, *, *, *, *, *, *)$	partial 10_b

(4.37)

Figure 4-9: Quiver diagram for Model III of dP_5.

The superpotential for this theory is

$$W_{III} = 16^2 \otimes 10_a + 16^2 \otimes 10_b \tag{4.38}$$

Note that the global symmetry invariant term $\mathbf{16}^4$ does not appear, since none of its components survives the projection onto gauge invariants. It is clear from looking at the 3-block quiver in Figure 4-9 that there are no quartic gauge invariants in this case.

4.3.4 del Pezzo 6

The final model we study is the toric phase of dP_6. There are some indications suggesting that this theory completes the list of toric phases of del Pezzo theories. In particular, the geometric computation of dibaryon R charges (the charges of bifundamental fields can be derived from them) determines that, if all gauge groups were $SU(N)$, the least possible R-charge for a bifundamental field is one for dP_7 and two for dP_8. In this case, the superpotential for dP_7 could only consist of quadratic mass terms, while it would be impossible to construct a superpotential for dP_8 [71]. Since we expect all del Pezzo theories to have nontrivial superpotentials, this seems to rule out such models. Some other particular features, that might be related to the previous one, and differentiate dP_7 and dP_8 from the rest of the del Pezzos arise in the context of (p, q) webs [45, 46], where webs without crossing external legs cannot be constructed beyond dP_6.

The toric phase of dP_6 has 27 fields. The associated divisors are listed in (4.39).

$Node$	L_α
1	E_1
2	E_2
3	E_3
4	$D - E_4$
5	$D - E_5$
6	$D - E_6$
7	D
8	0
9	$2D - E_4 - E_5 - E_6$

	$L_{\alpha\beta}$	J_1	J_2	J_3	J_4	J_5	J_6	R
X_{81}	E_1	-1	0	0	0	0	1	2/3
X_{82}	E_2	1	-1	0	0	0	1	2/3
X_{83}	E_3	0	1	-1	0	0	1	2/3
X_{47}	E_4	0	0	1	-1	0	0	2/3
X_{57}	E_5	0	0	0	1	-1	0	2/3
X_{67}	E_6	0	0	0	0	1	0	2/3
X_{93}	$D - E_1 - E_2$	0	1	0	0	0	-1	2/3
X_{92}	$D - E_1 - E_3$	1	-1	1	0	0	-1	2/3
X_{14}	$D - E_1 - E_4$	1	0	-1	1	0	0	2/3
X_{15}	$D - E_1 - E_5$	1	0	0	-1	1	0	2/3
X_{16}	$D - E_1 - E_6$	1	0	0	0	-1	0	2/3
X_{91}	$D - E_2 - E_3$	-1	0	1	0	0	-1	2/3
X_{24}	$D - E_2 - E_4$	-1	1	-1	1	0	0	2/3
X_{25}	$D - E_2 - E_5$	-1	1	0	-1	1	0	2/3
X_{26}	$D - E_2 - E_6$	-1	1	0	0	-1	0	2/3
X_{34}	$D - E_3 - E_4$	0	-1	0	1	0	0	2/3
X_{35}	$D - E_3 - E_5$	0	-1	1	-1	1	0	2/3
X_{36}	$D - E_3 - E_6$	0	-1	1	0	-1	0	2/3
X_{69}	$D - E_4 - E_5$	0	0	-1	0	1	1	2/3
X_{59}	$D - E_4 - E_6$	0	0	-1	1	-1	1	2/3
X_{49}	$D - E_5 - E_6$	0	0	0	-1	0	1	2/3
X_{71}	$2D - E_2 - E_3 - E_4 - E_5 - E_6$	-1	0	0	0	0	0	2/3
X_{72}	$2D - E_1 - E_3 - E_4 - E_5 - E_6$	1	-1	0	0	0	0	2/3
X_{73}	$2D - E_1 - E_2 - E_4 - E_5 - E_6$	0	1	-1	0	0	0	2/3
X_{48}	$2D - E_1 - E_2 - E_3 - E_5 - E_6$	0	0	1	-1	0	-1	2/3
X_{58}	$2D - E_1 - E_2 - E_3 - E_4 - E_6$	0	0	0	1	-1	-1	2/3
X_{68}	$2D - E_1 - E_2 - E_3 - E_4 - E_5$	0	0	0	0	1	-1	2/3

(4.39)

All fields are accommodated in the fundamental **27** representation of E_6, as shown in (4.41). The superpotential for this theory is simply

$$W = 27^3 \tag{4.40}$$

Fields	E_6
$(X_{81}, X_{82}, X_{83}, X_{47}, X_{57}, X_{67}, X_{93}, X_{92}, X_{14}$ $X_{15}, X_{16}, X_{91}, X_{24}, X_{25}, X_{26}, X_{34}, X_{35}, X_{36}$ $X_{69}, X_{59}, X_{49}, X_{71}, X_{72}, X_{73}, X_{48}, X_{58}, X_{68})$	27

(4.41)

Figure 4-10: Quiver diagram for dP_6.

4.4 Partial represention

We have discussed how the matter content of the quiver theories for each dP_n can be arranged into irreducible representations of the corresponding E_n group. The superpotential can therefore be expressed as the gauge invariant part of a combination of fields invariant under the global symmetry transformations. Our discussion of this classification will be extended in Section 4.6, where we will study how to relate the representation content of Seiberg dual theories.

In Section 4.3, we encoutered some examples (Model II of dP_4, and Models II and III of dP_5) that seem to challenge the applicability of our classification strategy. We mentioned there that in these cases we have to go a step further and consider *partial representations*, and postponed the explanation to this point. The purpose of this section is to give a detailed description of the concept of partial representations and to show that they are a natural construction that enables us to study all the toric del Pezzo quivers from the same unified perspective. We will devote this subsection to explaining the simple rules that can be derived for these theories from a field theory point of view. The next subsection will sharpen these concepts but bases the discussion on the geometry of partial representations.

Theories with *partial representations* are those in which it is not possible to arrange matter fields so that the corresponding E_n representations are completely filled. Naively, it is not clear what are the transformation properties that should be assigned to fields that seem not to fit into representations in these cases. It is not even clear that they can be organized into irreducible representations at all. As we will discuss, this situation neither implies a loss of predictive power nor that these models are exceptionl cases outside of the scope of our techniques, since in order for partial representations to exist, very specific conditions have to be fulfilled.

The idea is to find those fields that seem to be absent from the quiver, and that would join the fields that are present to form irreducible E_n representations. These bifundamental fields should appear in representations and have gauge charges such that, following the rules given in Section 4.3, quadratic terms appear in the superpotential. That is they can form quadratic invariants of the global symmetry group and, in quiver language, they appear as bidirectional arrows. These symmetric terms give masses to the fields under consideration, removing them from the low energy effective description.

Following the previous reasoning, partial representations appear in such a way that the same number of fields are missing from those representations that form quadratic terms. In some cases it is possible for the missing fields to lie on the same representation, which combines with itself to form a quadratic invariant. When this occurs, the number of missing fields is even. The R charges of fields in representations that combine into quadratic invariants and become partial representations add up to 2. Thus, for the specific case of self-combining representations, they should have $R = 1$ in order to be capable of becoming partial.

These general concepts are sufficient to classify the quivers into representations, but do not indicate which are the precise nodes that are connected by the missing fields. One possible way to determine them uses the assignation of divisors to bifundamental fields and is the motive of the next subsection.

4.4.1 The geometry of partial representations

An important question is what the location in the quiver of the fields that are needed in order to complete partial representations is. As we discussed in the previous section, fields missing from partial representations form bidirectional arrows and are combined into quadratic mass terms.

The lists in Section 3 summarize the baryonic $U(1)$ and R charges of the fields that are present in the quiver. For each arrow, these numbers indicate the intersection of its associated divisor with the $n+1$ curves in the non-orthogonal basis of (4.3). Thus, these charges define a set of $n+1$ equations from which the divisor associated to a given bifundamental field can be deduced. Furthermore, as explained in Section 2, the n flavor charges correspond to the Dynkin components of each state. Then, the Dynkin components of the missing fields can be inferred by looking for those that are absent from partial representations. Once these charges are determined, they can be used together with the R charge of the representation to follow the process explained above and establish the divisors for the missing fields.

Based on the divisors that correspond to each node, (4.7) gives the divisors for every possible bifundamental field. Comparing them with the ones for missing fields we determine where they are in the quiver. Let us remark that the examples in Section 4.3 show us that different bifundamentals can have the same associated divisors. In the cases we will study, it is straightforward to check that such ambiguity does not hold for the fields we are trying to identify.

Let us consider the example of Model II of dP_4. There are 19 fields in this theory. Some of them form a full $\mathbf{10}$ and a full $\bar{\mathbf{5}}$ representations. There are four remaining fields that cannot be arranged into full representations of E_4. From the Dynkin components in (4.27), we conclude that X_{27} and X_{37} sit in an incomplete $\mathbf{5}$, while Y_{21} and Y_{31} are part of a $\bar{\mathbf{5}}$. There are six missing fields that should complete the $\mathbf{5}$ and $\bar{\mathbf{5}}$. The Dynkin components ($U(1)$ charges) that are needed to complete the representations can be immediately determined. They are listed in the second column of (4.42). From those, the divisors in the third column are computed. The divisors for each node in the quiver appear in (4.27). Using them, we determine the nodes in

the quiver that are connected by the missing fields.

Representation	(J_1, J_2, J_3, J_4, R)	Divisor	Bifundamental
$\bar{5}$	$(-1,1,0,0,4/5)$	$D - E_2$	Y_{16}
	$(0,0,-1,1,4/5)$	$D - E_4$	Y_{14}
	$(0,0,0,-1,4/5)$	$2D - E_1 - E_2 - E_3 - E_4$	Y_{15}
5	$(1,-1,0,0,6/5)$	$2D - E_1 - E_3 - E_4$	X_{61}
	$(0,0,1,-1,6/5)$	$2D - E_1 - E_2 - E_3$	X_{41}
	$(0,0,0,1,6/5)$	D	X_{51}

(4.42)

The quiver with the addition of these extra fields is shown in Figure 4-11.

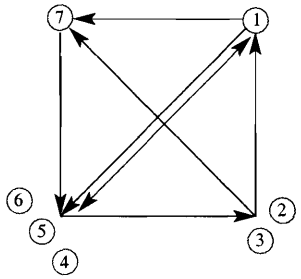

Figure 4-11: Quiver diagram for Model II of dP_4 showing the fields that are missing from partial representations (bidirectional arrow).

Now that we have identified the fields that are missing from the partial representations, we can rewrite the superpotential for this model in an expression that includes all the fields in the theory, both massless and massive. It becomes (note the mass term for the $\mathbf{5}$ and $\bar{\mathbf{5}}_\mathbf{b}$ representations)

$$W_{II} = [10 \otimes \bar{5}_a \otimes \bar{5}_a + 10 \otimes 10 \otimes 5 + 10 \otimes \bar{5}_a \otimes \bar{5}_b] + 10 \otimes \bar{5}_b \otimes \bar{5}_b + 5 \otimes \bar{5}_b \quad (4.43)$$

The products of representations between brackets are already present in (4.29). Keeping in mind that some of the fields in the $\mathbf{5}$ and $\bar{\mathbf{5}}_\mathbf{b}$ remain massless, it is straightforward to prove that the previous expression reduces to (4.29) (which only includes massless fields) when the massive fields are integrated out.

Let us now consider a different example. In Model II of dP_5, fields within a single representation are combined to form quadratic terms. The procedure described above can be applied without changes to this situation. The first step is to identify the Dynkin components and R charge of the missing fields. From them, the corresponding divisors are computed. Finally, the gauge charges of the missing fields are determined. This information is summarized in Table (4.44).

$(J_1, J_2, J_3, J_4, J_5, R)$	Divisor	Bifundamental
$(-1,0,0,0,0,1)$	$2D - E_2 - E_3 - E_4 - E_5$	X_{14}
$(1,-1,0,0,0,1)$	$2D - E_1 - E_3 - E_4 - E_5$	X_{15}
$(0,1,-1,0,0,1)$	$2D - E_1 - E_2 - E_4 - E_5$	X_{16}
$(1,0,0,0,0,1)$	$D - E_1$	X_{41}
$(-1,1,0,0,0,1)$	$D - E_2$	X_{51}
$(0,-1,1,0,0,1)$	$D - E_3$	X_{61}

(4.44)

Figure 4-12 shows where the fields that are missing from the partial **10** appear in the quiver for Model II of dP_5.

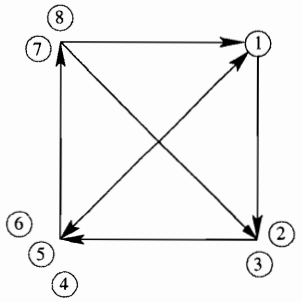

Figure 4-12: Quiver diagram for Model II of dP_5 showing the fields that are missing from partial representations (bidirectional arrow).

Including the massive fields, we can write the superpotential as

$$W_{II} = 16^2 \otimes 10 + 10^2 \tag{4.45}$$

which reproduces (4.35) when integrating out those fields in the **10** representation that are massive.

4.4.2 Partial representations and E_n subgroups

It is possible to make a further characterization of theories with partial representations using group theory. This is attained by considering the transformation properties of fields, both present and missing from the quiver, under subgroups of E_n. These subgroups appear when some of the nodes in a quiver theory fall into blocks. For a block containing n_i nodes, a subgroup $SU(n_i)$ of the enhanced global symmetry E_n becomes manifest. In the general case, the manifest subgroup of the enhanced global symmetry will be a product of such $SU(n_i)$ factors [2]. A matter field is charged under one of these factors if it is attached to one of the nodes in the corresponding block. Let us see how this works in the quivers where partial representations appear.

The first example is Model II of dP_4. Its quiver, shown in Figure 4-6, features two blocks, with two and three nodes each. The corresponding subgroup of E_4 is $SU(2) \times SU(3)$. There are two partial representations, a **5** and a $\bar{\mathbf{5}}$. The way they decompose under this subgroup is

$$\begin{aligned} 5 &\rightarrow (2,1) + (1,3) \\ \bar{5} &\rightarrow (2,1) + (1,\bar{3}). \end{aligned} \tag{4.46}$$

The fields which do not appear in the low energy limit are the ones in the $(1,3)$ and $(1,\bar{3})$ and run from nodes 4, 5, 6 to node 1 and vice versa, as was derived in Section 4.4.1. These fields form a quadratic gauge invariant which is a mass term and is the singlet in the product $(1,3)\otimes(1,\bar{3})$. The singlet in $(2,1)\otimes(2,1)$ is not gauge invariant

[2] dP_n quivers have $n+3$ nodes. For each block of n_i nodes, the associated $SU(n_i)$ factor has rank $n_i - 1$. Thus, we see that for the specific case of 3-block quivers the sum of the ranks of the three $SU(n_i)$ factors is n, corresponding to a maximal subgroup of the corresponding E_n.

so these fields are massless and make up the partial representations. The important observation is that fields present and missing from the quiver can be organized in representations of these relatively small subgroups of E_n, their classification becomes simpler.

A similar situation occurs for Model II of dP_5, depicted in Figure 4-8. The subgroup here is $SU(2) \times SU(2) \times SU(3)$ and we have a partial **10** representation which decomposes as

$$10 \rightarrow (2,2,1) + (1,1,3) + (1,1,\bar{3}). \tag{4.47}$$

The missing fields are the ones in $(1,1,3)$ and $(1,1,\bar{3})$, extending from node 1 to nodes $4,5,6$ and vice-versa respectively in the quiver. As before, the singlet of $(1,1,3) \otimes (1,1,\bar{3})$ is a quadratic gauge invariant that makes these fields massive.

The last example where partial representations occur is Model III of dP_5. This is a three block model and the manifest subgroup of E_5 is $SU(2) \times SU(2) \times SU(4)$, which is maximal. The **10** of $SO(10)$ breaks as

$$10 \rightarrow (2,2,1) + (1,1,6). \tag{4.48}$$

The four fields that appear in each of the two partial **10**'s are the ones in $(2,2,1)$, running from nodes 5, 6 to nodes 7, 8. The matter fields in $(1,1,6)$ are charged only under the $SU(4)$ factor and thus cannot extend between two blocks of nodes. These fields run between pairs of nodes in the $SU(4)$ block (there are exactly six distinct pairs). The fields coming from the two partial representations run in opposite directions making the arrows between the nodes bidirectional. The corresponding superpotential terms are given by the singlet of $(1,1,6) \otimes (1,1,6)$ and make the fields massive.

4.5 Higgsing

It is interesting to understand how the gauge theories for different del Pezzos are related to each other. The transition from dP_n to dP_{n-1} involves the blow-down of a

2-cycle. This operation appears in the gauge theory as a higgsing, by turning a non-zero VEV for a suitable bifundamental field. The determination of possible choices of this field has been worked out case by case in the literature.

The (p, q) web techniques introduced in [46] provide us with a systematic approach to the higgsing problem. In these diagrams, finite segments represent compact 2-cycles. The blow down of a 2-cycle is represented by shrinking a segment in the web and the subsequent combination of the external legs attached to it. The bifundamental field that acquires a non-zero VEV corresponds to the one charged under the gauge groups associated to the legs that are combined. The reader is referred to [46] to a detailed explanation of the construction, interpretation and applications of (p, q) webs in the context of four dimensional gauge theories on D3-branes on singularities. (p, q) webs are traditionally associated to toric geometries, since they represent the reciprocal lattice of a toric diagram (see [73] for a recent investigation of the precise relation). Nevertheless, their range of applicability can be extended to the determination of quivers [45] and higgsings of non-toric del Pezzos.

In this section, we will derive all possible higgsings from dP_n down to dP_{n-1} using (p, q) webs. The passage from dP_3 to dP_2 will be discussed in detail, and the presentation of the results for other del Pezzos will be more schematic. After studying these examples, it will be clear that this determination becomes trivial when using the information about global symmetries summarized in Section 3. The problem can be rephrased as looking for how to higgs the global symmetry group from E_n to E_{n-1} by giving a non-zero VEV to a field that transform as a non-singlet under E_n. We will conclude this section by writing down the simple group theoretic explanation of our findings.

4.5.1 Del Pezzo 3

As our first example, we proceed now to determine all possible higgsings from the four phases of dP_3 down to the two phases of dP_2.

Model I

The (p, q) webs representing the higgsing of this phase down to dP_2 are presented in Figure 4-13. We have indicated in lighter color, the combined external legs that result from blowing down 2-cycles. All the resulting webs in Figure 4-13 are related by $SL(2, \mathbb{Z})$ transformations, implying that in this case it is only possible to obtain Model II of dP_2 by higgsing.

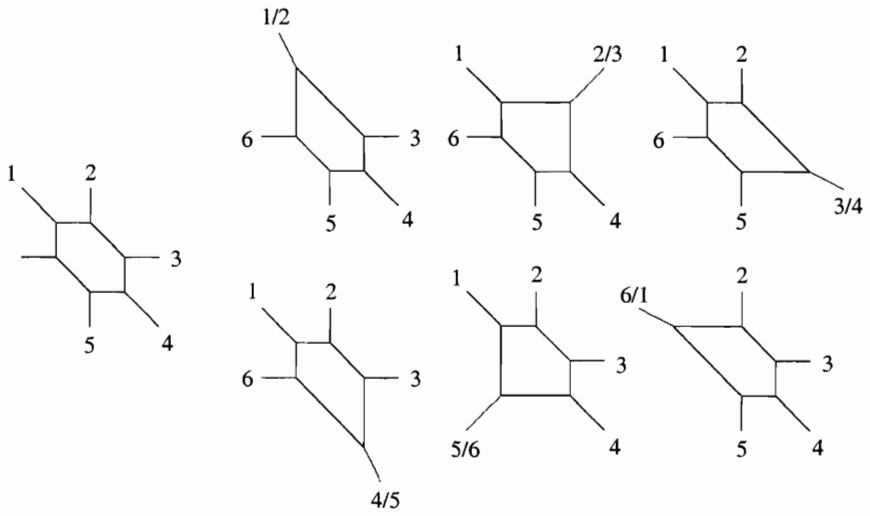

Figure 4-13: (p, q) webs describing all possible higgsings from Model I of dP_3 down to dP_2.

From the external legs that have to be combined in the (p, q) webs in Figure 4-13, we conclude that the lowest component of the following bifundamental chiral superfields should get a non-zero VEV in order to produce the higgsing

$$X_{12}, X_{23}, X_{34}, X_{45}, X_{56}, X_{61} \rightarrow \text{Model II} \Big\} \rightarrow (2, 3) \tag{4.49}$$

We notice that these fields form precisely a $(2, 3)$, i.e. a fundamental representation, of $E_3 = SU(2) \times SU(3)$. We will see that the same happens for all the del Pezzos.

Model II

The (p, q) web diagrams for this model are shown in Figure 4-14, along with the possible higgsings.

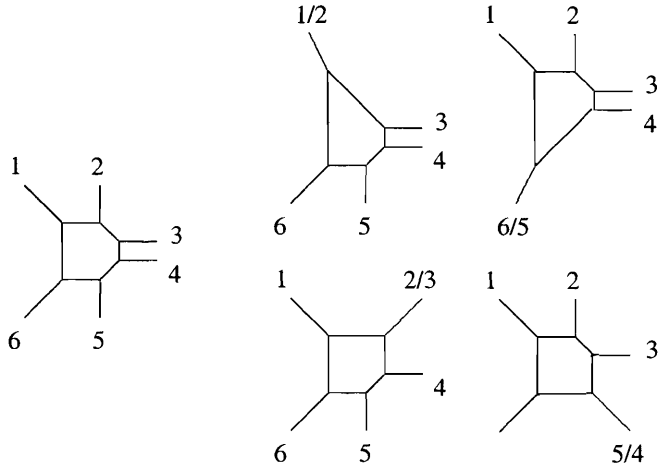

Figure 4-14: (p, q) webs describing all possible higgsings from Model II of dP_3 down to dP_2.

It is important to remind the reader of the node symmetries that appear in the gauge theory when parallel external legs are present [46]. This situation appears in this example, and we have drawn only one representative of each family of (p, q) webs related by this kind of symmetries. In the language of exceptional collections, each set of parallel external legs corresponds to a block of sheaves. The full list of bifundamental fields associated to the higgsings in Figure 4-14 is summarized in the following list

$$\left.\begin{array}{lll} X_{21}, X_{65} & \rightarrow & \text{Model I} \\ X_{32}, X_{42}, X_{53}, X_{54} & \rightarrow & \text{Model II} \end{array}\right\} \rightarrow (2,3) \tag{4.50}$$

Model III

Figure 4-15 shows the (p, q) webs describing the higgsings of this phase. Once again, we have included only one representative of each set of webs related by node symmetries.

Then, we have the following set of fields that produce a higgsing to dP_2.

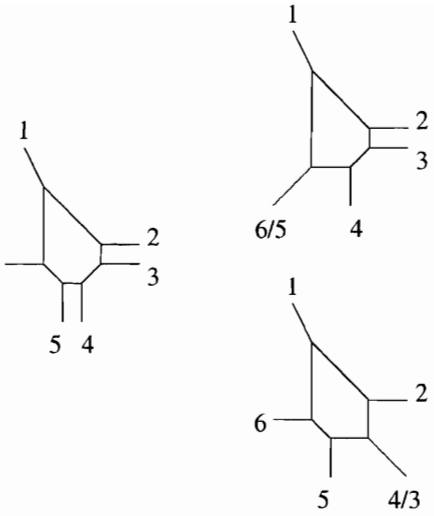

Figure 4-15: (p, q) webs describing all possible higgsings from Model III of dP_3 down to dP_2.

$$\left.\begin{array}{lcl} X_{64}, X_{65} & \rightarrow & \text{Model I} \\ X_{42}, X_{43}, X_{52}, X_{53} & \rightarrow & \text{Model II} \end{array}\right\} \rightarrow (2,3) \tag{4.51}$$

Model IV

Finally, for Model IV of dP_3, we have the webs shown in Figure 4-16

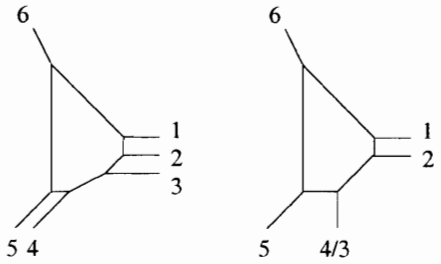

Figure 4-16: (p, q) webs describing all possible higgsings from Model IV of dP_3 down to dP_2.

Indicating that the following fields can take us from this phase to dP_2.

$$\left.\begin{array}{lcl} X_{41}, X_{42}, X_{43}, X_{51}, X_{52}, X_{53} & \rightarrow & \text{Model I} \end{array}\right\} \rightarrow (2,3) \tag{4.52}$$

Having studied the four toric phases of dP_3, we see that for all of them the fields

that produce a higgsing down to dP_2 are those in the fundamental $(2,3)$ representation of $E_3 = SU(2) \times SU(3)$. We will show below how the higgsing of all other del Pezzos is also attained by a non-zero VEV of any field in the fundamental representation of E_n.

4.5.2 Del Pezzo 4

Let us now analyze the two toric phases of dP_4.

Model I

A possible (p,q) web for this model is the one in Figure 4-17. From now on, for simplicity, we will only present the original webs but not the higgsed ones. From Figure 4-17, we determine the following higgsings

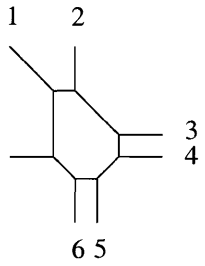

Figure 4-17: (p,q) web for Model I of dP_4.

$$\left.\begin{array}{lcl} X_{35}, X_{36}, X_{45}, X_{46} & \rightarrow & \text{Model I} \\ X_{23}, X_{24}, X_{57}, X_{67} & \rightarrow & \text{Model II} \\ X_{12}, X_{71} & \rightarrow & \text{Model III} \end{array}\right\} \rightarrow 10 \tag{4.53}$$

As expected, the fields that higgs the model down to some dP_3 phase form the fundamental **10** representation of E_4.

Model II

The (p,q) web for Model II is presented in (4-18).

The higgsings in this case become

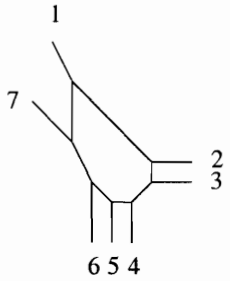

Figure 4-18: (p, q) web for Model II of dP_4.

$$\left.\begin{array}{lll} X_{42}, X_{52}, X_{62}, X_{43}, X_{53}, X_{63} & \rightarrow & \text{Model II} \\ X_{74}, X_{75}, X_{76} & \rightarrow & \text{Model III} \\ X_{17} & \rightarrow & \text{Model IV} \end{array}\right\} \rightarrow 10 \qquad (4.54)$$

4.5.3 Del Pezzo 5

There are three toric phases for dP_5. We study now their higgsing down to dP_4.

Model I

The web diagram corresponding to this theory is shown in Figure 4-19. From it, we see that the fields that can take us to dP_4 by getting a non-zero VEV are

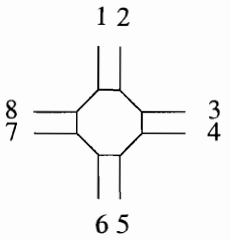

Figure 4-19: (p, q) web for Model I of dP_5.

$$\left.\begin{array}{lll} X_{13}, X_{14}, X_{23}, X_{24}, X_{35}, X_{36}, X_{45}, X_{46} & \rightarrow & \text{Model I} \\ X_{57}, X_{58}, X_{67}, X_{68}, X_{71}, X_{72}, X_{81}, X_{82} & & \end{array}\right\} \rightarrow 16 \qquad (4.55)$$

Model II

The web in this case is shown in Figure 4-20.

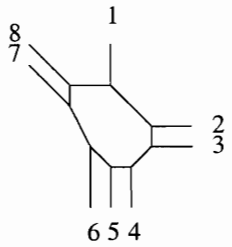

Figure 4-20: (p, q) web for Model II of dP_5.

The fields that higgs the theory down to dP_4 are

$$\left.\begin{array}{lll} X_{24}, X_{25}, X_{26}, X_{34}, X_{35}, X_{36}, X_{47}, X_{57}, X_{67}, X_{48}, X_{58}, X_{68} & \rightarrow & \text{Model I} \\ X_{12}, X_{13}, X_{71}, X_{81} & \rightarrow & \text{Model II} \end{array}\right\} \rightarrow 16 \tag{4.56}$$

Model III

From the (p, q) web in Figure 4-21, we see that the following fields higgs the theory down to dP_4

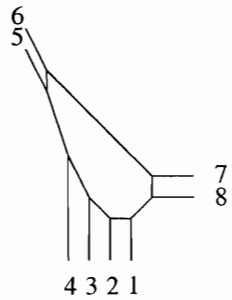

Figure 4-21: (p, q) web for Model III of dP_5.

$$\left.\begin{array}{lll} X_{71}, X_{72}, X_{73}, X_{74}, X_{81}, X_{82}, X_{83}, X_{84} & \rightarrow & \text{Model II} \\ X_{15}, X_{25}, X_{35}, X_{45}, X_{16}, X_{26}, X_{36}, X_{46} & & \end{array}\right\} \rightarrow 16 \tag{4.57}$$

4.5.4 Del Pezzo 6

Finally, we present the web for dP_6 in Figure 4-22, from where we read the following higgsings

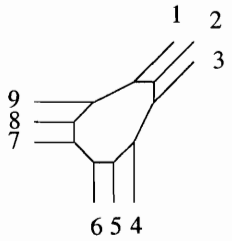

Figure 4-22: (p, q) web for dP_6.

$$\left.\begin{array}{l} X_{14}, X_{15}, X_{16}, X_{24}, X_{25}, X_{26}, X_{34}, X_{35}, X_{36} \\ X_{47}, X_{48}, X_{49}, X_{57}, X_{58}, X_{59}, X_{67}, X_{68}, X_{59} \\ X_{71}, X_{72}, X_{73}, X_{81}, X_{82}, X_{83}, X_{91}, X_{92}, X_{93} \end{array}\right\} \rightarrow \text{Model II} \rightarrow 27 \qquad (4.58)$$

4.5.5 Higgsing global symmetry groups

The results above show that, once the we classify quiver theories using their global symmetry groups, the identification of higgsings that correspond to blow-downs of the geometry becomes straightforward. In particular, we have seen for each dP_n quiver theories that turning on a non-zero VEV for any component field of the fundamental representation reduces the enhanced global symmetry from E_n to E_{n-1} and produces a toric phase of dP_{n-1}.

In the previous section, we established which fields produce the desired higgsing with the aid of (p, q) webs, and discovered that in all cases they form the fundamental representation of the corresponding E_n group. In fact, it is possible to determine which representation to choose for higgsing using solely group theoretic considerations. Generically, more than one representation are present in a given quiver theory. The representations that appear are always basic, meaning that their highest weight vectors are simple roots of the algebra. The clue to the right representation is provided by the Dynkin diagrams for the E_n Lie algebras. The higgsing, and the corresponding

enhanced symmetry breaking $E_n \to E_{n-1}$ can be depicted as the removal of a certain node from the E_n Dynkin diagram. The representation that must be used for the higgsing is the one corresponding to the removed node, in the sense that its highest weight vector is equal to the root corresponding to this node. Practically this means that the higgsed representation must contain a matter field with only one non-zero $U(1)$ charge in the same position as the removed node in the Dynkin diagram[3]. The numbering of the nodes in the Dynkin diagram is unique in the basis of $U(1)$'s that we have chosen, leaving no space for ambiguity.

Let us now discuss the blow-down as a Higgs mechanism in four dimensions. As explained in previous sections, we go down from dP_n to dP_{n-1} by blowing down one of the exceptional divisors E_i $(i = 1 \ldots n-1)$ of the del Pezzo. In fact, by acting on the E_i's with the Weyl group of E_n, other possible choices of cycles to blow down are generated. As we have seen, all these divisors form the fundamental representation of E_n and give precisely the divisors $L_{\alpha\beta}$ of the bifundamentals $X_{\alpha\beta}$ that can be used to appropriately higgs the gauge theory to one for dP_{n-1}. The bifundamental fields $X_{\alpha\beta}$ transform in the $(\bar{N}, N)$ representation of the four dimensional gauge groups $SU(N)_{(\alpha)} \times SU(N)_{(\beta)}$ of the nodes they connect. Blowing down $L_{\alpha\beta}$ corresponds to $X_{\alpha\beta}$ getting a VEV proportional to the $N \times N$ identity matrix, higgsing $SU(N)_{(\alpha)} \times SU(N)_{(\beta)}$ to the diagonal subgroup. The non-zero VEV introduces a scale in the otherwise conformal field theory, and the new quiver will correspond to a new fixed point at the IR limit of the renormalization group flow.

4.6 Global symmetries and Seiberg duality

Section 3 explained how to determine the divisors associated to bifundamental fields when blowing-up or blowing-down 2-cycles or when performing a Seiberg duality. We also saw there how the intersections with the divisors generating the $U(1)$ flavor symmetries determine the E_n Dynkin labels for each bifundamental field. Therefore,

[3]The case $E_3 \to E_2$ is slightly special, in that we have to remove two nodes from the (disconnected) Dynkin diagram. An obvious generalization of the described procedure shows that the representation we have to higgs is the (2,3).

given the representation structure of an original gauge theory, it is possible to determine how a Seiberg dual quiver is organized into E_n representations, by carefully following this algorithm.

The purpose of this section is to give a straightforward alternative procedure to determine the transformation properties under global symmetries of fields in a Seiberg dual theory. It consists of three simple rules, which have their origin in how E_n symmetries are realized in the quivers, and also admits a geometric interpretation. Before going on, it is important to remind the reader the key fact that the bifundamental fields transforming in an irreducible representation of the E_n global symmetry group do not necessarily have the same gauge quantum numbers (i.e. they can be charged under different pairs of gauge groups).

The three steps to deduce the representation structure of a theory based on that of a Seiberg dual are:

- **Step 1:** Fields that are neutral under the dualized gauge group remain in the same representations. Some places in those representations might be left empty by the fields (otherwise known as dual quarks) that are conjugated (their transformation properties are yet to be determined) and by fields that become massive. If the representation is such that it cannot appear in partial form (i.e. it is not possible to combine it with other representation or with itself to form a quadratic invariant), these places will be completed either by meson fields or the conjugated ones (dual quarks).

- **Step 2:** Seiberg mesons appear in the product of the representations of the constituent fields. The precise representation is chosen from all the ones appearing in the product by requiring that those superpotential terms that include the mesons are singlets under the global symmetry group. The geometric interpretation of this step is that the divisor associated to mesons is given by the composition of the two divisors corresponding to the component fields. As we studied above, the requirement that the superpotential terms are E_n singlets is translated to the geometric condition that the associated divisor lays in the

canonical class.

- **Step 3:** The representations for the conjugated fields are determined by requiring that the cubic meson terms added to the superpotential are singlets of the global symmetry group. When doing so, it is very useful to choose these representations based on the entries that were left vacant at step **(1)**, if this is possible. Once again, the geometric perspective is that the sum of the divisors appearing in a superpotential term should be in the canonical class.

We will now use this technique to determine the global symmetries for all toric phases starting from one of them, for del Pezzo surfaces from dP_3 to dP_5. As we will see, the results obtained this way are consistent with the Dynkin components assignations listed in Section 4.3, obtained using the geometric prescription.

4.6.1 Del Pezzo 3

Let us start by applying the above rules to the case of dP_3, deriving the symmetry properties of Models II, III and IV from Model I.

Model II of dP_3

Model II is obtained from Model I by dualizing node 1.

We get

$$\begin{aligned} X_{12} &\to X_{21} & \qquad X_{13} &\to X_{31} \\ X_{51} &\to X_{15} & \qquad X_{61} &\to X_{16} \end{aligned} \tag{4.59}$$

and the following mesons are added

$$\begin{aligned} M_{52} &= X_{51}X_{12} & \qquad M_{53} &= X_{51}X_{13} \\ M_{62} &= X_{61}X_{12} & \qquad M_{63} &= X_{61}X_{13} \end{aligned} \tag{4.60}$$

Applying the stepwise procedure described above:

Step 1:

$$\begin{array}{cc} & SU(2)\times SU(3) \\ (*, X_{23}, X_{34}, X_{45}, X_{56}, *) & (2,3) \\ (X_{24}, X_{46}, X_{62}) & (1,\bar{3}) \end{array} \tag{4.61}$$

One of the $(\mathbf{1},\bar{\mathbf{3}})$ representations has completely disappeared, while the other one stays unchanged. Note that M_{53} and X_{35} become massive and are in complex conjugate representations.

Step 2:

$$\begin{array}{rclcrcl} M_{52} & = & X_{51}X_{12} & = & (1,\bar{3})\otimes(2,3) & = & (2,1\oplus 8) \;\rightarrow\; (2,1) \\ M_{53} & = & X_{51}X_{13} & = & (1,\bar{3})\otimes(1,\bar{3}) & = & (1,3\oplus\bar{6}) \;\rightarrow\; (1,3) \\ M_{62} & = & X_{61}X_{12} & = & (2,3)\otimes(2,3) & = & (1\oplus 3,\bar{3}\oplus 6) \;\rightarrow\; (1,\bar{3}) \\ M_{63} & = & X_{61}X_{13} & = & (2,3)\otimes(1,\bar{3}) & = & (2,1\oplus 8) \;\rightarrow\; (2,1) \end{array} \tag{4.62}$$

Step 3:

In order to determine the transformation properties of X_{21}, X_{31}, X_{15} and X_{16}, we study the meson terms in the superpotential

$$M_{52}X_{21}X_{15} + M_{53}X_{31}X_{15} + M_{62}X_{21}X_{16} + M_{63}X_{31}X_{16} \tag{4.63}$$

Thus, we conclude that

$$\begin{array}{ll} X_{21}\in(1,\bar{3}) & X_{31}\in(2,3) \\ X_{15}\in(2,3) & X_{16}\in(1,\bar{3}) \end{array} \tag{4.64}$$

Putting all these results together

$$\begin{array}{cc} & SU(2)\times SU(3) \\ (X_{31},X_{23},X_{34},X_{45},X_{56},X_{15}) & (2,3) \\ (X_{24},X_{46},X_{62}) & (1,\bar{3}) \\ (M_{62},X_{21},X_{16}) & (1,\bar{3}) \\ (M_{52},M_{63}) & (2,1) \end{array} \tag{4.65}$$

which becomes (4.16) after relabeling the gauge groups according to $(1,2,3,4,5,6) \to (4,6,5,3,2,1)$.

Model III of dP_3

Model III is obtained by dualizing node 5 of Model II. The dual quarks are

$$\begin{array}{ll} X_{15} \to X_{51} & X_{65} \to X_{56} \\ X_{54} \to X_{45} & X_{53} \to X_{35} \end{array} \tag{4.66}$$

The Seiberg mesons are

$$\begin{array}{ll} M_{13} = X_{15}X_{53} & M_{14} = X_{15}X_{54} \\ M_{63} = X_{65}X_{53} & M_{64} = X_{65}X_{54} \end{array} \tag{4.67}$$

The following fields become massive and are integrated out: X_{31}, M_{13}, X_{41} and M_{14}. Let us now apply our set of rules.

Step 1:

$$\begin{array}{cc} & SU(2)\times SU(3) \\ (*,*,*,X_{32},X_{21},X_{42}) & (2,3) \\ (X_{63},*,X_{16}) & (1,\bar{3}) \\ (X_{64},*,Y_{16}) & (1,\bar{3}) \\ (X_{26},*) & (2,1) \end{array} \tag{4.68}$$

Step 2:

$$\begin{array}{rclcrcl} M_{13} & = & X_{15}X_{53} & = & (2,1)\otimes(2,3) & = & (1\oplus 3,3) \;\rightarrow\; (1,3) \\ M_{14} & = & X_{15}X_{54} & = & (2,1)\otimes(2,3) & = & (1\oplus 3,3) \;\rightarrow\; (1,3) \\ M_{63} & = & X_{65}X_{53} & = & (2,3)\otimes(2,3) & = & (1\oplus 3,\bar{3}\oplus 6) \;\rightarrow\; (1,\bar{3}) \\ M_{64} & = & X_{65}X_{54} & = & (2,3)\otimes(2,3) & = & (1\oplus 3,\bar{3}\oplus 6) \;\rightarrow\; (1,\bar{3}) \end{array} \tag{4.69}$$

Step 3:

We now determine the representations for X_{51}, X_{56}, X_{35} and X_{45}. The new terms in the superpotential are

$$M_{13}X_{35}X_{51} + M_{14}X_{45}X_{51} + M_{63}X_{35}X_{56} + M_{64}X_{45}X_{56} \tag{4.70}$$

Then,

$$\begin{array}{ll} X_{51} \in (2,3) & X_{56} \in (2,1) \\ X_{35} \in (2,3) & X_{45} \in (2,3) \end{array} \tag{4.71}$$

Putting all the fields together we have

$$\begin{array}{cc} & SU(2)\times SU(3) \\ (X_{51}, X_{35}, X_{45}, X_{32}, X_{21}, X_{42}) & (2,3) \\ (X_{63}, M_{64}, X_{16}) & (1,\bar{3}) \\ (M_{63}, X_{64}, Y_{16}) & (1,\bar{3}) \\ (X_{26}, X_{56}) & (2,1) \end{array} \tag{4.72}$$

which becomes (4.19) after renaming the gauge groups according to $(1,2,3,4,5,6) \rightarrow (6,2,3,1,4,5)$.

Model IV of dP_3

Model IV can be obtained for example by dualizing node 6 of Model III. Then,

$$\begin{aligned} X_{16} &\to X_{61} & Y_{16} &\to Y_{61} \\ X_{64} &\to X_{46} & X_{65} &\to X_{56} \end{aligned} \tag{4.73}$$

The following mesons are added

$$\begin{aligned} M_{14} &= X_{16}X_{64} & \tilde{M}_{14} &= Y_{16}X_{64} \\ M_{15} &= X_{16}X_{65} & \tilde{M}_{15} &= Y_{16}X_{65} \end{aligned} \tag{4.74}$$

There are no fields that become massive in this case.

Step 1:

$$\begin{array}{cc} & SU(2) \times SU(3) \\ (X_{42}, *, X_{43}, X_{53}, *, X_{52}) & (2,3) \\ (X_{21}, *, X_{31}) & (1,\bar{3}) \\ (Y_{21}, *, Y_{31}) & (1,\bar{3}) \\ (X_{15}, X_{14}) & (2,1) \end{array} \tag{4.75}$$

Step 2:

Meson fields transform according to

$$\begin{aligned} M_{14} &= X_{16}X_{64} = (1,\bar{3}) \otimes (2,3) = (2, 1 \oplus 8) \to (2,1) \\ \tilde{M}_{14} &= Y_{16}X_{64} = (1,\bar{3}) \otimes (2,3) = (2, 1 \oplus 8) \to (2,1) \\ M_{15} &= X_{16}X_{65} = (1,\bar{3}) \otimes (2,3) = (2, 1 \oplus 8) \to (2,1) \\ \tilde{M}_{15} &= Y_{16}X_{65} = (1,\bar{3}) \otimes (2,3) = (2, 1 \oplus 8) \to (2,1) \end{aligned} \tag{4.76}$$

Step 3:

We determine the representations for X_{46}, X_{56}, X_{61} and Y_{61} by requiring the meson superpotential terms to be invariant

$$M_{14}X_{46}X_{61} + \tilde{M}_{14}X_{46}Y_{61} + M_{15}X_{56}X_{61} + \tilde{M}_{15}X_{56}Y_{61} \tag{4.77}$$

And we see that

$$\begin{array}{ll} X_{46} \in (2,3) & X_{56} \in (2,3) \\ X_{61} \in (1,\bar{3}) & Y_{61} \in (1,\bar{3}) \end{array} \tag{4.78}$$

leading to

$$\begin{array}{cc} & SU(2) \times SU(3) \\ (X_{42}, X_{46}, X_{43}, X_{53}, X_{56}, X_{52}) & (2,3) \\ (X_{21}, X_{61}, X_{31}) & (1,\bar{3}) \\ (Y_{21}, Y_{61}, Y_{31}) & (1,\bar{3}) \\ (X_{15}, X_{14}) & (2,1) \\ (M_{15}, M_{14}) & (2,1) \\ (\tilde{M}_{15}, \tilde{M}_{14}) & (2,1) \end{array} \tag{4.79}$$

that reduces to (4.22) by renaming $(1,2,3,4,5,6) \to (6,1,3,5,4,2)$.

4.6.2 Del Pezzo 4

We will now derive the global symmetry properties of Model II of dP_4 from those of Model I.

Model II of dP_4

The preceding examples show in detail how to operate with the rules in Section 4.6 and classify the matter content of dual theories according to their global symmetry properties. We will now move on and apply our program to Model II of dP_4. This example is of particular interest because, as we mentioned in Sections 4.3 and 4.4, it is the first one to exhibit *partial representations*.

We obtain Model II by dualizing Model I on node 7. As usual, those bifundamental fields that are charged under the dualized gauge group reverse their orientation

$$\begin{array}{ll} X_{71} \to X_{17} & X_{72} \to X_{27} \\ X_{57} \to X_{75} & X_{67} \to X_{76} \end{array} \tag{4.80}$$

The following meson fields have to be incorporated

$$\begin{aligned} M_{51} &= X_{57}X_{71} & M_{52} &= X_{57}X_{72} \\ M_{61} &= X_{67}X_{71} & M_{62} &= X_{67}X_{72} \end{aligned} \tag{4.81}$$

There are no fields in this theory that become massive, so we end up in a theory with 19 fields. At this point, we see the first indications that this model is rather peculiar since, as long as singlets are not used, it seems impossible to arrange these 19 fields into a combination of $SU(5)$ representations. Let us apply the three step program as before.

Step 1:

$$\begin{array}{cc} \text{Fields} & SU(5) \\ (X_{45}, X_{23}, X_{46}, *, X_{36}, X_{24}, *, X_{35}, X_{12}, *) & 10 \\ (X_{51}, *, X_{61}, X_{13}, X_{14}) & \bar{5} \end{array} \tag{4.82}$$

Step 2:

$$\begin{aligned} M_{51} &= X_{57}X_{71} = 10 \otimes 10 = \bar{5} \oplus \bar{45} \oplus \bar{50} \rightarrow \bar{5} \\ M_{52} &= X_{57}X_{72} = 10 \otimes \bar{5} = 5 \oplus 45 \rightarrow 5 \\ M_{61} &= X_{67}X_{71} = 10 \otimes 10 = \bar{5} \oplus \bar{45} \oplus \bar{50} \rightarrow \bar{5} \\ M_{62} &= X_{67}X_{72} = 10 \otimes \bar{5} = 5 \oplus 45 \rightarrow 5 \end{aligned} \tag{4.83}$$

Both the $\mathbf{5}$ and $\bar{\mathbf{5}}$ representations will be partially filled with two fields each. The same number of fields are missing in both representations, as explained in Section 4.4.

Step 3:

Looking at the superpotential terms

$$M_{51}X_{17}X_{75} + M_{52}X_{27}X_{75} + M_{61}X_{17}X_{76} + M_{62}X_{27}X_{76} \tag{4.84}$$

we see that

$$\begin{aligned} X_{27} &\in 10 & X_{17} &\in \bar{5} \\ X_{75} &\in \bar{5} & X_{76} &\in 10 \end{aligned} \tag{4.85}$$

and we obtain (4.28). We thus see that partial representations appear naturally when we study the transformation of theories under Seiberg duality.

4.6.3 Del Pezzo 5

We will obtain in this section the global symmetry structure of Models II and III of dP_5 from Model I.

Model II of dP_5

Model II is obtained by dualizing Model I on node 2.

$$\begin{aligned} X_{23} &\to X_{32} & X_{24} &\to X_{42} \\ X_{72} &\to X_{27} & X_{82} &\to X_{28} \end{aligned} \tag{4.86}$$

The following mesons appear

$$\begin{aligned} M_{73} &= X_{72}X_{23} & M_{74} &= X_{72}X_{24} \\ M_{83} &= X_{82}X_{23} & M_{84} &= X_{82}X_{84} \end{aligned} \tag{4.87}$$

No fields become massive.

Step 1:

$$\begin{array}{cc} & SO(10) \\ (X_{81}, X_{57}, *, X_{36}, X_{46}, *, X_{58}, X_{13}, & \\ X_{14}, X_{71}, X_{45}, X_{35}, *, *, X_{67}, X_{68}) & 16 \end{array} \tag{4.88}$$

Step 2:

$$\begin{aligned} M_{73} &= X_{72}X_{23} = 16 \otimes 16 = 10 \oplus 120 \oplus 126 \rightarrow 10 \\ M_{74} &= X_{72}X_{24} = 16 \otimes 16 = 10 \oplus 120 \oplus 126 \rightarrow 10 \\ M_{83} &= X_{82}X_{23} = 16 \otimes 16 = 10 \oplus 120 \oplus 126 \rightarrow 10 \\ M_{84} &= X_{82}X_{24} = 16 \otimes 16 = 10 \oplus 120 \oplus 126 \rightarrow 10 \end{aligned} \tag{4.89}$$

Step 3:

The representations for X_{32}, X_{42}, X_{27} and X_{28} are determined by considering the superpotential terms

$$M_{73}X_{32}X_{27} + M_{74}X_{42}X_{27} + M_{83}X_{32}X_{28} + M_{84}X_{42}X_{28} \tag{4.90}$$

Thus,

$$X_{32}, X_{42}, X_{27}, X_{28} \in 16 \tag{4.91}$$

and we conclude that the matter is arranged as in (4.34).

Model III of dP_5

Dualizing Model II on node 1 we get Model III.

$$\begin{aligned} X_{71} &\rightarrow X_{17} \qquad & X_{81} &\rightarrow X_{18} \\ X_{12} &\rightarrow X_{21} \qquad & X_{13} &\rightarrow X_{31} \end{aligned} \tag{4.92}$$

The Seiberg mesons are

$$\begin{aligned} M_{72} &= X_{71}X_{12} \qquad & M_{82} &= X_{81}X_{12} \\ M_{73} &= X_{71}X_{13} \qquad & M_{83} &= X_{81}X_{13} \end{aligned} \tag{4.93}$$

There are no massive fields.

Step 1:

$$\begin{array}{cc} & SO(10) \\ (*, X_{25}, X_{24}, X_{67}, X_{68}, X_{34}, X_{35}, *, & \\ *, *, X_{58}, X_{57}, X_{48}, X_{47}, X_{26}, X_{36}) & 16 \\ (X_{73}, X_{83}, X_{72}, X_{82}, *, *, *, *, *, *) & \text{partial } 10 \end{array} \tag{4.94}$$

Step 2:

$$\begin{array}{rclcl} M_{72} & = & X_{71}X_{12} & = & 16 \otimes 16 = 10 \oplus 120 \oplus 126 \rightarrow 10 \\ M_{82} & = & X_{81}X_{12} & = & 16 \otimes 16 = 10 \oplus 120 \oplus 126 \rightarrow 10 \\ M_{73} & = & X_{71}X_{13} & = & 16 \otimes 16 = 10 \oplus 120 \oplus 126 \rightarrow 10 \\ M_{83} & = & X_{81}X_{13} & = & 16 \otimes 16 = 10 \oplus 120 \oplus 126 \rightarrow 10 \end{array} \tag{4.95}$$

Step 3:

Looking at the following superpotential terms, we determine the representations for X_{17}, X_{18}, X_{21} and X_{31}.

$$M_{72}X_{21}X_{17} + M_{82}X_{21}X_{18} + M_{73}X_{31}X_{17} + M_{83}X_{31}X_{18} \tag{4.96}$$

Then,

$$X_{17}, X_{18}, X_{21}, X_{31} \in 16 \tag{4.97}$$

and we recover (4.37).

4.7 Conclusions

We have identified the global symmetries of the gauge theories on D3-branes probing complex cones over del Pezzo surfaces dP_n , $3 \leq n \leq 6$. This has been possible due to the association of divisors in the del Pezzo surface to every bifundamental field in the quiver. The correspondence between bifundamental fields and divisors follows from the analogous correspondence for a special class of dibaryon operators. Each of them

is constructed by antisymmetrizing the gauge indices of a single bifundamental field in the quiver. For each dP_n , $3 \leq n \leq 6$, the global $U(1)$ charges of the bifundamental matter of the theories are the sets of Dynkin coefficients in irreducible representations of E_n. We presented the results in Section 4.3. This structure has been obscure in the past due to the fact that, in general, irreducible representation of E_n are formed by bifundamental fields charged under different pairs of gauge groups.

We encountered some theories in which the matter content seems, at a first glance, insufficient to complete representations. We discussed how all the models can be studied within the same framework. The fields that appear to be absent from partial representations sit in bidirectional arrows in the quiver (i.e. quadratic gauge invariants) and that also form quadratic invariants under the global symmetry group. Thus, following the same rules that apply to all other cases, mass terms for these fields are present in the superpotential, and they are integrated out when considering the low energy physics. The geometric interpretation of partial representations was discussed in Section 4.4.1, where we explained how to determine the location in the quiver of the massive fields.

The E_n classification of the models becomes particularly helpful in writing down superpotentials, both for toric and non-toric del Pezzos. The basic elements of their construction are the gauge invariant projections of the singlets under the action of E_n. We have seen how superpotentials become completly determined by this principle (and, in a few cases, information about the higgsing from a higher dP_n). This suggests the possibility of an enhanced E_n global symmetry at the point of infinite gauge coupling.

The blow-down of a 2-cycle takes us from dP_n to dP_{n-1}. This geometric action translates on the gauge theory side to a non-zero VEV for a bifundamental field that higgses the quiver. We have shown in Section 4.5 how to use the group theory classification of the quiver to identify the bifundamental fields that do the correct job. By turning on a VEV for any field in the fundamental representation of E_n, it is higgsed down to one of E_{n-1} and a dP_{n-1} quiver is produced. In this way, we have presented a clear systematic prescription that identifies all possible ways in which a

dP_n quiver can be higgsed to obtain another quiver that corresponds to dP_{n-1}.

It would be interesting to extend the discussion of this chapter to gauge theories on D3-branes probing different singularities, in which other groups of automorphisms will point towards global symmetries of the corresponding field theories. In the case that these symmetry groups include or are included in the ones for del Pezzo theories, the group theory concepts of Section 4.5.5 would indicate how to derive those theories by (un)higgsing.

In Section 4.6, we presented a simple set of rules that determine how the representation structure of a gauge theory transform under Seiberg duality. This was used to rederive the classification based on divisors obtained in Section 4.3.

Chapter 5

The Toric Phases of the $Y^{p,q}$ Theories

5.1 Introduction

As discussed in previous chapters, an interesting class of $\mathcal{N} = 1$ superconformal gauge theories can be geometrically engineered by placing a stack of D3 branes at the apex of a Calabi-Yau cone. These theories are always *quiver gauge theories*. For such a setup it is possible to take the near horizon limit [9, 12, 13], which gives a string dual, namely Type IIB string theory on $AdS_5 \times X_5$. X_5 is the compact Einstein base of the six-dimensional cone, which is Calabi-Yau if X_5 is *Sasaki-Einstein*.

Until about a year ago, the explicit metric on X_5 was known only for two homogeneous Sasaki-Einstein manifolds: S^5 and $T^{1,1}$. The first case corresponds to $\mathcal{N} = 4$ SYM. The second case, the conifold, was analysed in [47] and corresponds to a $\mathcal{N} = 1$ superconformal quiver with gauge group $SU(N) \times SU(N)$. Of course it is possible to take orbifolds of these spaces, leading to manifolds with local geometry of S^5 or $T^{1,1}$. A remarkable development in the field of Sasakian-Einstein geometry changed this situation: Gauntlett, Martelli, Sparks and Waldram in [48, 49] found a countably infinite family of explicit non-homogeneous five-dimensional Sasaki-Einstein metrics. The corresponding manifolds are called $Y^{p,q}$, where $q < p$ are positive integers.

The dual superconformal field theories were constructed in [50]. The theories bare

the name $Y^{p,q}$ and they are quiver gauge theories. The precise structure of the superpotential was found, allowing a comparison between the global symmetries of the gauge theories and the isometries of the manifolds. An analogous match was performed for the baryonic symmetry. As a further non-trivial check of the gauge/string duality, the volumes of the manifolds and of some supersymmetric three-cycles were computed in field theory and matched with geometric results. This was done using the general field theoretic technique of a-maximization, that was also applied to the known del Pezzo 1 (corresponding to $Y^{2,1}$, [51]) and del Pezzo 2 quivers in [52].

The metric on the $Y^{p,q}$ [48, 49, 51] in local form can be written as:

$$\begin{aligned} \mathrm{d}s_5^2 &= \frac{1-y}{6}(\mathrm{d}\theta^2+\sin^2\theta\mathrm{d}\phi^2)+\frac{1}{w(y)q(y)}\mathrm{d}y^2+\frac{q(y)}{9}(\mathrm{d}\psi-\cos\theta\mathrm{d}\phi)^2 \\ &+ w(y)\left[\mathrm{d}\alpha+f(y)(\mathrm{d}\psi-\cos\theta\mathrm{d}\phi)\right]^2 \end{aligned} \tag{5.1}$$

where

$$\begin{aligned} w(y) &= \frac{2(b-y^2)}{1-y} \\ q(y) &= \frac{b-3y^2+2y^3}{b-y^2} \\ f(y) &= \frac{b-2y+y^2}{6(b-y^2)} \ . \end{aligned} \tag{5.2}$$

The coordinate y ranges between the two smallest roots y_1, y_2 of the cubic $b-3y^2+2y^3$. The parameter b can be expressed in terms of the positive integers p and q:

$$b=\frac{1}{2}-\frac{(p^2-3q^2)}{4p^3}\sqrt{4p^2-3q^2} \ . \tag{5.3}$$

The topology of the five-dimensional $Y^{p,q}$ spaces is $S^2\times S^3$. The isometry group is $SO(3)\times U(1)\times U(1)$ for both p and q odd, and $U(2)\times U(1)$ otherwise. This shows up as global symmetry of the quiver gauge theories. We will not enter into the details of these metrics, and we refer the reader to [51] for an in-depth exposition.

On the other side of the correspondence one finds the $Y^{p,q}$ quiver gauge theories. These were constructed in [50] where it was shown that they can be obtained from

the $Y^{p,p}$ theory. The five-dimensional $Y^{p,p}$ space is not smooth, but can be formally added to the list of the $Y^{p,q}$ spaces, and is the base of the $\mathbb{C}^3/\mathbb{Z}_{2p}$ orbifold. The action of the orbifold group on the three coordinates of $\mathbb{C}^3$, $z_i, i = 1,2,3$ is given by $z_i \to \omega^{a_i} z_i$ with ω a $2p$–th root of unity, $\omega^{2p} = 1$, and $(a_1, a_2, a_3) = (1, 1, -2)$. The dual gauge theory is easily found. To get the $Y^{p,q}$ theories, one starts from $Y^{p,p}$ and applies an iterative procedure $p - q$ times. We will discuss the details of this method in the next section. At the IR fixed point, one can use Seiberg duality [1] to find an infinite class of theories that are inequivalent in the UV but flow to the same conformal fixed point in the IR. We call these the *phases* of the $Y^{p,q}$ theories. A finite subclass of these are the so-called *toric phases*. These theories have the property that all gauge groups in the quiver have the same rank and every bifundamental field appears in the superpotential exactly twice: once with a positive sign and once with a negative sign. These properties make explicit the fact that the geometry transverse to the D3 branes is toric (hence the name). The IR equivalence of such theories (also called 'toric duality') was discovered in [53], interpreted as Seiberg duality in [2, 3] and further elaborated in [27, 54].

In this chapter we construct all the *connected* toric phases of the $Y^{p,q}$ quivers. These are the toric phases that can be reached by applying Seiberg duality on self-dual gauge groups, i.e. $SU(N)$ gauge groups with $N_f = 2N_c$ flavors, whose rank remains the same after the duality. Starting from a toric phase, one gets another toric phase by dualizing a self-dual node of the quiver. By studying the phases we get from these dualisations we will derive a method for constructing all the connected toric phases of the $Y^{p,q}$ theories as combinations of different types of "impurities" on the $Y^{p,p}$ quiver. We also demonstrate the agreement between properties of these quivers and geometric predictions by computing the R–charges, and show how one can break conformal invariance (while preserving supersymmetry) by adding fractional branes.

5.2 The connected toric phases

In this section we construct the connected toric phases of the $Y^{p,q}$ quivers. As mentioned in the introduction, the term 'connected' means the that we are only considering the toric phases that can be reached by applying Seiberg duality on self-dual gauge groups. We do not have a general proof that these are all the toric phases, and it is in principle possible that there are toric phases that can only be reached by going through non-toric ones. However, our experience with a number of examples leads us to believe that this is in fact impossible. For instance, in the case of 3-block and 4-block chiral quivers, the classification of [55] implies that all the toric phases are indeed connected. It will be interesting to find a proof of this. A general property of the toric phases (when they exist, as is the case for the $Y^{p,q}$ quivers), for any superconformal quiver, is that they are always 'minimal models', or 'roots' of the Duality Tree. This can be seen in the following way. By the definition of the toric phase all the ranks of the gauge groups are equal. This implies that the 'relative number of flavors' $\mathrm{n}^{\mathrm{F}} \equiv \frac{N_f}{N_c}$ is always a positive integer number. For instance in the models constructed in [50] one always find $\mathrm{n}^{\mathrm{F}} = 2$ or $\mathrm{n}^{\mathrm{F}} = 3$, meaning that there are gauge groups with $N_f = 2N_c$ or $N_f = 3N_c$. Now, if successive application of Seiberg dualities results in a phase with some $\mathrm{n}^{\mathrm{F}} = 1$, a problem would occur, since the IR of a gauge group with $N_f = N_c$ is not superconformal. This would be a contradiction with the results obtained by Seiberg in [1]. The conclusion is that for any toric phase all the relative number of flavors are integer numbers satisfying $\mathrm{n}^{\mathrm{F}} \geq 2$. This is precisely the condition [55] for a model to be a root of the Duality Tree, i.e. a (local) minimum for the sum of the ranks of the gauge groups. In all the models discussed in this chapter, n^{F} will be equal to 2, 3, or 4.

The $Y^{p,q}$ gauge theories can be built starting from $Y^{p,p}$ through an iterative procedure described in detail in [50]. The $Y^{p,p}$ quiver has a particularly simple form. It has $2p$ nodes, each representing an $SU(N)$ gauge group, that can be placed at the vertices of a polygon. If we number the nodes with an index i, $i = 1, \ldots, 2p$ in a clockwise direction, then between nodes i and $i + 1$ there is a double arrow

$X_i^\alpha, \alpha = 1, 2$, representing two bifundamental fields that form a doublet of the $SU(2)$ global symmetry and between nodes i and $i-2$ there is a single arrow Y_i (a singlet of the same $SU(2)$). For example the quiver for $Y^{4,4}$ is shown in the upper left corner of Figure 5-1. Following the conventions of [50], we denote the doublets on the outer polygon as $U_i = X_{2i}, V_i = X_{2i+1}$. In Figure 5-1 the U fields are colored cyan, the V fields green and the Y fields blue. The superpotential for this theory consists of all possible cubic terms contracted in a fashion that makes it an invariant of the $SU(2)$ global symmetry. It is written:

$$W = \sum_{i=1}^{p} \epsilon_{\alpha\beta}(U_i^\alpha V_i^\beta Y_{2i+2} + V_i^\alpha U_{i+1}^\beta Y_{2i+3}). \tag{5.4}$$

The iterative procedure that produces $Y^{p,q}$ is as follows:

- Pick an edge of the polygon that has a V_i arrow[1] starting at node $2i+1$, and remove one arrow from the corresponding doublet to make it a singlet. Call this type of singlet Z_i.

- Remove the two diagonal singlets, Y that are connected to the two ends of this singlet Z. Since the V_i arrow which is removed starts at node $2i+1$ the Y fields which are removed are Y_{2i+2} and Y_{2i+3}. This action removes from the superpotential the corresponding two cubic terms that involve these Y fields.

- Add a new singlet Y_{2i+3} such that together with the two doublets at both sides of the singlet Z_i, an oriented rectangle is formed. Specifically this arrow starts at node $2i+3$ and ends at node $2i$. The new rectangle thus formed contains two doublets which as before should be contracted to an $SU(2)$ singlet. This term is added to the superpotential.

For $Y^{p,q}$ one has to apply the procedure $p-q$ times. For example, a phase of $Y^{4,2}$ is shown at the upper right side of Figure 5-1. The Z singlets are shown in red. The added Y singlets are shown in blue. That they have the same notation

[1] Picking a V arrow instead of a U is purely a matter of convention, since U and V are equivalent in $Y^{p,p}$.

is justified by the the fact that, as shown in [50], they have the same R-charge and global $U(1)$ charges as the Y singlets of $Y^{p,p}$. We will use the term 'impurity' for each 3-step substitution in the $Y^{p,p}$ quiver as above. In this language, $Y^{p,q}$ contains $p-q$ impurities. An important point is that $Y^{p,p-1}$, and in general $Y^{p,q}$, is a conformal gauge theory with $c=a$ only at the IR fixed point.

We must emphasize that what we call IR fixed point is really a manifold of fixed points, as also discussed in [31]. On the string theory side, it is possible to modify the background changing the vev of the axion-dilaton, and giving a vev for the complex B-field over the S^2 (there is precisely one such possible vev since the second Betti number of the $Y^{p,q}$ manifolds is always 1). On the gauge theory side this corresponds, respectively, to a simultaneous rescaling of the gauge and superpotential couplings, and to a relative change in the gauge couplings (there is precisely one gauge coupling deformation since the kernel of the quiver matrix is always two). This discussion implies that the conformal manifold is at least two-complex dimensional. It would be nice to see if there are additional marginal directions, corresponding in the gauge theory to exactly marginal superpotential deformations and in the supergravity to continuosly turning on vevs for the other Type IIB forms (these deformations would probably break the $SU(2)$ global symmetry).

Also note that these IR fixed points, for finite $q \neq p$, are not perturbatively accessible. One way to see this is that there are always *finite* anomalous dimensions for the bifundamental fields (and so for all chiral operators), and this is clearly inconsistent with a fixed point were all the couplings are infinitesimal. A simple way to see that there are always finite anomalous dimensions is by noting that in all the phases of the quivers there are always some gauge groups with $\mathrm{n}^{\mathrm{F}}=2$; the numerator of the NSVZ beta function vanishes with infinitesimal anomalous dimensions only if $\mathrm{n}^{\mathrm{F}}=3$. All Seiberg dual phases share the same property, since the chiral spectrum is invariant under Seiberg duality.

5.2.1 Seiberg duality moves the impurities

The above procedure gives toric phases of $Y^{p,q}$. All nodes (gauge groups) have rank N and every field enters the superpotential exactly twice. However, there is a freedom involved in this construction, namely the choice of positions for the impurities. There are p available positions (the positions of the V doublets) and $p-q$ impurities to distribute. The resulting theories are generally different in the UV. We will now show that they are equivalent at the IR fixed point, related by Seiberg duality. First note that all nodes in $Y^{p,p}$ have $\mathrm{n^F}=3$, so none of them is self-dual. Placing the impurities changes the relative number of flavors from three to two for the nodes at the ends of

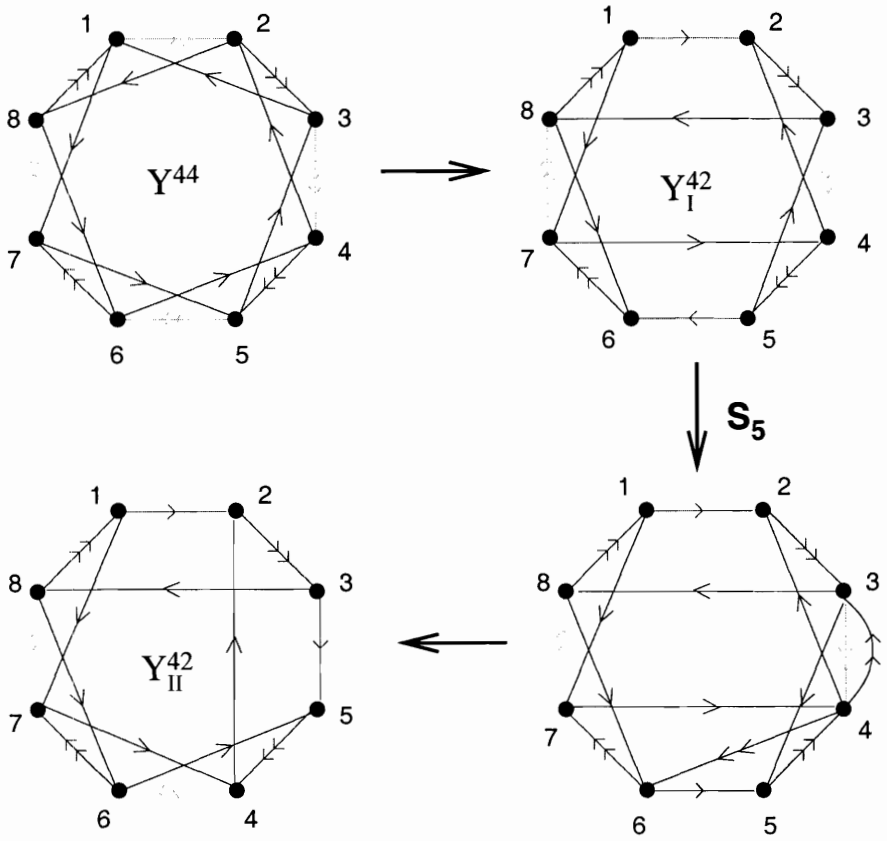

Figure 5-1: Seiberg duality moves the impurities. The notation S_5 means Seiberg duality on node 5.

the Z arrows. So the only self-dual nodes in $Y^{p,q}$ are the ones at the ends of the Z arrows. Dualising any one of these nodes will result in a different toric phase. We illustrate this using the example of $Y^{4,2}$. Phase I (the notation is arbitrary) is shown

in the upper right side of Figure 5-1. We have four choices on which node to dualise: Nodes 1, 2, 5, 6 are self-dual. We choose node 5 and dualise as usual. The new quarks and mesons are shown in black in the lower right side of Figure 5-1. Note that the mesons M_{43}^{α} and M_{46}^{α} are products of a doublet and a singlet of the $SU(2)$ isometry and thus transform as doublets. The quartic term in the superpotential involving nodes 4, 5, 6, 7 becomes a cubic term with nodes 4, 6, 7, and another cubic term, $\epsilon_{\alpha\beta}X_{54}^{\alpha}M_{46}^{\beta}X_{65}$ is added to the superpotential. The cubic term involving nodes 3, 4, 5 becomes a quadratic term $\epsilon_{\alpha\beta}V_1^{\alpha}M_{43}^{\beta}$ which gives mass to these fields, so it must be integrated out in the IR limit. Integrating out these fields we get a new quartic term involving nodes 2, 3, 5, 4. After eliminating the fields that are integrated out and exchanging nodes 4 and 5 we obtain the quiver shown in the lower left side of Figure 5-1. But this is exactly what we get from a different placement of the two impurities. We can describe the effect of Seiberg duality by saying that the impurity has moved by one step. This was also shown in [31] and put to good use in computing duality cascades for $Y^{p,p-1}$ and $Y^{p,1}$. It is easy to see that if we had dualised node six the impurity would have moved one step in the opposite direction in exactly the same fashion. Also, the result of the dualisation depends only on the fact that there is no impurity between nodes 3 and 4. The rest of the quiver goes along for the ride. So dualising one of the nodes at the ends of a Z field moves the impurity one step in the direction of the dualised node, as long as there is no impurity already there. We have shown that the different phases one gets from applying the iterative procedure are indeed toric duals. This fact was briefly mentioned in [50].

5.2.2 Double impurities

The next step in constructing the toric phases of $Y^{p,q}$ is to examine what happens when two impurities 'collide'. We saw before how Seiberg duality on a self dual-node moves the impurity by one step. However, when two impurities are adjacent something different happens. We can illustrate this using $Y^{4,2}$ as an example. It will become clear that the result can be generalized to any $Y^{p,q}$ because the duality affects only the vicinity of the dualised node. We can start from phase II of $Y^{4,2}$

(Figure 5-2). Nodes 1, 2, 3, 4 are self-dual. Dualising nodes 1 or 4 will move the impurities as before. Dualising nodes 2 or 3 leads to a new phase. We choose to dualise node 3. The new quarks and mesons are shown in black. The quartic terms associated with the impurities become cubic terms with nodes 1, 2, 8 and 2, 4, 5, and new cubic terms $\epsilon_{\alpha\beta}X^{\alpha}_{32}M^{\beta}_{24}X_{43}$ and $\epsilon_{\alpha\beta}X^{\alpha}_{32}M^{\beta}_{28}X_{83}$ are added to the superpotential according to the prescription of Seiberg duality. After rearranging the nodes we see the new phase $Y^{4,2}_{III}$ in Figure 5-2. The mesons M^{α}_{28} are shown in golden because as we will see they have different R-charges than the fields we have encountered so far. We denote these fields as C^{α}.

This is a new toric phase, different from the ones constructed from the procedure of [50], but equivalent to these at the IR fixed point. An interesting thing to note is that this phase includes only cubic terms in the superpotential (true only for two impurities) and therefore it is a perturbatively renormalizable gauge theory. A closer look at this quiver shows that it actually can be seen formally as a result of applying the procedure of [50] *twice* on the same V doublet. We call this a *double impurity.* So applying Seiberg duality to a self dual node moves the impurity when there is an 'empty slot', but in the case where there is already another impurity there, the two impurities fuse into a double impurity. It is clear that the result of this dualisation does not depend on the rest of the quiver and so it is not specific to $Y^{4,2}_{II}$. Two adjacent single impurities can be 'fused' in this fashion in any $Y^{p,q}$. In $Y^{4,2}_{III}$, the only self dual nodes are 1 and 3. Dualising node 3 will lead back to $Y^{4,2}_{II}$, since two successive dualisations on the same node always give back the same theory. In exactly the same way, dualising node 1 will break up the double impurity into two adjacent single impurities, giving back the $Y^{4,2}_{II}$ model.

A picture is starting to emerge: Single impurities can be moved around and fused into double impurities, double impurities can be broken into single impurities and all these models are toric phases. In this fashion one can think of Seiberg duality as the 'motion of free particles on a circle'. It remains to see what happens when double impurities 'collide' with single impurities or other double impurities. The answer is that nothing new happens, and single and double impurities are the only possible

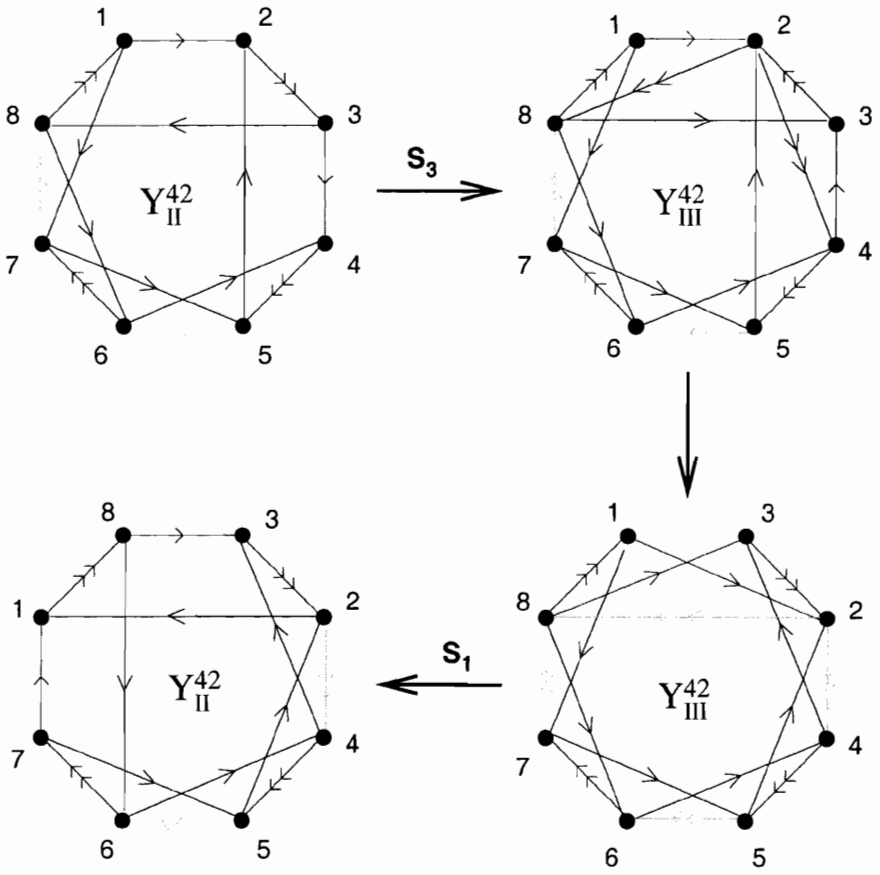

Figure 5-2: Single impurities can fuse into double impurities.

configurations in toric phases. Figure 5-3 illustrates this. We see a phase of $Y^{4,1}$ with a double impurity next to a single impurity, labeled $Y^{4,1}_{I}$. Node 3 has $\mathrm{n}^{\mathrm{F}} = 3$ and dualising it will give a non-toric phase. Nodes 1, 2, 4 are self dual. We already know that dualising node 1 will separate the double impurity into two single ones, and give a model with three single impurities. Dualising 4 will move the single impurity by one step in a clockwise direction. Dualising 2 will also break the double impurity, but the single impurity that is created fuses with the single impurity next to it to give another double impurity. We get a different phase with one single and one double impurity, labeled $Y^{4,1}_{II}$ in Figure 5-3 (note the rearrangement of nodes 2 and 3). A phase of Y^{40} with two double impurities is also shown in the figure. The only self-dual nodes are 1 and 4. Dualising either one separates the corresponding double impurity as before.

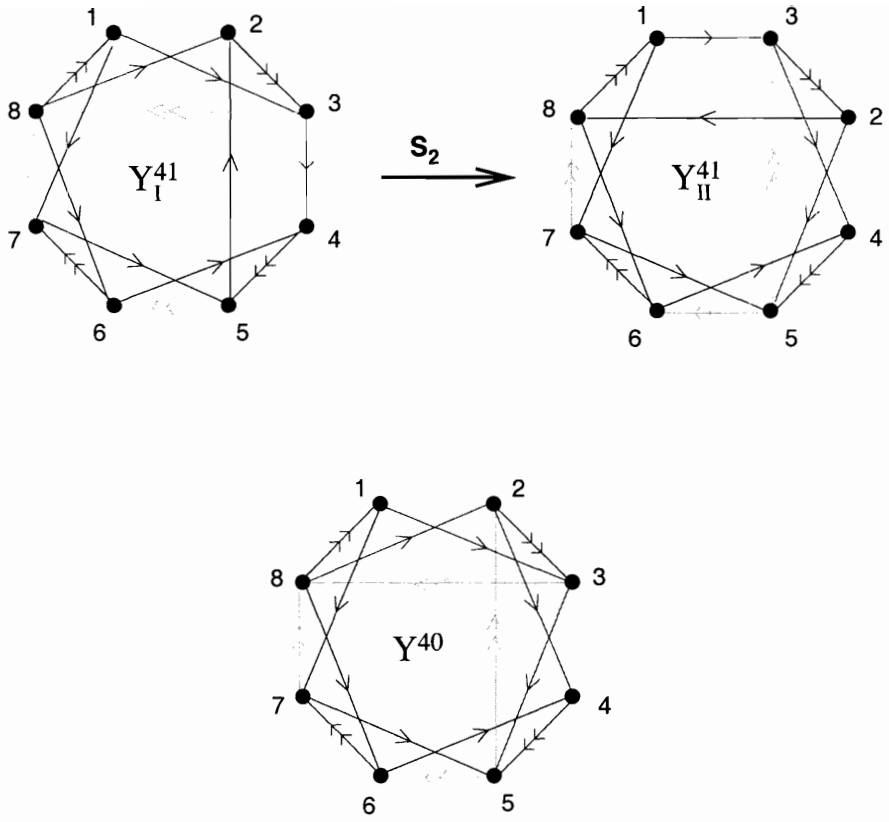

Figure 5-3: Models with one single and one double impurity and with two double impurities.

In all these models, all cubic and quartic gauge invariants in the quiver enter the superpotential. Each of these terms contains two $SU(2)$ doublets which are contracted into an $SU(2)$ singlet. Single impurities contribute quartic terms, double impurities cubic terms, and we also have the cubic terms carried over from $Y^{p,p}$. We can now state the final result: All connected toric phases of $Y^{p,q}$ can be constructed by placing n_1 single impurities and n_2 double impurities, with $n_1 + 2n_2 = p - q$, on $n_1 + n_2$ of the p available positions[2] of the V doublets of $Y^{p,p}$. We have also seen how Seiberg duality connects all these models by moving, fusing and separating the impurities. It is worth mentioning that those models that contain only double impurities have cubic superpotentials and therefore are renormalizable quantum field theories. We note that a double impurity still 'occupies' 4 nodes of the quiver, in the sense that there are 4 consecutive nodes with $\mathrm{n}^{\mathrm{F}} \neq 3$. This explains why it is impossible to

[2]Note that only the relative positions of the impurities matter.

merge together a lot of impurities, and is consistent with the fact that there are only single and double impurities. It is also easy to see that turning on a non-zero vev for the $p-q$ Z fields in all these models higgses the quiver to the one for the orbifold $\mathbb{C}^3/\mathbb{Z}_{p+q}$. We will now proceed to compute the R–charges for a generic toric phase.

5.3 R–charges for a generic toric phase

We can compute the R–charges of any toric phase using a-maximization [23]. The non-R global symmetry group in all of the models that we have constructed is $SU(2)\times U(1)_B \times U(1)_F$. All fields transform in either singlets or doublets of the $SU(2)$ and are charged under the global $U(1)$'s. Since there are two $U(1)$'s with which the R symmetry can mix there will be two unknowns in the a-maximization. Because of the presence of the $U(1)$-flavor the R–charges can be irrational (if only baryonic $U(1)$ symmetries, with vanishing cubic 't Hooft anomalies, are present, one has to maximize a quadratic function). The trial R–charge must be anomaly-free (which is equivalent to the vanishing of the NSVZ beta functions for the $2p$ gauge groups) and all terms in the superpotential must have R–charge two.

The following assignment satisfies these conditions:

- The $(p-q)$ singlets Z have R–charge x.
- The $(p+q)$ diagonal singlets Y have R–charge y.
- The p doublets U have R–charge $1-\frac{1}{2}(x+y)$.
- The $p-(n_1+n_2)$ doublets V have R–charge $1+\frac{1}{2}(x-y)$.
- The n_2 doublets C have R–charge $1-\frac{1}{2}(x-y)$

The quiver structure of the gauge theory automatically implies that the linear 't Hooft anomaly $\mathrm{tr}R$ vanishes, since it is given by a weighted sum of the gauge coupling beta functions $\mathrm{tr}R=\sum N_i\beta_i$ [55]. The cubic 't Hooft anomaly $\mathrm{tr}R^3$, proportional to the gravitational central charges $c=a$ [?, ?], is given by:

$$\begin{aligned}\mathrm{tr}R^3_{\mathrm{trial}}(x,y) &= 2p+(p-q)(x-1)^3+(p+q)(y-1)^3-\frac{p}{4}(x+y)^3+\frac{p-n_1-n_2}{4}(x-y)^3-\frac{n_2}{4}(x-y)^3 \\ &= 2p+(p-q)(x-1)^3+(p+q)(y-1)^3-\frac{p}{4}(x+y)^3+\frac{q}{4}(x-y)^3\ . \end{aligned} \tag{5.5}$$

We have used the relation $n_1+2n_2=p-q$. The expression for $\mathrm{tr}R^3_{\mathrm{trial}}(x,y)$ is the same as the one in [50] and is independent of n_1, n_2. As a consequence, the result is the same for all the toric phases of a given $Y^{p,q}$. This is expected of course, since all toric phases are related by Seiberg duality. The straightforward maximization leads to

$$\begin{aligned} x_{max} &= \frac{1}{3q^2}\left[-4p^2-2pq+3q^2+(2p+q)\sqrt{4p^2-3q^2}\right] \\ y_{max} &= \frac{1}{3q^2}\left[-4p^2+2pq+3q^2+(2p-q)\sqrt{4p^2-3q^2}\right]\ . \end{aligned} \tag{5.6}$$

The R–charges and global U(1) charges for the fields are shown in Table 6.2. The

Field	number	$R-$charge	$U(1)_B$	$U(1)_F$
Z	$p-q$	$(-4p^2+3q^2-2pq+(2p+q)\sqrt{4p^2-3q^2})/3q^2$	$p+q$	1
Y	$p+q$	$(-4p^2+3q^2+2pq+(2p-q)\sqrt{4p^2-3q^2})/3q^2$	$p-q$	-1
U^α	p	$(2p(2p-\sqrt{4p^2-3p^2}))/3q^2$	$-p$	0
V^α	$p-(n_1+n_2)$	$(3q-2p+\sqrt{4p^2-3q^2})/3q$	q	$+1$
C^α	n_2	$(3q+2p-\sqrt{4p^2-3q^2})/3q$	$-q$	-1

Table 5.1: Charge assignments for the five different types of fields in the general toric phase of $Y^{p,q}$.

R–charges and the central charge computed via field theory methods match exactly with the geometric data of the volume of supersymmetric three-cycles and the $Y^{p,q}$ manifolds themselves [50, 51].

The determination of the baryonic charges leads immediately to the determination of the vector of the ranks of the gauge groups in the presence of fractional branes, useful in the study of duality cascades [56, 57, 30], [31]. The reason is that the $U(1)_B$ symmetry is a linear combination of the $2p$ decoupled gauge $U(1)$s, corresponding to

one of the two null vectors of the quiver matrix. It is important that in Table 6.2 we chose the convention that the baryonic charges are always integers numbers.

The procedure for changing the ranks, without developing ABJ anomalies (corresponding to the addition of fractional branes), is very simple and is as follows.

- Start with all the ranks of the gauge groups equal to N. This corresponds to the absence of fractional branes.

- Pick a node I and change the gauge group from $SU(N)$ to, say, $SU(N+M)$.

- Pick an arrow starting from I and arriving at node J. This arrow $I \to J$ has a well defined integer baryonic charge $U(1)_B^{I\to J}$. The rank of the group at node J is precisely $N + M + U(1)_B^{I\to J} M$. For instance, if there is a U-field one has $N + M - pM$, if there is a Z-field one has $N + M + (p+q)M$.

- Pick an arrow starting from J and arriving at node K. Apply the same procedure as above with $U(1)_B^{J\to K}$.

- Go on until all nodes are covered. In case there are only single-impurities, it is enough to do the full loop of lenght $2p$, using the baryonic charges of the doublets U and the singlets Z.

It is clear that in this way the new gauge theory, while not conformal if $M \neq 0$, is still free of ABJ gauge anomalies. Of course there are two possible freedoms in the previous construction. First, one can add an "overall" M to the gauge groups, this is equivalent to a shifting in the number of D3 branes at the singularity. Second, it is possible to rescale M, this is equivalent to a rescaling in the number of wrapped D5 branes (or fractional branes).

As check of the procedure, note that after any closed loop one will always find precisely the initial value. This is due to the fact that any "mesonic" operator (corresponding to close loops in the quiver) has vanishing baryonic charge. We note that this simple procedure is valid for any quiver, also in the case where there are more than one $U(1)$-baryonic symmetries.

5.4 Conclusions

In this chapter we have shown how to construct the toric phases of the $Y^{p,q}$ quivers using a combination of single and double impurity modifications of $Y^{p,p}$. There is an infinity of Seiberg duals for each of the $Y^{p,q}$ theories, forming a duality tree and the toric phases lie at the roots of this tree. The natural question in this context is to understand the structure of the full duality tree, including the non toric phases. It would be nice to understand if the various phases are classified by the solutions of some Diophantine equation, as is the case for higher del Pezzo quivers and for all 3 and 4-block chiral models.

Another related problem is the computation of the duality cascades both from the gauge theory and supergravity perspectives. Very significant progress on this has already been made in [31].

Chapter 6

An Infinite Family of Quiver Gauge Theories

6.1 Introduction

In this last chapter we build upon the knowledge obtained from the $Y^{p,q}$ theories and construct another infinite family of quiver gauge theories which we call $X^{p,q}$. These theories can be Higgsed to $Y^{p,q}$ or $Y^{p,q-1}$ by the right choice of the field that gets a vev, and this property allows us to pinpoint their structure. This adds a new set of examples to the the theories that can be geometrically engineered in string theory.

The first such examples of $\mathcal{N} = 1$ superconformal field theories constructed by placing a stack of D3-branes at the tip of a non-compact Calabi-Yau cone were given for Calabi-Yau spaces which are orbifolds of $\mathbb{C}^3$ [58]. The AdS/CFT correspondence [9, 10, 11] says that there is a gauge/string duality which can be seen by taking the near horizon limit of the D3-branes. The simplest example, where the branes are placed in flat ten dimensional space, gives a duality between type IIB string theory on $AdS_5 \times S^5$ and $\mathcal{N} = 4$ SUSY Yang-Mills. More generally, however, we can place the D3-branes at the tip of a Calabi-Yau cone whose base is a five-dimensional Einstein-Sasaki manifold X_5; the near-horizon limit of this is then Type IIB on $AdS_5 \times X_5$ [12, 13]. This setup breaks additional supersymmetry, generically leaving an $\mathcal{N} = 1$ theory on the D3-branes. These $\mathcal{N} = 1$ theories are quiver gauge theories [58],

i.e. theories with product gauge groups and matter transforming in bifundamental representations.

Ideally, one would like to know the metric on the Calabi-Yau manifold, since this would provide a great deal of information (e.g. volumes of calibrated submanifolds) which could be translated into data about the field theory. In practice, however, it is a difficult task to find these metrics, and until recently the metrics on only two Einstein-Sasaki five-manifolds were known: S^5 and $T^{1,1}$. In [49] an infinite family of Einstein-Sasaki manifolds with topology $S^2 \times S^3$ were found by Gauntlett, Sparks, Martelli and Waldram. These extend previous work by these authors on compactifications of M-theory [48]. These Einstein-Sasaki spaces have been dubbed $Y^{p,q}$, where p and q are integers with $0 < q < p$; the Calabi-Yau cones over these spaces are toric. Sparks and Martelli [51] computed the corresponding toric diagrams and found that $Y^{2,1}$ was in fact the horizon of the complex cone over the first del Pezzo surface dP_1. The corresponding gauge theory is known, having been computed via partial resolution of the orbifold $\mathbb{C}^3/\mathbb{Z}_3 \times \mathbb{Z}_3$ [59].the gauge theories dual to the other $Y^{p,q}$ were constructed by the authors of [50] and can be built through an iterative procedure as explained in Chapter 5. Aspects of the $Y^{p,q}$ theories have been studied in [55, 31, 60, 61, 62, 63, 64, 65].

Some of the $Y^{p,q}$ theories and geometries are already familiar. We can formally extend the range of q to $0 \leq q \leq p$ and find that $Y^{p,p} = S^5/\mathbb{Z}_{2p}$, and $Y^{p,0} = T^{1,1}/\mathbb{Z}_p$. These spaces are not smooth, but can be used as interesting string backgrounds. The corresponding gauge theories to these spaces are well-known [58, 59, 47, 53], and the rest of the $Y^{p,q}$ gauge theories were constructed by a simple procedure that generalizes the method for going from $Y^{2,2} = S^5/\mathbb{Z}_2 \times \mathbb{Z}_2$ to $Y^{2,1} = dP_1$ to $Y^{2,0} = \mathbb{F}_0$.

The fact that the $Y^{p,q}$ spaces are toric is crucial to the above calculations. The toric diagram for a given geometry can be described as points in a three-dimensional lattice; these points describe a $\mathbb{C}^*$ action and uniquely specify the resulting geometry. In this sense, toric geometries are generalizations of $\mathbb{CP}^n$. Equivalently, we can describe the geometry with a *toric fan*, which is a series of vectors ending on the specified lattice points. A toric Calabi-Yau cone then satisfies the additional restriction that the

endpoints of these vectors lie in a plane. For this reason, all the toric diagrams we study can be represented on a two-dimensional lattice.

The construction of quiver gauge theories from toric singularities is a difficult task and many attempts at getting a general formula have been made so far with some or partial success. The general problem is to start with a geometric description, given by the toric data, and then to use it in order to find the corresponding gauge theory that lives on a D3 brane probing the corresponding Calabi-Yau cone. There are a few steps in finding the quiver gauge theory: First, one looks for the gauge groups. The second step is to determine the matter bifundamental fields, and finally one must find the corresponding superpotential which encodes the interaction terms. We have listed these three steps in order by level of difficulty; the third step is often a really hard problem to solve. If for some reason in an independent computation we have a good guess for the quiver gauge theory then it is a straightforward task to compute the corresponding toric data [59]. However, the current known techniques are very long in computation time and are practical only for relatively small (few gauge groups and few matter fields) quiver gauge theories.

Until the computation of the $Y^{p,q}$ quiver gauge theories there were only finitely many toric singularities with known quiver gauge theories, most of which were centered around del Pezzo surfaces and toric diagrams with one or no internal points. This situation changed when the $Y^{p,q}$'s were found. This leads to the hope that there are many more such infinite families of quiver gauge theories for which the computation is a relatively simple task. This is the point of this chapter - to introduce another infinite family of quiver gauge theories for which we know the toric data.

Shortly after the computation of the $Y^{p,q}$ quivers it was realized that the toric diagrams had actually been studied before in a seemingly unrelated environment. In [39, 41] the $Y^{p,q}$ toric diagrams were shown to be dual to a 5-brane web which describes the dynamics of a five dimensional SYM $SU(p)$ gauge theory with 8 supercharges, with q denoting the coefficient of a Chern Simons term. Only a few computations have been made since then [66, 68] and many more may be found. Using the connection to five dimensional gauge theories, we are able to borrow ideas from the construction

of such theories using branes. In particular the process of adding flavors to the five dimensional gauge theory is a useful tool. As we will see this will be interpreted as an inverse Higgs mechanism (unhiggsing) for the quiver gauge theories and essentially is the main tool which allows the construction of the new infinite family of quiver theories. The correspondence with five dimensional theories thus turns out to be useful and may be used in future attempts to find other quiver theories.

In this chapter, we describe a new infinite class of toric geometries and the corresponding gauge theories. To motivate this construction, consider the case of the (complex cone over the) second del Pezzo surface dP_2. Since dP_2 is simply $\mathbb{P}^2$ blown up at two points, it is easy to see that one can blow down an exceptional $\mathbb{P}^1$ to arrive at dP_1. This fact is reflected in the corresponding gauge theories via Higgsing of the dP_2 theory to the dP_1 theory by giving an appropriate bifundamental field a vacuum expectation value. Additionally, however, one can also blow down dP_2 to $\mathbb{F}_0$. As with dP_1, this can also be seen from the gauge theory via Higgsing. Thus, dP_2 is an example of a theory which can be Higgsed to give two different $Y^{p,q}$ theories. The goal of the present chapter is to generalize this construction. The analogous phenomenon in the context of five dimensional gauge theories with $SU(2)$ gauge group was studied in [39, 41, 69], where it is associated with a discrete θ angle and the limit of a gauge theory with one flavor that has a large mass. The sign of the mass then implies which of the resulting theories is either $\mathbb{F}_0$ or dP_1.

The outline of this chapter is as follows. In Section 2, we motivate the construction of the $X^{p,q}$ theories by doing two simple examples. We first explore the relationship between dP_2, dP_1, and $\mathbb{F}_0$ from both the gauge theory and the toric perspectives. In addition, we describe an analogous relationship between the Suspended Pinch Point (SPP), conifold, and $\mathbb{C}^3/\mathbb{Z}_2$. In Section 3, we describe the construction of one phase of the $X^{p,q}$ spaces. It is necessary to treat two cases, $q = p$ and $1 \leq q \leq p-1$, which we do. As a detailed example, we write down the quivers and superpotentials for the $X^{3,1}$, $X^{3,2}$, and $X^{3,3}$ theories. Finally, we discuss the toric diagrams for the dual $X^{p,q}$ geometries. In Section 4, we review the relationship of toric geometry with webs of (p,q) 5-branes, and describe how the Higgsing process can be seen from this

perspective. We discuss how many parameters of the four dimensional theory are related to parameters of the five dimensional theory. In Section 5, we discuss the Seiberg dual phases of the $X^{p,q}$ theories that still have gauge group $SU(N)^{2p+1}$; these are usually called the "toric phases" of the theory. There is a general relationship between the number of bifundamentals in the different toric phases of the $X^{p,q}$ with the number of bifundamentals in the different toric phases of $Y^{p,q}$ and $Y^{p,q-1}$, which we discuss. Finally, in section 6, we discuss the R-charges for the $X^{p,q}$ theories. The calculation is in general computationally quite difficult but can be done for some small values of p. We calculate the R-charges for $X^{2,2}$ and $X^{3,3}$ and find that they not quadratic irrational but instead the roots of quartic equations. In addition, we discuss how although $X^{2,1}$ has a two-dimensional basis of R-charges, this property does not appear to be true for larger values of p.

6.2 Warm-Ups: del Pezzo 2 and the Suspended Pinch Point

Before we proceed to the general construction, we review the case of the gauge theory dual to the cone over dP_2. This theory provides a template for constructing the more general quivers, and as such is a useful example to explore.

Although we do not know the explicit metric on dP_2, the gauge theory has been constructed by partially resolving the space $\mathbb{C}^3/\mathbb{Z}_3 \times \mathbb{Z}_3$ [53, 59]. One quiver for this theory is given in Figure 6-1.

The superpotential is given by

$$\begin{aligned} W &= X_{34}X_{45}X_{53} - X_{53}Y_{31}X_{15} - X_{34}X_{42}Y_{23} && (6.1) \\ &+ Y_{23}X_{31}X_{15}X_{52} + X_{42}X_{23}Y_{31}X_{14} - X_{23}X_{31}X_{14}X_{45}X_{52}. && (6.2) \end{aligned}$$

This superpotential has 3 cubic terms, 2 quartics, and one quintic.

For our purposes in this work, the interesting thing to notice about the dP_2 quiver is that it can be Higgsed to either $Y^{2,1}$ or $Y^{2,0}$ by giving a vev to (for example) X_{52} or

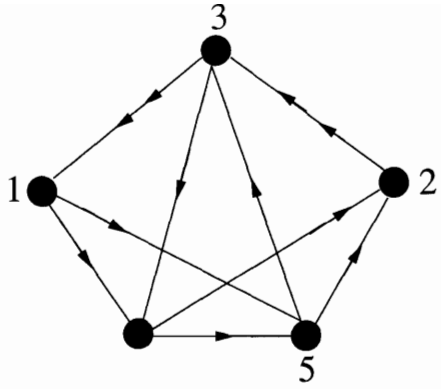

Figure 6-1: One quiver for the dP_2 gauge theory.

X_{45}, respectively. See Figure 6-2 for these quivers. The Higgsing is straightforward: Giving a vev to a bifundamental field simply breaks the $SU(N) \times SU(N)$ group under which it transforms to the diagonal. This means that we should combine those two nodes in the quiver and delete the bifundamental from the theory this flows to in the IR. If there is a cubic term with the bifundamental in it, then we should also delete the other bifundamental fields; the vev will give them a mass and they should be integrated out of the IR theory.

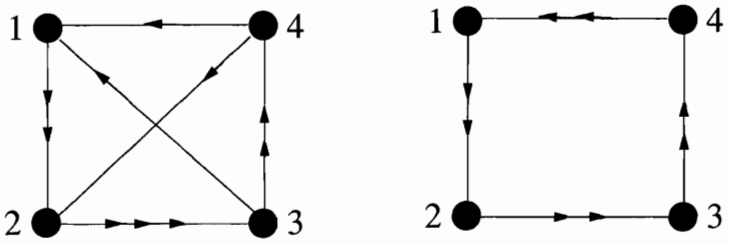

Figure 6-2: The quivers for $Y^{2,1}$ (left) and $Y^{2,0}$ (right)

To be complete, we must also check that the superpotential behaves as it should under Higgsing. Giving a vev to X_{52} is straightforward: Since this bifundamental only appears in terms with four or more fields, we simply delete it from the appropriate terms and relabel the remaining fields. This yields the superpotential

$$\begin{aligned} W_{dP_1} &= X_{31}Y_{12}X_{23} - X_{23}Y_{34}X_{42} - X_{31}X_{12}Y_{23} \\ &+ Y_{23}X_{34}X_{42} + X_{12}Z_{23}Y_{34}X_{41} - Z_{23}X_{34}X_{41}Y_{12}. \end{aligned} \tag{6.3}$$

This is the superpotential for the gauge theory dual to the complex cone over the first del Pezzo surface dP_1. Note that we have relabelled some nodes for aesthetic reasons.

Now, let's see what happens when we set $\langle X_{45} \rangle \neq 0$. Since X_{45} appears in a cubic term $X_{45}X_{53}X_{34}$ in the dP_2 superpotential, this vev has the effect of giving a mass to X_{53} and X_{34}. These fields should then be integrated out of the IR theory. The classical equations of motion are

$$\frac{\partial W}{\partial X_{53}} = X_{45} - Y_{31}X_{15} = 0, \qquad \frac{\partial W}{\partial X_{34}} = X_{53} - X_{42}Y_{23} = 0. \tag{6.4}$$

The resulting superpotential is then purely quartic and is given by

$$W_{\mathbb{F}_0} = X_{12}Y_{23}X_{34}Y_{41} - X_{12}X_{23}X_{34}X_{41} - Y_{12}Y_{23}Y_{34}Y_{41} + Y_{12}X_{23}Y_{34}X_{41}, \tag{6.5}$$

which is indeed the superpotential for $\mathbb{F}_0$. Notice that dP_2 has 11 fields, dP_1 has 10, and $\mathbb{F}_0$ has 8. The cubic term has had the effect of removing two additional fields from the spectrum, as it must.

The R-charges for this theory must be computed via a-maximization [23]. There are *a priori* 11 different R-charges, subject to 5 constraints from anomaly freedom and 6 constraints from the superpotential. One can easily check that there are, however, 4 undetermined R-charges; the maximization must then be done over the space of these 4 charges [52]. This will be a general feature of the new quivers.

Let's now recall the toric presentations of the complex cones over $\mathbb{F}_0, dP_1$, and dP_2. Since these cones are Calabi-Yau, we may represent the toric data with a two dimensional lattice. A perhaps familiar presentation of the toric data for these three surfaces is given in Figure 6-3. The toric diagram can be used to read off the number of 2- and 4-cycles in the corresponding Calabi-Yau cone: The number of internal points is the number of 4-cycles, and the number of 2-cycles can be derived from the requirement that #(0-cycles) + #(2-cycles) + #(4-cycles) = 2(Area). This is the simply the Euler characteristic of the Calabi-Yau. This number is also the same as the number of gauge groups in the dual gauge theory. The Euler characteristic is

also the number of gauge groups in the dual quiver theory, as one can check for these examples[1]. Since each space here is connected, the number of 0-cycles is always 1. It is then straightforward to figure out that the number of 2-cycles for $\mathbb{F}_0, dP_1$, and dP_2 is two, two, and three, respectively. This corresponds exactly with out geometric intuition: Since $\mathbb{F}_0 = \mathbb{P}^1 \times \mathbb{P}^1$, we expect two independent 2-cycles on $\mathbb{F}_0$, and since dP_n is just $\mathbb{P}^2$ blown up at n points, we expect $n+1$ 2-cycles for dP_n.

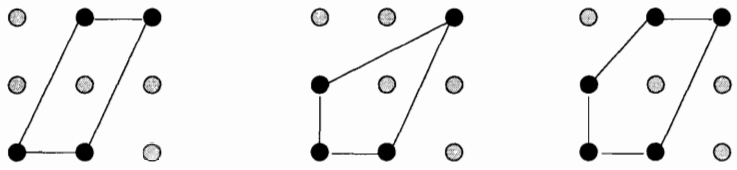

Figure 6-3: The toric data for $\mathbb{F}_0$ (left), dP_1 (center), and dP_2 (right).

Other (and for our purposes later on, more convenient) toric presentations of these spaces are also possible. For future reference, we include these alternate presentations in Figure 6-4. One can easily check that these toric diagrams yield the same number of 2- and 4-cycles as the ones in Figure 6-3. The relation between the two toric presentations is simply that the points along the diagonal in Figure 6-3 have been brought to lie along a vertical line in Figure 6-4; the two toric diagrams correspond to different projections of the full three-dimensional toric diagram for the Calabi-Yau cones. The presentations of Figure 6-3 can be mapped to those of Figure 6-4 by an affine transformation, whose form we do not record here.

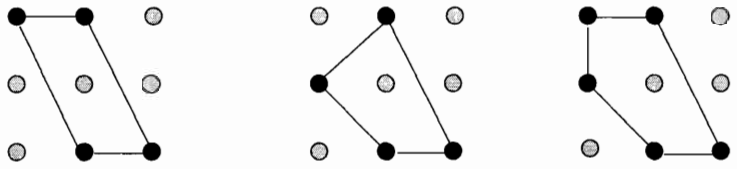

Figure 6-4: Alternate toric data for $\mathbb{F}_0$ (left) dP_1 (center), and dP_2 (right).

Note that it is possible to see Higgsing from the toric diagram. Since twice the area of the toric diagram (i.e. the number of triangles in a triangulation) is the number of gauge groups in the dual superconformal theory, Higgsing corresponds to

[1]This rule was discovered empirically with B. Kol; the brane dimer picture [64, 65] provides a proof.

removing an external point from the toric diagram. All the processes we consider here will never decrease the number of triangles by more than one, meaning that we only consider Higgsings that break $SU(N)^m \to SU(N)^{m-1}$ (cases for which this is not true are more mysterious and not well understood). In the example above, it's easy to see how the toric diagram for dP_2 can be altered to give the toric diagrams for dP_1 and $\mathbb{F}_0$: To get dP_1, delete the top left point from the dP_2 diagram in Figure 6-4; to get $\mathbb{F}_0$, delete the other point on the left side of the toric diagram. Note that the external lines in the toric diagrams correspond to places where the T^3 fiber of the toric geometry has a degenerate cycle. Removing an external line is thus the same as blowing down a 2-cycle; this matches our intuition for how to get from dP_2 to dP_1 or $\mathbb{F}_0$. It is also possible to see this process from the corresponding (p,q)-brane web, which is straightforward to read off the toric diagram. We postpone the discussion of (p,q) webs until Section 4.

As a final warm-up example, we recall the theory that blows down to the gauge theories dual to the conifold and $S^5/\mathbb{Z}_2$. This theory is known as the Suspended Pinch Point (SPP), and was first described in [13]. This theory can be Higgsed to the simplest $Y^{p,q}$ spaces, $Y^{1,0}$ and $Y^{1,1}$. $Y^{1,0}$ is simply the conifold theory, and $Y^{1,1}$ is the $\mathcal{N} = 2$ theory dual to $\mathbb{C}^3/\mathbb{Z}_2$. This Higgsing is illustrated in Figure 6-5.

The superpotential for the SPP is given by

$$W_{SPP} = X_{12}X_{23}X_{32}X_{21} - X_{23}X_{31}X_{13}X_{32} + X_{13}X_{31}X_{11} - X_{12}X_{21}X_{11}. \qquad (6.6)$$

It is easy to see that upon setting $\langle X_{23} \rangle \neq 0$, the superpotential becomes purely cubic. This is exactly as expected for the $\mathcal{N} = 2$ theory, since it is an orbifold of $\mathbb{C}^3$. Giving X_{21} a vev results in a mass term for the fields X_{12} and X_{11}, which must then be integrated out. Doing so reproduces the superpotential for the conifold, given by two quartic terms.

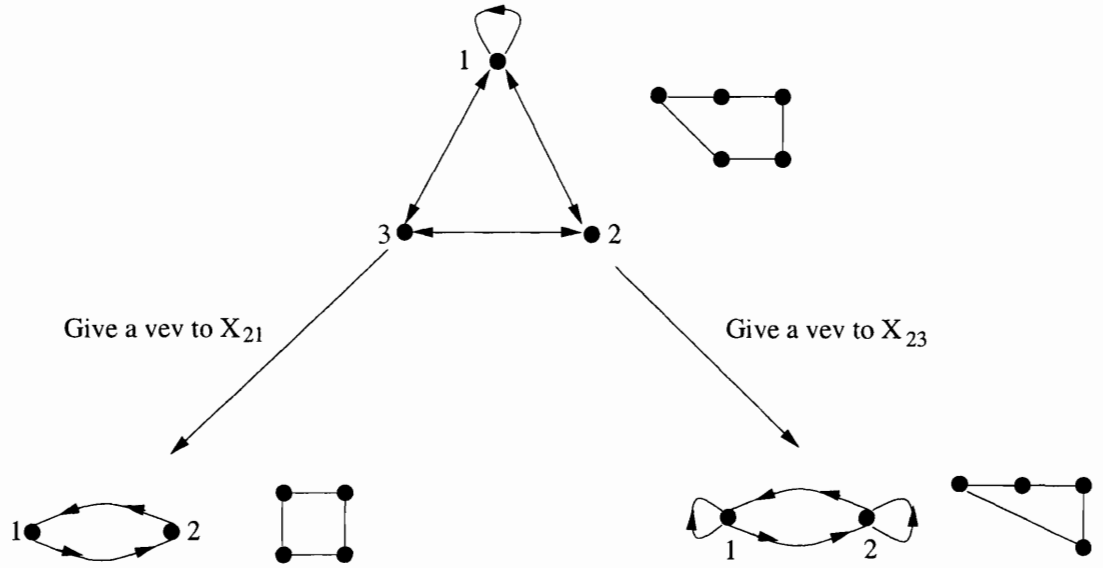

Figure 6-5: The SPP quiver (top) can be Higgsed to the conifold (bottom left) or the $\mathbb{C}^3/\mathbb{Z}_2$ theory (bottom right).

6.3 New quiver theories: $X^{p,q}$

In this section we give a procedure for constructing quivers which blow down to $Y^{p,q}$ and $Y^{p,q-1}$. The general idea is to start with a known quiver gauge theory, say $Y^{p,q}$, blow up its corresponding toric diagram and then to find the effect on the quiver. This procedure was done for several examples in [67]. In many situations there is a unique way to perform such a blow up; this gives the resulting quiver gauge theory. It turns out that in the case we study here we have such a situation in which a blow up gives a unique answer and therefore allows the construction of a new infinite family of quiver gauge theories. We denote the quivers we construct in this chapter by $X^{p,q}$; in this language, the dP_2 quiver would be called $X^{2,1}$, and the SPP would be $X^{1,1}$. We will see that the procedure for constructing dP_2 generalizes nicely to general p and q. The blow-up we construct is the unique possiblity for blowing up the specified node, but of course one could always choose to blow up a different node. In a later section, we will show that blowing up a different node simply results in a theory which is Seiberg dual to the one presented here.

Before we continue on to the $X^{p,q}$ spaces, however, we briefly review the $Y^{p,q}$

quivers. This will be a quick discussion; for more details the reader is referred to [50].

6.3.1 Review of the $Y^{p,q}$ quivers

The $Y^{p,q}$ theories were constructed in [50], following the discovery of the dual geometries and their toric descriptions in [49, 48, 51]. It was shown there that they can be obtained as modifications of $Y^{p,p}$, which happens to be the theory living on a stack of D3 branes placed on the singular point of the orbifold $\mathbb{C}^3/\mathbb{Z}_2 \times \mathbb{Z}_p$. The orbifold theory can be constructed by standard methods as a projection of $\mathcal{N} = 4$ SYM. The gauge group is $SU(N)^{2p}$ where N is the number of D3 branes in the stack. The $Y^{p,p}$ theory has $6p$ bifundamental matter fields transforming in $2p$ doublets $U^\alpha, \alpha = 1, 2$, and $2p$ singlets Y of the $SU(2)$ nonabelian part of the global symmetry group. The superpotential for this theory descends from that of $\mathcal{N} = 4$ and consists of $4p$ cubic terms. The quiver for $Y^{3,3}$ can be seen in the top left corner of Figure 6-6. The superpotential for this theory is

$$\begin{aligned} W_{Y^{3,3}} &= \epsilon^{\alpha\beta} U^\alpha_{12} U^\beta_{23} Y_{31} + \epsilon^{\alpha\beta} U^\alpha_{23} U^\beta_{34} Y_{42} + \epsilon^{\alpha\beta} U^\alpha_{34} U^\beta_{45} Y_{53} \\ &+ \epsilon^{\alpha\beta} U^\alpha_{45} U^\beta_{56} Y_{64} + \epsilon^{\alpha\beta} U^\alpha_{56} U^\beta_{61} Y_{15} + \epsilon^{\alpha\beta} U^\alpha_{61} U^\beta_{12} Y_{26}. \end{aligned} \tag{6.7}$$

The doublets are contracted in a way that respects the $SU(2)$ global symmetry.

To construct the $Y^{p,p-1}$ theory, one picks a doublet in $Y^{p,p}$, say the one between nodes i and $i+1$, and removes one of the two bifundamentals. Then one removes the singlets $Y_{i+2,i}$, $Y_{i+1,i-1}$ and adds a new singlet $Y_{i+2,i-1}$. Four of the cubic terms in the superpotential are eliminated by these removals. Finally, one adds two quartic terms to the superpotential, involving the remaining of the two U fields (now called Z), the new singlet and two U doublets. As an example, the quiver for $Y^{3,2}$ is shown in the top right corner of Figure 6-6. The superpotential for this theory reads:

$$W_{Y^{3,2}} = \epsilon^{\alpha\beta} U^\alpha_{12} U^\beta_{23} Y_{31} + \epsilon^{\alpha\beta} U^\alpha_{23} Z_{34} U^\beta_{45} Y_{52} \tag{6.8}$$

$$+ \quad \epsilon^{\alpha\beta} U^{\alpha}_{45} U^{\beta}_{56} Y_{64} + \epsilon^{\alpha\beta} U^{\alpha}_{56} U^{\beta}_{61} Y_{15} + \epsilon^{\alpha\beta} U^{\alpha}_{61} U^{\beta}_{12} Y_{26}.$$

This procedure repeated $p - q$ times for non-consecutive U doublets yields $Y^{p,q}$. In the lower half of Figure 6-6 we show the quivers for $Y^{3,1}$ and $Y^{3,0}$. Each time q descreases by one, four cubic terms are eliminated and two quartic terms appear in the superpotential. The superpotential of $Y^{p,q}$ therefore has $4q$ cubics and $2(p-q)$ quartics. The modifications to the $Y^{p,p}$ quiver are called *single impurities*; we say that there is a single impurity between any two nodes where there is a bifundamental Z. The specific choice of sites on the quiver where single impurities are placed is not important, since the different theories obtained this way are related by Seiberg duality [63] and have the same IR dynamics. In fact, single impurities can be brought on top of each other and combine into *double impurities*, which contribute cubic terms to the superpotential. We shall say more about these in a later section.

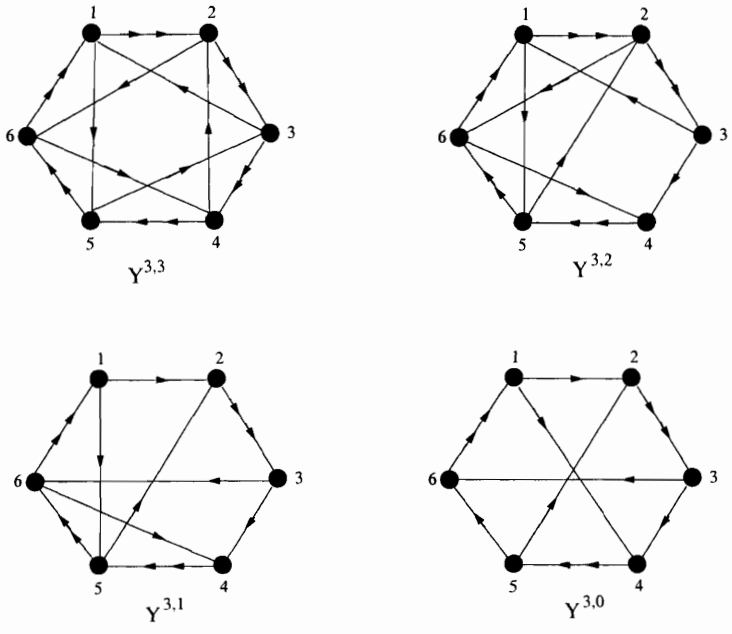

Figure 6-6: Quivers for the $Y^{3,q}$ theories.

6.3.2 $X^{p,q}$ for $1 \leq q \leq p-1$

Now that we have reviewed the $Y^{p,q}$ theories, constructing the $X^{p,q}$ quivers is straightfoward. We first consider the case $0 \leq q \leq p-1$, since the procedure we give here must be altered slightly when $q = p$; this latter case will be described subsequently. Consider the quiver for $Y^{p,q}$. One toric phase of this theory will have $p-q$ single impurities, where double arrows on the outside of the $Y^{p,p}$ quiver have been replaced with single arrows. Since we only consider cases where $q \leq p-1$, there will always be at least one single arrow on the outside of the $Y^{p,q}$ quiver. Without loss of generality, we can choose this arrow to be as close as possible to the leg which is impurified when constructing the $Y^{p,q-1}$ quiver; if the single arrow is farther away, it is always possible to perform a sequence of Seiberg dualities to bring it to the desired position. See Figure 6-7.

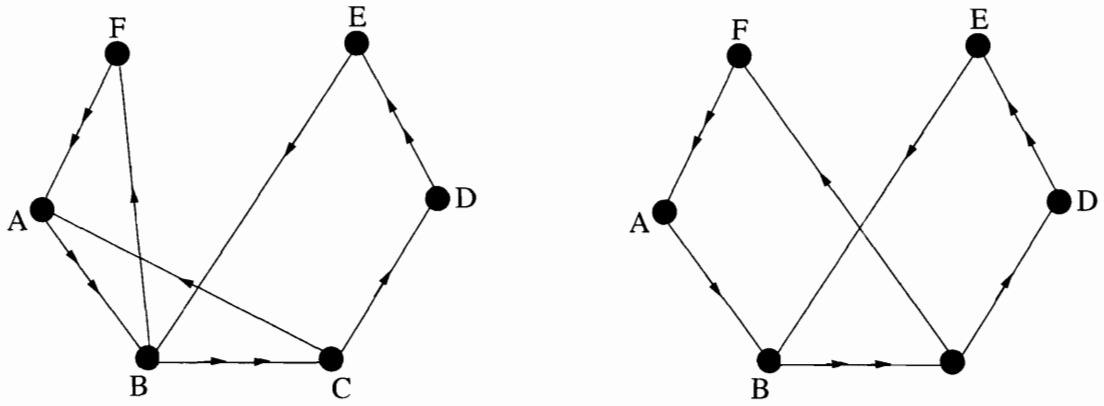

Figure 6-7: The relevant portions of the quivers for $Y^{p,q}$ (left) and $Y^{p,q-1}$ (right). The rest of the quiver is assumed to be in between nodes E and F and is not drawn.

Let's call the node we blow up node B, which we blow up into the two nodes B_1 and B_2. Denote the node before B by A, and the node after B by C. The new $X^{p,q}$ quiver is constructed as follows:

- Draw bifundamentals $X_{AB_1}, X_{B_1B_2}, X_{B_2C}, X_{AB_2}, X_{B_1C}$.
- For all single bifundamentals in the $Y^{p,q}$ quiver of the form X_{nB} (i.e. entering B), draw a bifundamental X_{nB_1}.

- For all single bifundamentals in the $Y^{p,q}$ quiver of the form X_{Bn} (i.e. exiting B), draw a bifundamental X_{B_2n}.
- All other bifundamentals should be left as they are in the $Y^{p,q}$ quiver.

For a graphical depiction of this process, see Figure 6-8.

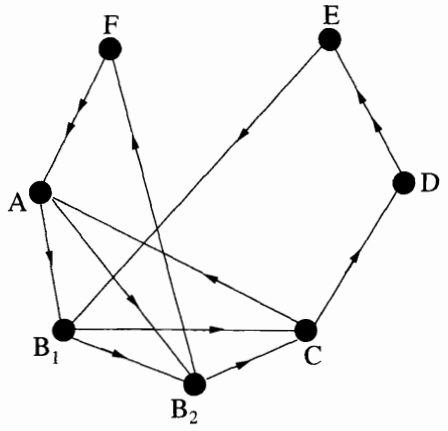

Figure 6-8: The relevant portions of the quivers for $Y^{p,q}$ (left) and $Y^{p,q-1}$ (right).

Notice that there are $4p+2q$ bifundamentals in the $Y^{p,q}$ quiver. Four of them are the double arrows entering and exiting node B, which get replaced with five single arrows in the $X^{p,q}$ quiver. Thus there is a net increase of one in the number of arrows, meaning that this phase of our $X^{p,q}$ theories will always have $4p+2q+1$ bifundamentals. As we saw in the previous section, this is exactly the case with dP_2, which has 11 fields, compared to the 10 fields of dP_1 and the 8 fields of $\mathbb{F}_0$.

Obtaining the superpotential is straightforward. We know that in the superpotential for a $Y^{p,q}$ quiver theory, there are $4q$ cubic terms and $2(p-q)$ quartic terms. To reproduce this upon Higgsing, we must have the superpotential

$$\begin{aligned} W_{X^{p,q}} &= U^{(2)}_{DE} Y_{EB_1} Z_{B_1B_2} Z_{B_2C} Z_{CD} + Z_{AB_1} Y_{B_1C} Y_{CA} + U^{(2)}_{FA} Y_{AB_2} Y_{B_2F} && (6.9) \\ &- Y_{EB_1} Y_{B_1C} Z_{CD} U^{(1)}_{DE} - Y_{AB_2} Z_{B_2C} Y_{CA} - U^{(1)}_{FA} Z_{AB_1} Z_{B_1B_2} Y_{B_2F} && (6.10) \\ &+ \text{unchanged}, && (6.11) \end{aligned}$$

where "unchanged" simply denotes all the other terms in the original $Y^{p,q}$ superpotential, which are unaffected by the blowup. In this sense, blowing up a node is a

"local" procedure – it only affects the fields within 3 nodes of the blown up node.

That the $X^{p,q}$ quivers Higgs to $Y^{p,q}$ and $Y^{p,q-1}$ is now easy to see. Setting $\langle Z_{B_1B_2} \rangle \neq 0$ collapses the nodes B_1 and B_2 back into node B. We lose the field $Z_{B_1B_2}$ and the other fields remain, although we should rewrite any B_1 and B_2 indices as B. This gives (as it should, by our construction), the $Y^{p,q}$ quiver. The superpotential (6.11) also does exactly what it must. Setting $\langle Z_{B_1B_2} \rangle \neq 0$ changes the quintic term into a quartic, and one of the quartics into a cubic. This gives the superpotential for $Y^{p,q}$, where it is obvious that the global $SU(2)$ symmetry has been restored: The doublets are $(Z_{AB_1}, Y_{AB_2}), (Y_{B_1C}, Z_{B_2C}), (U^{(1)}_{FA}, U^{(2)}_{FA})$, and $(U^{(1)}_{DE}, U^{(2)}_{DE})$.

Giving a vev to Z_{B_2C} yields the quiver for $Y^{p,q-1}$. This affects the superpotential in a mildly more nontrivial way than the previous case, since now the fields Y_{AB_2} and Y_{CA} get a mass and should be integrated out. Since these two fields appear in only cubic terms, the net effect of integrating them out is to replace the three cubic terms with one quartic. This quartic is exactly what we'd expect; it is paired with $U^{(1)}_{FA} Z_{AB_1} Z_{B_1B_2} Y_{B_2F}$ under the newly restored $SU(2)$ symmetry. For completeness, we note that the new $SU(2)$ doublets are given by $(U^{(1)}_{FA}, U^{(2)}_{FA}), (U^{(1)}_{DE}, U^{(2)}_{DE})$, and $(Z_{B_1B_2}, Y_{B_1C})$.

We note here that the total number of terms of a given degree in the superpotential for $X^{p,q}$ is easy to figure out. There is always one quintic, $2(p-q)$ quartics, and $4q-1$ cubic terms. The reason is clear: In the $Y^{p,q}$ quiver, there are $2(p-q)$ quartics and $4q$ cubics. Since blowing down the $X^{p,q}$ quiver to $Y^{p,q}$ involves shifting a quintic to a quartic and a quartic to a cubic, we see that the number of quintic terms in the $X^{p,q}$ superpotential is one, whereas the net number of cubic terms decreases by one and the net number of quartics remains the same.

6.3.3 $X^{p,q}$ for $q = p$

Now, let's consider the case $q = p$. The above procedure clearly must be modified, since a quintic term in the superpotential may no longer exist since there is nothing for it to descend to in the $Y^{p,p}$ theory. Nevertheless, the procedure is more or less the same as above, the only difference being that instead of drawing a bifundamental

between node E and node B_1, we draw one between D and B_1. This is shown in Figure 6-9; as before, the parts of the quiver that do not change are not shown.

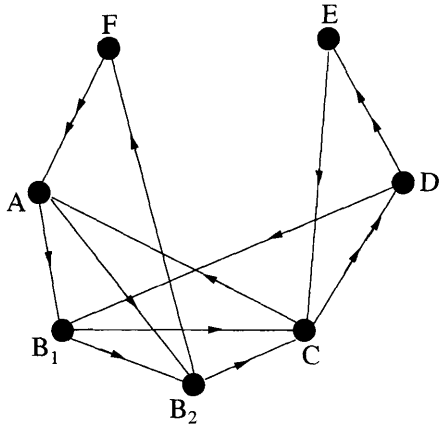

Figure 6-9: The relevant portions of the quivers for $Y^{p,q}$ (left) and $Y^{p,q-1}$ (right).

The superpotential is now given by

$$W_{X^{p,q}} = Z_{B_2C}Y_{CA}Y_{AB_2} + U^{(2)}_{CD}Y_{DB_1}Y_{B_1C} - Y_{B_1C}Y_{CA}Z_{AB_1} - Y_{AB_2}Y_{B_2F}U^{(2)}_{FA} \quad (6.12)$$

$$- Z_{B_2C}U^{(1)}_{CD}Y_{DB_1}Z_{B_1B_2} + Z_{B_1B_2}Y_{B_2F}U^{(1)}_{FA}Z_{AB_1} \quad (6.13)$$

$$+ \text{unchanged}, \quad (6.14)$$

Notice that, as before, when we set $\langle Z_{B_1B_2}\rangle \neq 0$, the theory flows to $Y^{p,p}$, and when we set $\langle Z_{B_1C}\rangle \neq 0$, the theory flows to $Y^{p,p-1}$. In the latter case, the fields Y_{AB_2} and Y_{AC} acquire a mass and should be integrated out; this yields the correct superpotential for $Y^{p,p-1}$.

For general p, then, we see that this $X^{p,p}$ theory has $6p+1$ fields. The superpotential has 2 quartic terms and $4p-2$ cubics. Going to the $Y^{p,p}$ theory simply changes both quartics into cubics, which recovers the $4p$ cubic terms required for this theory. Flowing to the $Y^{p,p-1}$ theory involves shifting one quartic to a cubic, and taking three cubics into one quartic. Thus, the resulting theory has two quartic terms and $4(p-1)$ cubics, which is correct for $Y^{p,p-1}$.

It is worth pointing out again that the above prescription gives merely one way

of constructing the $X^{p,q}$ theories, and there are many different possible toric phases of these theories. We will explore these dualities in a later section.

6.3.4 An example: $X^{3,1}$, $X^{3,2}$, and $X^{3,3}$

As an illustrative example, we now present quivers for $X^{3,1}$, $X^{3,2}$, and $X^{3,3}$. These theories will Higgs to the quivers for $Y^{3,0}, Y^{3,1}, Y^{3,2}$, and $Y^{3,3}$ in Figure 6-6. Apply the procedure outlined in the previous sections is straightforward, and yields the quivers in Figure 6-10.

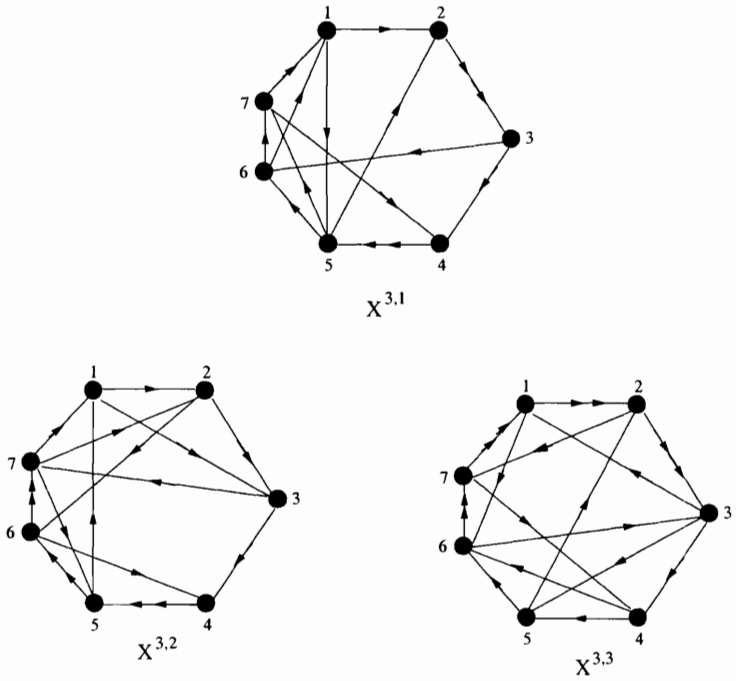

Figure 6-10: Quivers for a particular phase of $X^{3,1}$, $X^{3,2}$, and $X^{3,3}$.

We can easily write down the superpotentials for these theories. They are

$$\begin{aligned} W_{X^{3,1}} &= U_{23}^{(2)} Y_{36} Z_{67} Z_{71} Z_{12} + Z_{56} Y_{61} Y_{15} + U_{45}^{(1)} Y_{57} Y_{74} \\ &- Y_{36} Y_{61} Z_{12} U_{23}^{(1)} - Y_{57} Z_{71} Y_{15} - U_{45}^{(2)} Z_{56} Z_{67} Y_{74} \\ &+ \epsilon^{\alpha\beta} U_{23}^{\alpha} Z_{34} U_{45}^{\beta} Y_{52}, \end{aligned} \tag{6.15}$$

$$
\begin{aligned}
W_{X^{3,2}} &= U_{45}^{(2)} Y_{51} Z_{12} Z_{23} Z_{34} + Z_{71} Y_{13} Y_{37} + U_{67}^{(1)} Y_{72} Y_{26} \\
&- Y_{51} Y_{13} Z_{34} U_{45}^{(1)} - Y_{72} Z_{23} Y_{37} - U_{67}^{(2)} Z_{71} Z_{12} Y_{27} \\
&+ \epsilon^{\alpha\beta} U_{45}^{\alpha} U_{56}^{\beta} Y_{64} + \epsilon^{\alpha\beta} U_{56}^{\alpha} U_{67}^{\beta} Y_{71},
\end{aligned}
\tag{6.16}
$$

and

$$
\begin{aligned}
W_{X^{3,3}} &= Z_{56} Y_{63} Y_{35} + U_{67}^{(2)} Y_{74} Y_{46} - Y_{46} Y_{63} Z_{34} - Y_{35} Y_{52} U_{23}^{(2)} \\
&- Z_{56} U_{67}^{(1)} Y_{74} Z_{45} + Z_{45} Y_{52} U_{23}^{(1)} Z_{34} \\
&+ \epsilon^{\alpha\beta} U_{67}^{\alpha} U_{71}^{\beta} Y_{16} + \epsilon^{\alpha\beta} U_{71}^{\alpha} U_{12}^{\beta} Y_{27} + \epsilon^{\alpha\beta} U_{12}^{\alpha} U_{23}^{\beta} Y_{31}.
\end{aligned}
\tag{6.17}
$$

As they must, these become the $Y^{3,q}$ superpotentials upon giving vevs to the appropriate fields and integrating out where necessary.

6.3.5 Toric Diagrams for $X^{p,q}$

We now describe the toric presentation of the $X^{p,q}$ spaces. As discussed in the introduction, it is a rare occurrence to know the toric diagram corresponding to a given quiver. The Forward Algorithm [59] can be used to extract the toric data for simple quivers, but it is computationally prohibitive for quivers with many nodes. So knowing the toric data dual to an infinite number of quivers is highly nontrivial. Finding the toric data for the $X^{p,q}$ theories is straightforward, since we can use our intuition from dP_2 to simply write down the answer and then check that it is correct. First, we note two different toric presentations of the space $Y^{p,q}$; these are given in Figure 6-11. The toric data on the left is the presentation used in [51, 50]; the toric data on the right is simply an alternate projection which is particularly useful for our purposes[2]. Notice that for a given p, the only point that moves is the point along the left edge of the lattice. As q decreases, this point moves **up**; at $q = 0$ we recover the expected

[2]This representation was also used in [60].

parallelogram for $Y^{p,0}$.

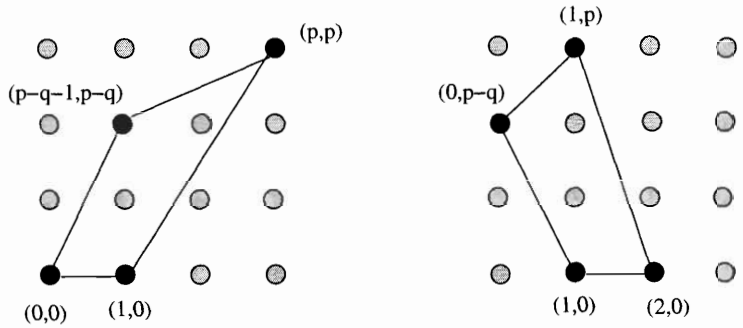

Figure 6-11: Two different presentations of the toric data for $Y^{p,q}$. The figures here are $Y^{3,1}$.

The toric data for $X^{p,q}$ is now easy to intuit. Since we need a space which blows down to both $Y^{p,q}$ and $Y^{p,q+1}$, we simply include both points on the left edge of the lattice, as in Figure 6-12. Removing the top left point leaves the toric diagram for $Y^{p,q}$, and removing the one below it yields the toric diagram for $Y^{p,q-1}$. Note that, as for $Y^{p,q}$, these two points move **up** as q decreases.

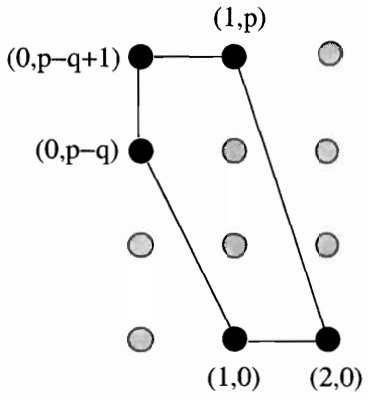

Figure 6-12: The toric data for $X^{p,q}$. This diagram is for $X^{3,1}$, which blows down to $Y^{3,0}$ and $Y^{3,1}$.

There are many checks that these are the correct toric diagrams dual to the $X^{p,q}$ quivers. First, one may use the Forward Algorithm of [59] to extract the toric data. These have been checked for small p, and yield the expected results [3]. We may also check the number of gauge groups, which is equal to the number of triangles in a

[3]We thank Alan Dunn for this calculation.

triangluation of the toric diagram. This should be equal to $2p + 1$ in general, and it is straightforward to see that this is correct: The $Y^{p,q}$ theories have $2p$ triangles, and the effect of adding the extra node is to add one more. Additionally, we can read off the even Betti numbers of the Calabi-Yau cone. There are $p - 1$ internal points, corresponding to $p - 1$ 4-cycles, and since the space is connected there is only one 0-cycle. Therefore, there must be $p + 1$ 2-cycles. Thus, the number of 2-cycles for the $X^{p,q}$ theories is one greater than it is in the lower $Y^{p,q}$ theories, as we expect by analogy to dP_2.

Notice that we can rephrase the above as follows: If I is the number of internal points in the toric diagram and E is the number of external points, then the number of 4-cycles is I, and the number of 2-cycles is $I + E - 3$. This has an interpretation in the related five dimensional gauge theory, as we will discuss in the next section.

We also can find some properties of the corresponding Sasaki-Einstein manifold at the base of the Calabi-Yau cone[4]. For a Sasaki-Einstein space whose toric diagram has d external lines, $H_3 = \mathbb{Z}^{d-3}$, so here we find $H_3(X^{p,q}) = \mathbb{Z}^2$. Thus there are always two 3-cycles available for a D3-brane to wrap; this will be discussed further in Section 6. The topological possibilities for five-dimensional spaces are known, thanks to Smale's Theorem. Here, we can say that the $X^{p,q}$ Sasaki-Einstein manifolds for $p \neq q$ (the $p = q$ case is singular) are a connected sum $(S^2 \times S^3)\#(S^2 \times S^3)$.

Knowing that the toric diagram in Figure 6-12 gives a Calabi-Yau dual to the $X^{p,q}$ theories is highly nontrivial. Although our construction of the gauge theories is done without ever considering the dual geometry, it is important to point out that we know information about **both** sides of the AdS/CFT duality. The metrics on the $X^{p,q}$ geometries are not known, and appear to be quite difficult to calculate. The $Y^{p,q}$ theories had a global $SU(2)$ symmetry; the existence of this non-Abelian symmetry was crucial to figuring out the metrics on the Sasaki-Einstein manifolds [49]. The $X^{p,q}$ gauge theories have only $U(1)$ global symmetries, so we lose the power of the non-Abelian isometry when trying to find the dual metrics. Thus, the Sasaki-Einstein metrics on these spaces are unknown, and probably rather difficult to derive.

[4]We thank James Sparks for discussions on this.

6.4 (p,q)-brane webs and 5d gauge theories

It is known that one can get a five-dimensional theory associated to the theory living on the D3-branes at the tip of the Calabi-Yau cone by writing down a web of (p,q)[5] 5-branes [39]; the procedure for deriving the brane web from the corresponding toric diagram is well-known [40, 41]. More mysterious, however, is what one can say about the resulting 5-dimensional gauge theory living on the 4+1 dimensions common to all the 5-branes. Some things are known about the correspondence between the five dimensional theory and the related four dimensional quiver [46], but much still remains unkown. Let us now briefly review what is known about (p,q)-webs and the associated 5 dimensional gauge theories.

Type IIB string theory has a vast armada of 5+1 dimensional branes, the (p,q) 5-branes. (p,q) 5-branes are bound states of different numbers of D5-branes and NS5-branes; we take the convention that a (1,0) brane is a D5-brane, and a (0,1) brane is an NS5-brane. A (p,q) 5-brane is simply the magnetic dual of a (p,q) string, and may be thought of as coming from an M5-brane wrapped on a (p,q)-cycle of a T^2. The tension of an arbitrary (p,q) brane is then given by $T_{(p,q)} = |p + \tau q| T_{D5}$, where τ is the Type IIB axion-dilaton. These (p,q) 5-branes are useful tools for studying 5d gauge theories, via arranging the branes in a network such that they share 4+1 dimensions. The remaining dimension can be taken to lie in a plane, and the branes can be arranged in a network called a (p,q) web. Of course, placing branes at generic angles will break all supersymmetry. The requirement that a web be stable and preserve supersymmetry can be summed up in the conditions

$$\frac{\Delta x}{\Delta y} = \frac{p}{q} \qquad \text{and} \qquad \sum_i p_i = \sum_i q_i = 0. \tag{6.18}$$

In (6.18), the first condition states that the slope of a brane in the (x, y) plane is equal to the ratio of its (p,q) charges, and the second condition is simply conservation of p and q charge at each vertex (the sum is over all branes ending at a given vertex). The

[5]Here we run into the problem of using the grouping (p,q) in two different contexts. (p,q) for 5-branes will always be in Roman, and (p, q) for $Y^{p,q}$ will be in math (italic).

slope condition ensures that one quarter of the supersymmetry is preserved, giving the 8 supercharges for a five-dimensional $\mathcal{N} = 1$ theory.

It is now well-known that one can associate a toric diagram to a (p,q) web via a straightforward procedure, which we now review. First, one needs to pick a triangulation of the toric diagram. We have done this for dP_1 in Figure 6-13. The brane web is now essentially just the dual of this diagram: To construct it, just draw the lines orthogonal to the lines in the triangulated toric diagram. External lines in the toric diagram correspond to semi-infinite branes, and internal lines correspond to branes with finite extent in the (x, y)-plane. Notice that a consequence of this is that the number of internal points in the toric diagram corresponds to the number of closed polygons in the brane web.

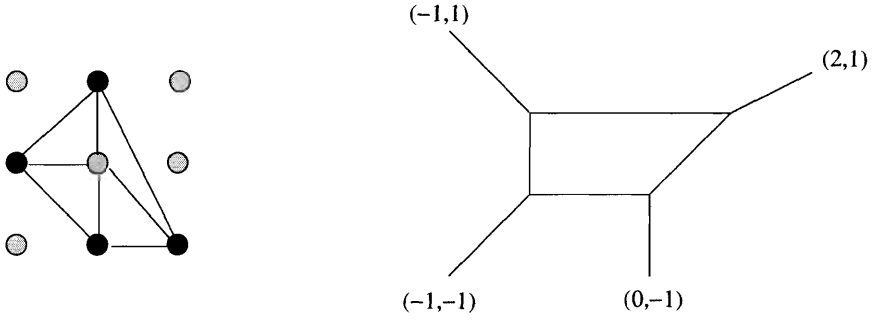

Figure 6-13: A triangulation of the toric data for dP_1 and the corresponding brane web.

As a warm-up for finding the $X^{p,q}$ brane webs, let's see how one can use the web for dP_2 to get the associated webs for dP_1 and $\mathbb{F}_0$. Related discussion can be found near Figure 12 of [39]. The brane webs for dP_2, dP_1, and $\mathbb{F}_0$ are shown in Figure 6-14; we have used the toric data of Figure 6-4 to construct them. Notice that the dP_2 web has a semi-infinite horizontal brane, which we have drawn in red. This is a D5-brane, and shows up in the 5d theory as a massive flavor. As we move this brane up or down, the mass of the flavor changes and it may then be integrated out of the theory. Interestingly, the resulting theory is different depending how one increases the mass: By moving the (-1,0) D5-brane up, it hits the (0,1) brane and results in a (-1,1) brane, giving the web for dP_1. By moving the D5-brane down, it hits the (-1,-1) brane at the bottom and results in a (-2,-1) brane, giving the $\mathbb{F}_0$ brane web. We will see analogous

behavior in the $X^{p,q}$ brane webs when we generate the two possible descendant $Y^{p,q}$ webs.

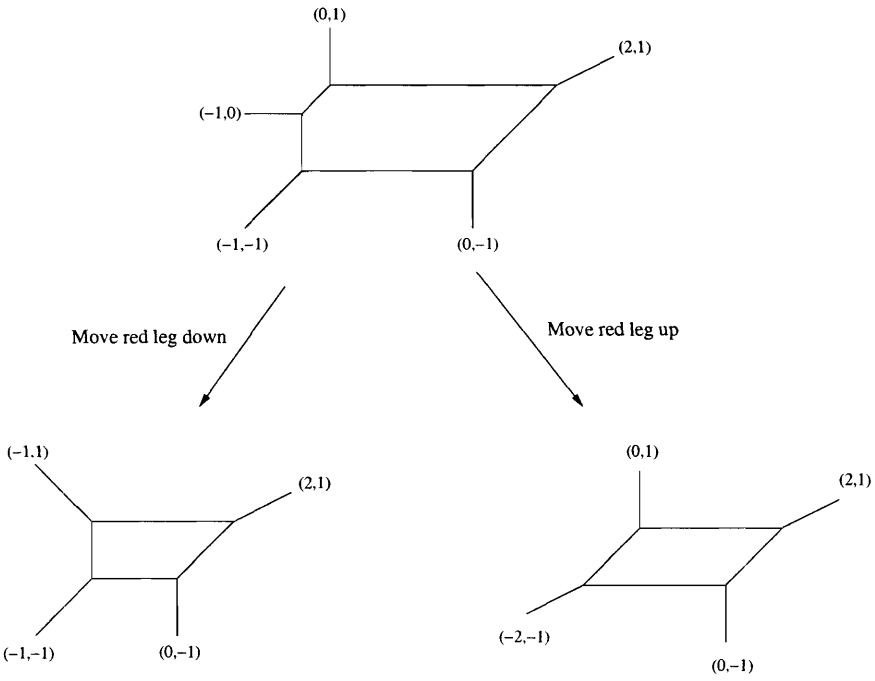

Figure 6-14: By moving the horizontal (red) brane in the above dP_2 brane web up or down, one can get a brane web for dP_1 (left) or $\mathbb{F}_0$ (right).

We now see that knowing the toric diagram is tantamount to knowing the brane web. One can easily see in Figure 6-12 that we'll always get a flavor D5-brane which can be moved up or down; this is just the external line dual to the one external vertical line in the toric diagram. We do note that the situation is mildly more complicated for many internal points, since moving the flavor D5 past any brane junction means that one must change the (p,q) charges of the branes at the junction. One example of this procedure is done, for $X^{3,1}$, in Figure 6-15.

We also note here that integrating out the massive flavor is equivalent, geometrically, to blowing down a 2-cycle. This is especially simple to see in the dP_2 example, since we know that dP_2 blows down to either dP_1 or $\mathbb{F}_0$. This is also easy to see from the toric diagram, since external lines correspond to 2-cycles. For the general $X^{p,q}$ theories this interpretation of blowing down a 2-cycle remains true. For an interesting discussion of the transitions between some of the $X^{p,q}$ and $Y^{p,q}$ theories, see Figure

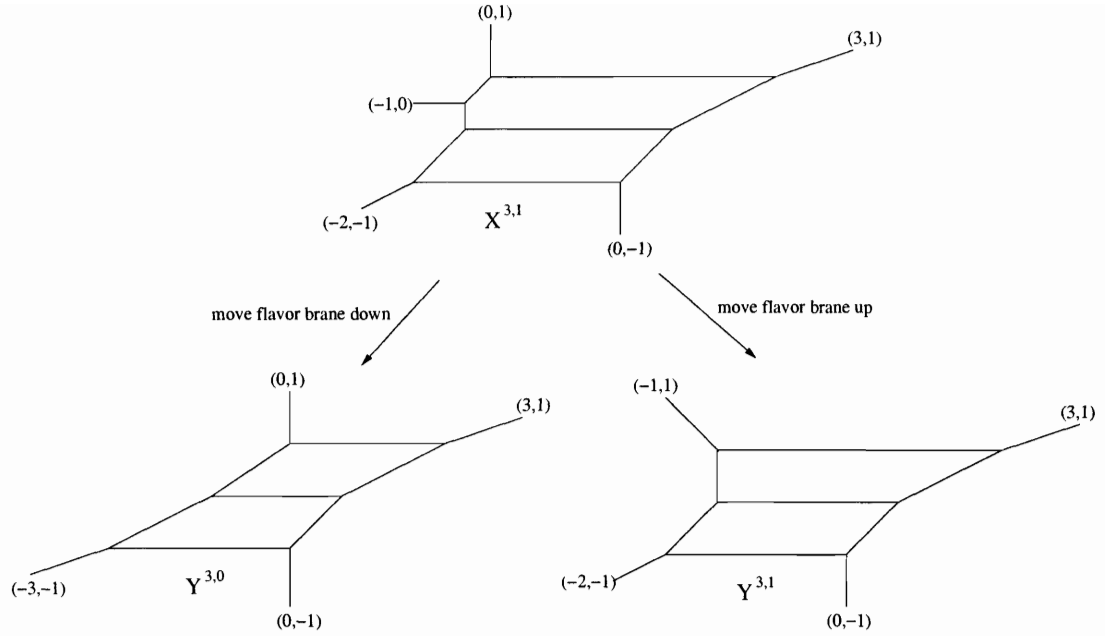

Figure 6-15: The process of going from the $X^{3,1}$ web to that of $Y^{3,0}$ or $Y^{3,1}$.

25 of [41] and the surrounding discussion.

The dP_2 theory, or $X^{2,1}$ as we call it in this chapter, corresponds to a five dimensional $SU(2)$ gauge theory with one flavor. Taking the mass of this flavor to positive infinity yields one of two different theories: If we define the sign of the mass to correspond to the positive y direction in Figure 6-14, this theory is $\mathbb{F}_0$. Taking the mass to negative infinity gives the other theory, dP_1. The distinction between these two theories is related to the value of the discrete θ angle, which follows from the fact that the 4th homotopy group of the gauge group is $\pi_4(SU(2)) = \mathbb{Z}_2$. This distinction is special to the case of $SU(2)$ as this is the only unitary group with a non-trivial 4th homotopy group. For higher values of the rank of the unitary group the five dimensional theory can admit a Chern-Simons term. This term is absent for the $SU(2)$ case since the completely symmetric rank 3 invariant for $SU(2)$ vanishes, while for the other $SU(p)$ theories it is non-vanishing. As a result, for the 5d theories living on the brane webs dual to the $Y^{p,q}$ toric diagrams with $p > 2$ we can introduce a Chern-Simons term which turns out to have a coefficent equal to q. As discussed in detail in [37] a massive flavor contributes at the one loop level to the effective Chern-

Simons coupling a value of $1/2$ and the sign of this contribution is proportional to the sign of the mass of this flavor. As a result when going from a large positive mass to a large negative mass and vice versa, the value of the Chern-Simons coefficient changes by 1. As we identify the Chern-Simons coupling with q, taking the mass from one sign to another precisely maps to the process of changing q by 1. This is the process we have discussed above in which we start with $X^{p,q}$, corresponding to a small mass in the 5d theory, and Higgs to either $Y^{p,q}$ or $Y^{p,q-1}$ by giving a large positive or negative mass, respectively, to the 5d flavor.

One more interesting point to note about the $Y^{p,q}$ theories is that from a five dimensional point of view, the allowed values for p and q which give interacting UV fixed points in five dimensions are $p > q \geq 0$. The case with $q = 0$ is the simplest five dimensional SYM $SU(p)$ gauge theory where there is no Chern-Simons term. The case with $q = p$ does not lead to an interacting UV fixed point since the brane web involves parallel legs; see a discussion in [41]. The conditions which were written in [37] for an interacting fixed point coincide nicely with the allowed range of the $Y^{p,q}$ theories as required by the geometry side to have smooth metrics. These conditions can be extended to the case of more flavors. If we denote the number of flavors of the five dimensional gauge theory by N_f then this number is related to the number of external nodes E in the corresponding toric diagram by $E = N_f + 4$. The condition for an interacting UV fixed point is then $N_f + 2q < 2p$. For $N_f = 0$ this recovers the known limits on $Y^{p,q}$ discussed above while for $N_f = 1$ we get a new bound which is consistent with the limits that we have found in this chapter. We further get a prediction for the allowed ranges of theories for higher values of N_f.

As discussed in [41], for a given five dimensional gauge theory with $SU(p)$ gauge group and for any Chern-Simons coefficient q the number of parameters in the Lagrangian is the number of external legs E in the (p,q) web minus 3. As an example, for $N_f = 0$ the number of parameters is 1; this parameter is simply the gauge coupling of the five dimensional gauge theory. For $N_f = 1$ there is an additional parameter given by the mass of the flavor, etc. This number $E - 3$ actually counts the number of baryonic $U(1)$ global symmetries in the corresponding quiver gauge theory. Thus

for the $Y^{p,q}$ theories we have one $U(1)_B$ and for $X^{p,q}$ we expect two baryonic $U(1)$ global symmetries.

There are additional matchings we can make between the five dimensional theory and the quiver gauge theory. The number of moduli for the five dimensional theory is equal to the rank of the gauge group, $p-1$. This number gives the number of distinct monopole solutions in the five dimensional gauge theory as well as the various vacuum expectation values which can spontaneously break gauge invariance. For the geometry this number is the number of internal points in the toric diagram and is therefore the number of vanishing 4-cycles for the singular geometry. The number of 2-cycles in the singular geometry has yet another simple expression as $p-1+E-3$. This number also counts the number of different BPS charges B that particles can carry in the five dimensional theory. As is well known the number of gauge groups for the quiver gauge theory is given by the total number of all even (0-,2-,and 4-) dimensional cycles. Therefore we get a relation which states that the number of different monopole solutions, denoted M, is given in terms of p and the number of external lines as $M+B+1=2M+N_f+2=2M+E-2=2p+N_f$. For the cases $N_f=0$ and $N_f=1$ we recover the known cases of $Y^{p,q}$ and $X^{p,q}$, respectively. See related discussions in [41]. We summarize the above discussion in Table 6.1.

5d SU(p) theory	$Y^{p,q}$ Toric Geometry
Number of Monopoles M	$p-1$
Number of BPS States B	Number of $2-$cycles, $p-1+E-3$
5d Moduli	Number of $4-$cycles, $p-1$
Chern – Simons Coefficient	q
Number of Flavors N_f	$E-4$

Table 6.1: The relationship between different parameters in the 5d theories and $Y^{p,q}$ toric geometries.

6.5 Toric Phases of the $X^{p,q}$ theories

The $X^{p,q}$ quiver gauge theories we present in this chapter each flow to a superconformal fixed point at the infrared. At that point one can apply Seiberg duality [1] to any of the gauge groups and get a new theory which has a different matter content and superpotential but flows to the same IR fixed point as the original theory. By repeating this process it is possible to obtain an infinite number of UV inequivalent theories that fall into the same universality class. In this section we will discuss a particularly simple finite subclass of these theories, the *connected toric phases*. We define the term *toric phase* to mean that all the gauge groups have the same rank. The term "connected" refers to the theories generated by starting from a toric phase, like the ones discussed above, and only dualizing nodes with number of flavors (N_f) equal to twice the number of colors (N_c). These are sometimes called *self-dual* nodes, because the gauge group is unchanged by the dualization. The resulting gauge theory is again in a toric phase, with gauge group $SU(N)^{2p+1}$ and every field appearing in the superpotential exactly twice. For the sake of brevity we will omit the tedious details of the dualizations. Instead we shall outline the general structure of these toric phases, using a few of the results of [63] for the corresponding $Y^{p,q}$ quivers.

The toric phases of the $Y^{p,q}$ theories can be described as modifications of the quiver for $Y^{p,p}$. These can be seen very clearly in the "ladder" depiction of the quiver, in which the nodes are placed in two parallel rows and numbered in a crenellating fashion. The quiver is then made up of "blocks," i.e. square sections between rungs of the ladder. All the blocks are identical in $Y^{p,p}$ and each one can be replaced by a single or double impurity. The numbers of single impurities (n_1) and double impurities (n_2) are restricted by the relation $n_1 + 2n_2 = p - q$. An example of this construction is shown in Figure 6-16.

In these toric phases of the $Y^{p,q}$ theories, the only self-dual nodes are the ones at the ends of a single or double impurity. The blow-up procedure which produces the $X^{p,q}$ theories creates new self-dual nodes. More precicely, node B in $Y^{p,q}$ Figure 6-7 is replaced by self-dual nodes B_1 and B_2 in $X^{p,q}$ Figure 6-8. Dualizing gauge groups that

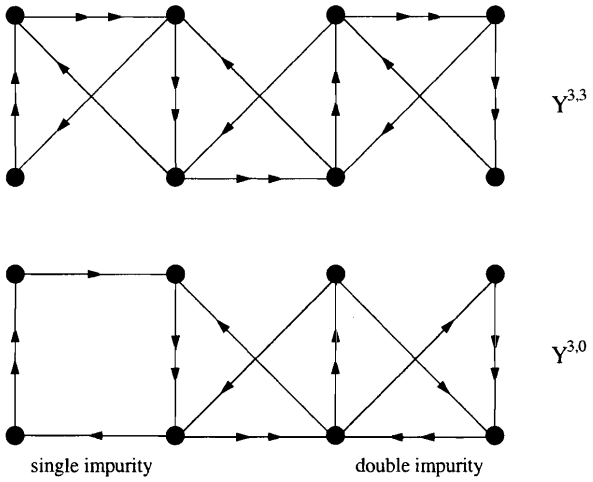

Figure 6-16: The quivers for Y^{33} and Y^{30} with one single (left block) and one double impurity (right block).

do not share any bifundamentals with these two nodes has exactly the same effect as in the case of $Y^{p,q}$. The impurities of $Y^{p,q}$ can be moved around the quiver, fusing into double impurities when they collide. As an example, we show the result of dualizing node 6 of $X^{3,1}$ below. The two impurities fuse into a double impurity exactly as they would in the absence of the blow up. Dualizing node 7 has an essentially identical effect.

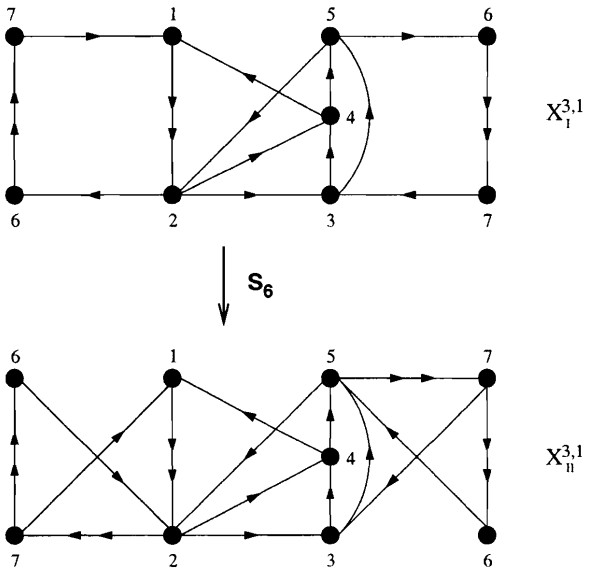

Figure 6-17: The notation S_6 means Seiberg duality on node 6. The resulting double impurity is located between nodes 1 and 6.

On the other hand, dualizing nodes connected by an arrow to the new self-dual nodes leads to new theories, not always accounted for by the toric phase structure of $Y^{p,q}$. Again we will use $X^{3,1}$ as a showcase. Dualizing node 4 leads to the quiver shown in Figure 6-18. We have moved node 4 between nodes 1 and 2 to make clear the result of this dualization: The theory we get is the same as the one we would get by blowing up node 2 instead of 3, as mentioned in Section 3. Higgsing X_{14} in this quiver gives $Y^{3,1}$ with two single impurities, while Higgsing X_{42} gives $Y^{3,0}$ with three single impurities. Dualizing 5 gives a theory completely equivalent to this one.

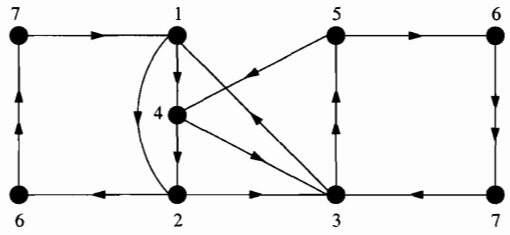

Figure 6-18: Seiberg duality on node 4 corresponds to blowing up a different node of $Y^{3,1}$.

The phases of $X^{3,1}$ we have described so far have either 15 or 19 fields. When we Higgs them down to $Y^{3,1}$ only the field that gets a vev disappears and we get the phases with with 14 and 18 fields respectively. Higgsing to $Y^{3,0}$ gives mass to two fields which are integrated out and removed from the massless spectrum together with the field that gets the expectation value, producing the toric phases with 12 and 16 fields. The difference in the number of fields simply comes from the difference in the distribution of impurities in $Y^{3,1}$. Whenever two single impurities fuse into a double impurity in $Y^{p,q}$, the number of fields goes up by four. In addition to these, there are also "intermediate" toric phases of $X^{3,1}$ that have 17 fields. These blow down to the phase of $Y^{3,1}$ that has 14 fields and to the phase of $Y^{3,0}$ with 16 fields. The details of the Higgsing are now reversed: two additional fields are integrated out when going to $Y^{3,1}$, but only the field with a vev disappears when we blow down to $Y^{3,0}$. For $X^{3,1}$ there are precisely two such phases, produced by dualizing nodes 1 or 3. In Figure 6-19 we show the first of these two, and the phases of $Y^{p,q}$ to which it

blows down.

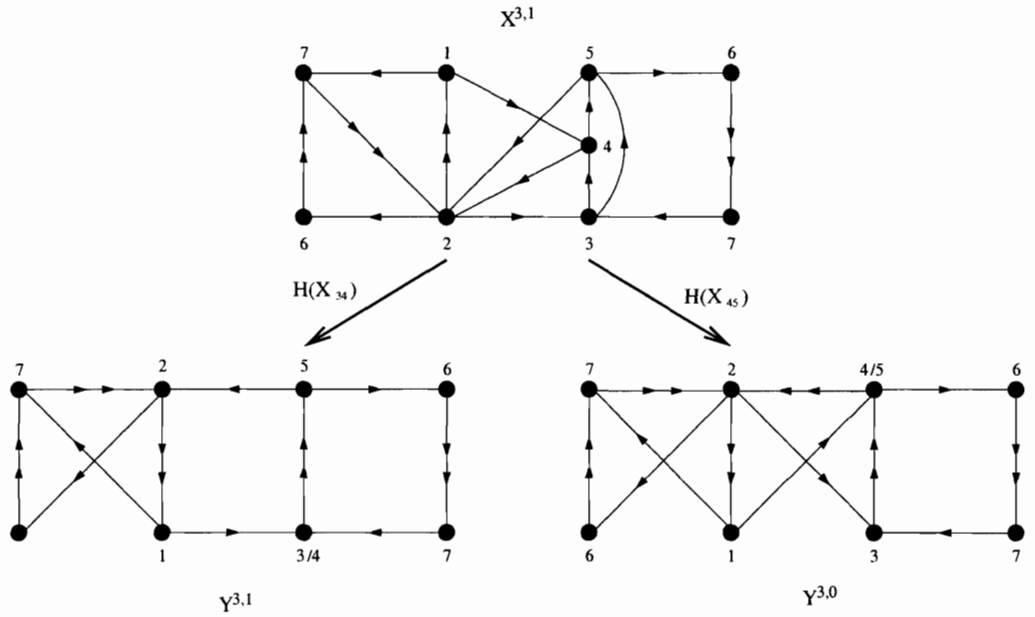

Figure 6-19: One of the two toric phases of $X^{3,1}$ with 17 fields. The notation $H(X_{ij})$ means giving a vev to the scalar component of X_{ij}.

More generally, we expect the toric phases of all $X^{p,q}$ to fall in this pattern. Increasing p does not change the story, because the blow up is localized on the quiver graph. The $Y^{p,q}$ theories have toric phases with $4p + 2q + 4n_2$ fields where $n_2 = 0, 1, \ldots \left[\frac{p-q}{2}\right]$ is the number of double impurities. For each of these models there will be toric phases of $X^{p,q}$ with one additional field that Higgs down to $Y^{p,q}$ and $Y^{p,q-1}$ like the examples in Figures 6-17,6-18. On top of these we have the "intermediate" phases with $4p + 2q + 4n_2 + 3$ fields, where $n_2 = 0, 1, \ldots \left[\frac{p-q}{2}\right] - 1$. These also blow down to $Y^{p,q}$, $Y^{p,q-1}$ in the way described for the example in Figure 6-19. This is summarized in in Figure 6-20 for the case of $X^{3,1}$. It would be interesting to have a more general understanding of the Seiberg dual phases of $X^{p,q}$, including non-toric ones, since it may be easier to extract information about the infrared dynamics from some of these models than from others.

The toric phases of $Y^{p,q}$ can be easily enumerated. The problem is the same as counting the ways of coloring the p vertices of a p-gon using three different colors (corresponding to a single impurity, a double impurity, or no impurity) modulo the

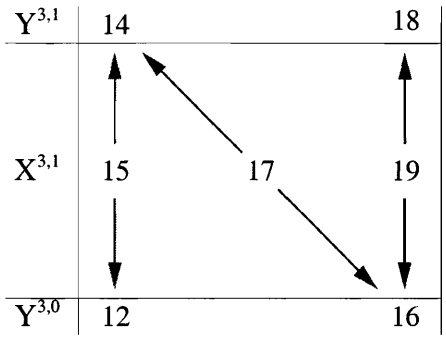

Figure 6-20: The number of fields for the toric phases of X^{31}, Y^{31}, Y^{30} and the possible higgsings (shown with arrows). Note that several different toric phases can have the same number of fields.

action of the dihedral group D_p. This is a standard application of Pólya's enumeration theorem [?]. The cycle index of the dihedral group is

$$\begin{aligned} \mathcal{Z}(D_p) &= \frac{1}{2}\mathcal{Z}(Z_p) + \frac{1}{2}x_1 x_2^{(p-1)/2} \qquad (p \text{ odd}) \\ \mathcal{Z}(D_p) &= \frac{1}{2}\mathcal{Z}(Z_p) + \frac{1}{4}(x_2^{p/2} + x_1^2 x_2^{(p-2)/2}) \qquad (p \text{ even}) \end{aligned} \tag{6.19}$$

where $\mathcal{Z}(Z_p)$ is the cycle index of the cyclic group of order p :

$$\mathcal{Z}(Z_p) = \frac{1}{p}\sum_{n|p} \phi(n) x_n^{p/n} \tag{6.20}$$

and $\phi(n)$ is Euler's totient function. To implement the condition $n_1 + 2n_2 = p - q$ we assign weight 1 for no impurity, λ to a single impurity and λ^2 to a double impurity. Then $x_n = 1 + \lambda^n + \lambda^{2n}$, and after plugging this into (6.19) the number of toric phases is given by the coefficient of λ^{p-q} in the resulting polynomial. Because of the way the $X^{p,q}$ theories Higgs to $Y^{p,q}$ and $Y^{p,q-1}$, we expect the number of toric phases of $X^{p,q}$ to be essentially determined by (and in fact greater than) the number of toric phases of $Y^{p,q}$, but we shall leave a detailed counting to future work.

Finally, we note that when performing Seiberg duality one must alter the superpotential as well as the quiver. This is done by including cubic interactions of the form $Mq\tilde{q}$, where q and $\tilde{q}$ are the dual quarks and M is a composite field in the original theory which maps to a singlet in the dual. One must be careful when applying this

procedure to bifundamentals, since here the field M is only a singlet under the dualized group but still transforms as a bifundamental in the dual theory. This procedure works as expected for the $X^{p,q}$ theories and produces the necessary $Y^{p,q}$ superpotentials upon giving a vev to the appropriate bifundamentals. For more details, we refer the reader to [2, 3].

6.6 R-charges

An important test of the AdS/CFT correspondence is that the dimensions of operators in the field theory match with the volumes of the different supersymmetric (calibrated) submanifolds D3-branes can wrap in the geometry [14, 16]. These dimensions, or equivalently R-charges, can be figured out in the gauge theory via a-maximization, and in the geometry via a volume calculation. These charges have also been computed via techniques from algebraic geometry [32, 70, 44, 71]. It is also possible to derive some of the R-charges purely from the toric data [72].

Let's briefly review the situation for dP_2, which will reveal an interesting aspect of the $X^{p,q}$ theories. The quiver for dP_2 is given in Figure 6-1. The R-charges for this theory are known [52], and given in Table 6.2. Since baryonic operators in the SCFT correspond to D3-branes wrapping 3-cycles, we may associate to each bifundamental a 3-manifold in the dual geometry. Since dP_2 has two 3-cycles, we expect two baryonic $U(1)$ global symmetries. Similarly, we expect dP_2 to have a $U(1) \times U(1)$ isometry, which should translate to an additional $U(1)^2$ flavor symmetry. The baryonic $U(1)$'s do not mix with the R-symmetry, as discussed in [23, 32]. Therefore there should be a two-dimensional space of $U(1)$ symmetries which can potentially mix with the R-symmetry. Indeed, we note that we may assign a 2-dimensional basis of R-charges to the fields in dP_2 as given in Table 6.2. One can see a similar agreement for the $Y^{p,q}$ theories: With one non-baryonic $U(1)$ symmetry, one can reduce the R-charges to a one-dimensional basis. This is what allowed the authors of [50] to compute the R-charges of these theories.

Equivalently, we can rephrase the above discussion as follows: Since the baryonic

symmetries do not mix with the R-charges, it should be possible to do a-maximization over a two-dimensional space of parameters for dP_2 and over a one-dimensional space for $Y^{p,q}$. Naively, one might think from the field theory that dP_2 would require a-maximization over four parameters; this is what comes out of solving the linear equations given by the constraints of anomaly freedom at each node, and that the superpotential terms all have R-charge equal to two. However, we know that this is not the whole story; if one were able to pick the two flat directions properly, a-maximization could be done over only two parameters. This is easy to do once we know the right R-charges. From these, it is possible to work backwards and assign a good two-dimensional basis of charges as in Table 6.2. Doing a-maxmization over these two-dimensional basis, treating these charges as free parameters, yields the correct result.

Field	$R-$charge	Linear Combination
X_{52}	$\frac{3}{16}(19-3\sqrt{33})$	Σ_1
X_{14}	$\frac{3}{16}(19-3\sqrt{33})$	Σ_1
X_{53}	$\frac{1}{4}(9-\sqrt{33})$	Σ_2
X_{34}	$\frac{1}{4}(9-\sqrt{33})$	Σ_2
X_{42}	$\frac{1}{16}(-21+5\sqrt{33})$	$\Sigma_2-\Sigma_1$
X_{51}	$\frac{1}{16}(-21+5\sqrt{33})$	$\Sigma_2-\Sigma_1$
X^1_{23}	$\frac{1}{16}(-21+5\sqrt{33})$	$\Sigma_2-\Sigma_1$
X^1_{31}	$\frac{1}{16}(-21+5\sqrt{33})$	$\Sigma_2-\Sigma_1$
X^2_{23}	$\frac{1}{16}(17-\sqrt{33})$	$\Sigma_2-\frac{1}{3}\Sigma_1$
X^2_{31}	$\frac{1}{16}(17-\sqrt{33})$	$\Sigma_2-\frac{1}{3}\Sigma_1$
X_{45}	$\frac{1}{2}(-5+\sqrt{33})$	$\Sigma_2-\frac{4}{3}\Sigma_1$

Table 6.2: R-charges for dP_2. All R-charges can be expressed as a linear combination of two basis charges.

One would naively think that just as the dP_1 results extended to general $Y^{p,q}$, we could extend the dP_2 results to general $X^{p,q}$. Since the number of baryonic $U(1)$'s is always the number of external legs of the toric diagram minus three, there should always be two $U(1)_B$ symmetries in the $X^{p,q}$ theories that do not mix with the R-symmetry. Since we expect there to be naively four free parameters for the $X^{p,q}$

theories in general (we have verified this for e.g. $X^{3,1}$ although not for general $X^{p,q}$), there should be a remaining two-dimensional basis of R-charges.

Unfortunately, however, we have not been able to reduce the R-charges of these theories to a two-dimensional basis. One difficulty is that since a-maximization for the $X^{p,q}$ theories must be done over four parameters (at least initially, since it is difficult to pick the flat directions in practice), it is very difficult to obtain exact numbers for $p > 2$. We have, however, numerically computed the R-charges for $X^{3,q}$. Since the numbers are not particularly illuminating, we do not record the R-charges here. We do note that it appears **not** to be true that there is a two-dimensional basis of R-charges for general $X^{p,q}$ theories. One can easily check if, given three R-charges, there is any integer linear combination of them that equals another integer. To the precision allowed by Mathematica, we have not found any such linear combination of R-charges for $X^{3,q}$ for any $1 \leq q \leq 3$. Thus, it appears that our naive guess that there are only two $U(1)$ flavor symmetries in the Einstein-Sasaki manifold is incorrect. We note that the $X^{p,p}$ theory is special in that the quiver and superpotential have a $\mathbb{Z}_2$ symmetry which gives a nontrivial constraint on the R-charges; in these cases we may reduce the number of independent R-charges to three. Thus, we have a puzzle: Since the baryonic $U(1)$'s should not mix with the R-symmetry, there should be relations between the R-charges. Our inability to find such relations may be a consequence of our numerical computation; since we cannot find the **exact** R-charges for the $X^{p,q}$, we can only check that things sum to zero up to a given numerical precision. However, it is possible that there is a deeper issue here as well.

Finally, we note that there are some $X^{p,q}$ where we can actually find the R-charges exactly. We have done the calculation for $X^{2,2}$ and $X^{3,3}$, and found that in these cases the R-charges are not quadratic irrational, but instead the roots of **quartic** polynomials. These are the first examples of theories whose R-charges are not quadratic irrationals. This is not in contradiction to the prediction from a-maximization, since the charges are still algebraic numbers. Since a is a cubic function over many variables, derivatives of a will be quadratic functions over many variables. In general the solutions of these equations will not be quadratic irrational, although

they have been for every case studied so far. Although we do not record the exact values of all the R-charges for $X^{2,2}$ and $X^{3,3}$ here, we do note for the sake of reference two R-charges. For $X^{3,3}$ (shown in Figure 6-10), the R-charge of the bifundamental X_{56} is given by a root of the polynomial $27x^4 - 198x^3 - 180x^2 + 650x - 250$. For $X^{2,2}$ (also known as Pseudo-del Pezzo 2), the R-charge of one of the fields (X_{53} in Figure 6 of [73]) is given by a root of $9x^4 - 78x^3 + 112x^2 + 16x + 32$.

6.7 Conclusions

We have seen how to generate a new class of quiver gauge theories for which the dual geometries are known in terms of toric varieties. In general, the study of the relation between the geometry which the branes probe and the theory living on their worldvolume contributes to the more ambitious effort for completely understanding the holographic duality between gauge theories and string theory. The theories we studied are for the most part supersymmetric, as this is required for the stability of the brane configuration. This is obviously a limitation if one wants to make use of the duality to analyze non-supersymmetric theories like standard QCD. However, as noted in the introduction, the motivation is still sound, both because of the good possibility that supersymmetry is real (and broken at low energies) and because of the structural features shared by both classes of theories. Recently, serious progress has been made through the introduction of the brane dimer concept [64, 65] which provides an "intermediary" between the geometry and the gauge theory. It is now very possible that in the very near future we will have a fast, comprehensive and physically meaningful algorithm for moving between the two poles of the duality. The purpose of course is not to generate increasingly complicated theories, but to uncover the mechanics of how the dynamics of the gauge theories are related to the gravity/string theory description. In this context, the most interesting question is to describe the physical reality of the brane dimer, and how it can replace the singularity. This will provide answers to important questions, such as the precise string theoretic origin of a-maximization.

Bibliography

[1] N. Seiberg, "Electric - magnetic duality in supersymmetric nonAbelian gauge theories," Nucl. Phys. B **435**, 129 (1995) [arXiv:hep-th/9411149].

[2] C. E. Beasley and M. R. Plesser, "Toric duality is Seiberg duality," JHEP **0112**, 001 (2001) [arXiv:hep-th/0109053].

[3] B. Feng, A. Hanany, Y. H. He and A. M. Uranga, "Toric duality as Seiberg duality and brane diamonds," JHEP **0112**, 035 (2001) [arXiv:hep-th/0109063].

[4] J. Polchinski, "Dirichlet-Branes and Ramond-Ramond Charges," Phys. Rev. Lett. **75**, 4724 (1995) [arXiv:hep-th/9510017].

[5] J. Dai, R. G. Leigh and J. Polchinski, "New Connections Between String Theories," Mod. Phys. Lett. A **4**, 2073 (1989).

[6] R. G. Leigh, "Dirac-Born-Infeld Action From Dirichlet Sigma Model," Mod. Phys. Lett. A **4**, 2767 (1989).

[7] E. Witten, "Bound states of strings and p-branes," Nucl. Phys. B **460**, 335 (1996) [arXiv:hep-th/9510135].

[8] D. R. Morrison and M. Ronen Plesser, "Summing the instantons: Quantum cohomology and mirror symmetry in toric varieties," Nucl. Phys. B **440**, 279 (1995) [arXiv:hep-th/9412236].

[9] J. M. Maldacena, "The large N limit of superconformal field theories and supergravity," Adv. Theor. Math. Phys. **2**, 231 (1998) [Int. J. Theor. Phys. **38**, 1113 (1999)] [arXiv:hep-th/9711200].

[10] S. S. Gubser, I. R. Klebanov and A. M. Polyakov, "Gauge theory correlators from non-critical string theory," Phys. Lett. B **428**, 105 (1998) [arXiv:hep-th/9802109].

[11] E. Witten, "Anti-de Sitter space and holography," Adv. Theor. Math. Phys. **2**, 253 (1998) [arXiv:hep-th/9802150].

[12] A. Kehagias, "New type IIB vacua and their F-theory interpretation," Phys. Lett. B **435**, 337 (1998) [arXiv:hep-th/9805131].

[13] D. R. Morrison and M. R. Plesser, "Non-spherical horizons. I," Adv. Theor. Math. Phys. **3**, 1 (1999) [arXiv:hep-th/9810201].

[14] E. Witten, "Baryons and branes in anti de Sitter space," JHEP **9807**, 006 (1998) [arXiv:hep-th/9805112].

[15] S. Gukov, M. Rangamani and E. Witten, "Dibaryons, strings, and branes in AdS orbifold models," JHEP **9812**, 025 (1998) [arXiv:hep-th/9811048].

[16] D. Berenstein, C. P. Herzog and I. R. Klebanov, "Baryon spectra and AdS/CFT correspondence," JHEP **0206**, 047 (2002) [arXiv:hep-th/0202150].

[17] I. R. Klebanov and M. J. Strassler, "Supergravity and a confining gauge theory: Duality cascades and chiSB-resolution of naked singularities," JHEP **0008**, 052 (2000) [arXiv:hep-th/0007191].

[18] B. Fiol, "Duality cascades and duality walls," JHEP **0207**, 058 (2002) [arXiv:hep-th/0205155].

[19] M. J. Strassler, "Duality in Supersymmetric Field Theory and an Application to Real Particle Physics," Talk given at International Workshop on Perspectives of Strong Coupling Gauge Theories (SCGT 96), Nagoya, Japan. Available at http://www.eken.phys.nagoya-u.ac.jp/Scgt/proc/

[20] A. Hanany and J. Walcher, "On duality walls in string theory," JHEP **0306**, 055 (2003) [arXiv:hep-th/0301231].

[21] V. A. Novikov, M. A. Shifman, A. I. Vainshtein and V. I. Zakharov, "Exact Gell-Mann-Low Function Of Supersymmetric Yang-Mills Theories From Instanton Calculus," Nucl. Phys. B **229**, 381 (1983).

[22] R. G. Leigh and M. J. Strassler, "Exactly marginal operators and duality in four-dimensional N=1 supersymmetric gauge theory," Nucl. Phys. B **447**, 95 (1995) [arXiv:hep-th/9503121].

[23] K. Intriligator and B. Wecht, "The exact superconformal R-symmetry maximizes a," Nucl. Phys. B **667**, 183 (2003) [arXiv:hep-th/0304128].

[24] F. Cachazo, B. Fiol, K. A. Intriligator, S. Katz and C. Vafa, "A geometric unification of dualities," Nucl. Phys. B **628**, 3 (2002) [arXiv:hep-th/0110028].

[25] S. Cecotti and C. Vafa, "On classification of N=2 supersymmetric theories," Commun. Math. Phys. **158**, 569 (1993) [arXiv:hep-th/9211097].

[26] O. DeWolfe, T. Hauer, A. Iqbal and B. Zwiebach, "Uncovering the symmetries on (p,q) 7-branes: Beyond the Kodaira classification," Adv. Theor. Math. Phys. **3**, 1785 (1999) [arXiv:hep-th/9812028].

[27] B. Feng, A. Hanany, Y. H. He and A. Iqbal, "Quiver theories, soliton spectra and Picard-Lefschetz transformations," JHEP **0302**, 056 (2003) [arXiv:hep-th/0206152].

[28] C. P. Herzog, I. R. Klebanov and P. Ouyang, "D-branes on the conifold and N = 1 gauge / gravity dualities," [arXiv:hep-th/0205100].

[29] C. P. Herzog, I. R. Klebanov and P. Ouyang, "Remarks on the warped deformed conifold," [arXiv:hep-th/0108101].

[30] S. Franco, Y. H. He, C. Herzog and J. Walcher, "Chaotic duality in string theory," Phys. Rev. D **70**, 046006 (2004) [arXiv:hep-th/0402120].

[31] C. P. Herzog, Q. J. Ejaz and I. R. Klebanov, "Cascading RG flows from new Sasaki-Einstein manifolds," JHEP **0502**, 009 (2005) [arXiv:hep-th/0412193].

[32] K. Intriligator and B. Wecht, "Baryon charges in 4D superconformal field theories and their AdS duals," arXiv:hep-th/0305046.

[33] K. A. Intriligator and N. Seiberg, "Mirror symmetry in three dimensional gauge theories," Phys. Lett. B **387**, 513 (1996) [arXiv:hep-th/9607207].

[34] M. Porrati and A. Zaffaroni, "M-theory origin of mirror symmetry in three dimensional gauge theories," Nucl. Phys. B **490**, 107 (1997) [arXiv:hep-th/9611201].

[35] A. Hanany and E. Witten, "Type IIB superstrings, BPS monopoles, and three-dimensional gauge dynamics," Nucl. Phys. B **492**, 152 (1997) [arXiv:hep-th/9611230].

[36] N. Seiberg, "Five dimensional SUSY field theories, non-trivial fixed points and string dynamics," Phys. Lett. B **388**, 753 (1996) [arXiv:hep-th/9608111].

[37] K. A. Intriligator, D. R. Morrison and N. Seiberg, "Five-dimensional supersymmetric gauge theories and degenerations of Calabi-Yau spaces," Nucl. Phys. B **497**, 56 (1997) [arXiv:hep-th/9702198].

[38] B. Feng and A. Hanany, "Mirror symmetry by O3-planes," JHEP **0011**, 033 (2000) [arXiv:hep-th/0004092].

[39] O. Aharony and A. Hanany, "Branes, superpotentials and superconformal fixed points," Nucl. Phys. B **504**, 239 (1997) [arXiv:hep-th/9704170].

[40] N. C. Leung and C. Vafa, "Branes and toric geometry," Adv. Theor. Math. Phys. **2**, 91 (1998) [arXiv:hep-th/9711013].

[41] O. Aharony, A. Hanany and B. Kol, "Webs of (p,q) 5-branes, five dimensional field theories and grid diagrams," JHEP **9801**, 002 (1998) [arXiv:hep-th/9710116].

[42] O. DeWolfe, A. Hanany, A. Iqbal and E. Katz, "Five-branes, seven-branes and five-dimensional E(n) field theories," JHEP **9903**, 006 (1999) [arXiv:hep-th/9902179].

[43] S. S. Gubser and I. R. Klebanov, "Baryons and domain walls in an N = 1 superconformal gauge theory," Phys. Rev. D **58**, 125025 (1998) [arXiv:hep-th/9808075].

[44] C. P. Herzog and J. Walcher, "Dibaryons from exceptional collections," [arXiv:hep-th/0306298].

[45] A. Hanany and A. Iqbal, "Quiver theories from D6-branes via mirror symmetry," JHEP **0204**, 009 (2002) [arXiv:hep-th/0108137].

[46] S. Franco and A. Hanany, "Geometric dualities in 4d field theories and their 5d interpretation," JHEP **0304**, 043 (2003) [arXiv:hep-th/0207006].

[47] I. R. Klebanov and E. Witten, "Superconformal field theory on threebranes at a Calabi-Yau singularity," Nucl. Phys. B **536**, 199 (1998) [arXiv:hep-th/9807080].

[48] J. P. Gauntlett, D. Martelli, J. Sparks and D. Waldram, "Supersymmetric AdS_5 solutions of M-theory," Class. Quant. Grav. **21** 4335, [arXiv:hep-th/0402153].

[49] J. P. Gauntlett, D. Martelli, J. Sparks and D. Waldram, "Sasaki-Einstein metrics on $S^2 \times S^3$," [arXiv:hep-th/0403002].

[50] S. Benvenuti, S. Franco, A. Hanany, D. Martelli and J. Sparks, "An infinite family of superconformal quiver gauge theories with Sasaki-Einstein duals," [arXiv:hep-th/0411264].

[51] D. Martelli and J. Sparks, "Toric Geometry, Sasaki-Einstein Manifolds and a New Infinite Class of AdS/CFT Duals," [arXiv:hep-th/0411238].

[52] M. Bertolini, F. Bigazzi and A. Cotrone, "New checks and subtleties for AdS/CFT and a-maximization," [arXiv:hep-th/0411249].

[53] B. Feng, A. Hanany and Y. H. He, "Phase structure of D-brane gauge theories and toric duality," JHEP **0108**, 040 (2001) [arXiv:hep-th/0104259].

[54] B. Feng, S. Franco, A. Hanany and Y. H. He, "Symmetries of toric duality," JHEP **0212**, 076 (2002) [arXiv:hep-th/0205144].

[55] S. Benvenuti and A. Hanany, "New results on superconformal quivers," [arXiv:hep-th/0411262].

[56] S. Franco, A. Hanany, Y. H. He and P. Kazakopoulos, "Duality walls, duality trees and fractional branes," [arXiv:hep-th/0306092].

[57] S. Franco, A. Hanany and Y. H. He, "A trio of dualities: Walls, trees and cascades," Fortsch. Phys. **52**, 540 (2004) [arXiv:hep-th/0312222].

[58] M. R. Douglas and G. W. Moore, "D-branes, Quivers, and ALE Instantons," [arXiv:hep-th/9603167].

[59] B. Feng, A. Hanany and Y. H. He, "D-brane gauge theories from toric singularities and toric duality," Nucl. Phys. B **595**, 165 (2001) [arXiv:hep-th/0003085].

[60] S. Franco, A. Hanany and A. M. Uranga, "Multi-flux warped throats and cascading gauge theories," arXiv:hep-th/0502113.

[61] A. Bergman, "Undoing orbifold quivers," arXiv:hep-th/0502105.

[62] S. S. Pal, "A new Ricci flat geometry," arXiv:hep-th/0501012.

[63] S. Benvenuti, A. Hanany and P. Kazakopoulos, "The toric phases of the Y(p,q) quivers," arXiv:hep-th/0412279.

[64] A. Hanany and K. D. Kennaway, "Dimer models and toric diagrams," arXiv:hep-th/0503149.

[65] S. Franco, A. Hanany, K. D. Kennaway, D. Vegh and B. Wecht, "Brane dimers and quiver gauge theories," arXiv:hep-th/0504110.

[66] A. Iqbal and V. S. Kaplunovsky, "Quantum deconstruction of a 5D SYM and its moduli space," JHEP **0405**, 013 (2004) [arXiv:hep-th/0212098].

[67] B. Feng, S. Franco, A. Hanany and Y. H. He, "Unhiggsing the del Pezzo," JHEP **0308**, 058 (2003) [arXiv:hep-th/0209228].

[68] A. Iqbal and A. K. Kashani-Poor, "SU(N) geometries and topological string amplitudes," arXiv:hep-th/0306032.

[69] M. R. Douglas, S. Katz and C. Vafa, "Small instantons, del Pezzo surfaces and type I' theory," Nucl. Phys. B **497**, 155 (1997) [arXiv:hep-th/9609071].

[70] C. P. Herzog, "Exceptional collections and del Pezzo gauge theories," JHEP **0404**, 069 (2004) [arXiv:hep-th/0310262].

[71] C. P. Herzog and J. McKernan, "Dibaryon spectroscopy," JHEP **0308**, 054 (2003) [arXiv:hep-th/0305048].

[72] D. Martelli, J. Sparks and S. T. Yau, "The geometric dual of a-maximisation for toric Sasaki-Einstein manifolds," arXiv:hep-th/0503183.

[73] B. Feng, Y. H. He and F. Lam, "On correspondences between toric singularities and (p,q)-webs," Nucl. Phys. B **701**, 334 (2004) [arXiv:hep-th/0403133].